

# **SANDIA REPORT**

SAND2005-4331  
Unlimited Release  
Printed July 2005

## **An Analysis of Uranium Dispersal and Health Effects Using a Gulf War Case Study**

**Albert C. Marshall**

Prepared by  
Sandia National Laboratories  
Albuquerque, New Mexico 87185 and Livermore, California 94550

Sandia is a multiprogram laboratory operated by Sandia Corporation,  
a Lockheed Martin Company, for the United States Department of Energy's  
National Nuclear Security Administration under Contract DE-AC04-94AL85000.



**Sandia National Laboratories**

Issued by Sandia National Laboratories, operated for the Issued by Sandia National  
Laboratories, operated for the United States Department of Energy by Sandia  
Corporation.

**NOTICE:** This report was prepared as an account of work sponsored by an agency  
of the United States Government. Neither the United States Government, nor any agency  
thereof, nor any of their employees, nor any of their contractors, subcontractors, or their  
employees, make any warranty, express or implied, or assume any legal liability or  
responsibility for the accuracy, completeness, or usefulness of any information,  
apparatus, product, or process disclosed, or represent that its use would not infringe  
privately owned rights. Reference herein to any specific commercial product, process, or  
service by trade name, trademark, manufacturer, or otherwise, does not necessarily  
constitute or imply its endorsement, recommendation, or favoring by the United States  
Government, any agency thereof, or any of their contractors or subcontractors. The  
views and opinions expressed herein do not necessarily state or reflect those of the United  
States Government, any agency thereof, or any of their contractors.

Printed in the United States of America. This report has been reproduced directly from  
the best available copy.

Available to DOE and DOE contractors from

U.S. Department of Energy  
Office of Scientific and Technical Information  
P.O. Box 62  
Oak Ridge, TN 37831

Telephone: (865)576-8401

Facsimile: (865)576-5728

E-Mail: [reports@adonis.osti.gov](mailto:reports@adonis.osti.gov)

Online ordering: <http://www.osti.gov/bridge>

Available to the public from

U.S. Department of Commerce  
National Technical Information Service  
5285 Port Royal Rd  
Springfield, VA 22161

Telephone: (800)553-6847

Facsimile: (703)605-6900

E-Mail: [orders@ntis.fedworld.gov](mailto:orders@ntis.fedworld.gov)

Online order: <http://www.ntis.gov/help/ordermethods.asp?loc=7-4-0#online>



SAND2005-4331  
Unlimited Release  
Printed July 2005

# **An Analysis of Uranium Dispersal and Health Effects Using a Gulf War Case Study**

Albert C. Marshall,  
National Security Studies Department  
Sandia National Laboratories  
P.O. Box 5800  
Albuquerque, NM 87185-0431

## **Abstract**

The study described in this report used mathematical modeling to estimate health risks from exposure to depleted uranium (DU) during the 1991 Gulf War for both U.S. troops and nearby Iraqi civilians. The analysis found that the risks of DU-induced leukemia or birth defects are far too small to result in an observable increase in these health effects among exposed veterans or Iraqi civilians. Only a few veterans in vehicles accidentally struck by U.S. DU munitions are predicted to have inhaled sufficient quantities of DU particulate to incur any significant health risk (i.e., the possibility of temporary kidney damage from the chemical toxicity of uranium and about a 1% chance of fatal lung cancer). The health risk to all downwind civilians is predicted to be extremely small. Recommendations for monitoring are made for certain exposed groups. Although the study found fairly large calculational uncertainties, the models developed and used are generally valid. The analysis was also used to assess potential uranium health hazards for workers in the weapons complex. No illnesses are projected for uranium workers following standard guidelines; nonetheless, some research suggests that more conservative guidelines should be considered.

## **Acknowledgements**

This work was performed for the U.S. Department of Energy. The author is grateful for the detailed review of this analysis by Dr. Leonard Connell and the support and encouragement of Dr. Clyde Layne and Dr. Jon Rogers from Sandia National Laboratories National Securities Studies Department. The author is also grateful for the review of the medical aspects of this study by Dr. Larry Clevenger from Sandia National Laboratories Medical Department, the review of environmental aspects of DU contamination by Dr. Don Wall from Sandia National Laboratories Repository Performance Department, and the review by Dr. Charles Potter from Sandia National Laboratories National Radiation Protection and Lab Services Department. The help provided by Dr. Celeste Drewien from Sandia National Laboratories System Analysis Department, in performing a Monte Carlo analysis for gamma emission from DU penetrators and for her detailed review of the report is greatly appreciated. This study benefited significantly from previous work on the topic. The comments and suggestions provided by Dr. Michael Bailey of the Royal Society's DU working group and the detailed analysis provided in the Royal Society's DU study were especially helpful.

# Contents

Executive Summary .....	9
1.0. Basis, Scope, and Approach .....	17
1.1 Basis for Study .....	17
1.2 Scope and Study Approach .....	19
1.2.1 Veterans Studied .....	19
1.2.2 Iraqi Civilians Studied .....	20
1.2.3 DU Sources Studied.....	21
1.2.4 General Approach .....	21
1.3 Report Organization .....	22
2.0. Background .....	25
2.1 DU Nuclear Characteristics.....	25
2.1.1 DU Radioactivity .....	26
2.1.2 DU Decay Properties .....	27
2.2 Military Use of DU .....	30
2.2.1 DU Weapons Used .....	30
2.2.2 Quantity and Locations of DU Weapons Use.....	32
2.3 Exposure Pathways .....	33
2.4. Chemical Health Effects of DU .....	34
2.5 Radiological Health Effects of DU .....	35
2.5.1 External vs. Internal Exposure.....	35
2.5.2 Cancers .....	36
2.5.3 Birth Defects.....	37
2.5.4 Guidelines .....	37
2.6 Iraqi Population and Environment .....	38
2.6.1 Population and Terrain.....	38
2.6.2 Water and Food Sources .....	39
2.6.3 Prevailing Weather .....	41
2.6.4 Gulf War Aftermath.....	41
3.0. DU Source Terms and Internalized Mass.....	43
3.1 Types of Exposures and Methodologies .....	43
3.2 Method I: During Battle .....	45
3.3 Method 2: Post Battle.....	46
3.3.1 Level II Veterans .....	46
3.3.2 Level III Veterans .....	47
3.3.3 Child at Play .....	47
3.4 Aerosol Generation and Dispersal (1 Target) .....	48
3.4.1 DU Particulate Masses Generated .....	48
3.4.2 Atmospheric Dispersal.....	49
3.5 Aerosol Generation and Dispersal (Multi-Target) .....	51
3.5.1 Tank Battle Array .....	51
3.5.2 Very High Density of Targets.....	53
3.6 Methods 3 and 4: Ex-Vehicle.....	55
3.6.1 Level III Veteran.....	55
3.6.2 Downwind Civilian.....	55
3.6.3 Child at Play .....	56
3.7 Method 5: Food/Water Contamination .....	56
3.8 Summary of Internalized DU Mass.....	59

4.0. Biokinetic Analysis .....	61
4.1 Biokinetic Model.....	62
4.2 Acute Inhalation and Ingestion .....	64
4.2.1 Acute Inhalation.....	64
4.2.2 Acute Ingestion.....	66
4.3 Biokinetics for Veterans.....	67
4.3.1 Level I.....	67
4.3.2 Levels II and III .....	69
4.4 Biokinetics for Civilians .....	69
4.4.1 Child at Play .....	70
4.4.2 Downwind Civilians .....	70
5.0. Health Effect Estimates .....	73
5.1 Kidney Heavy Metal Effect .....	73
5.1.1 Estimated Concentrations vs. Guidelines .....	73
5.1.2 Kidney Health Effects Assessment.....	75
5.2 Other Heavy Metal Effects.....	75
5.3 Veteran Internal Radiation Exposure .....	76
5.3.1 Veteran Doses.....	76
5.3.2 Cancer Risks .....	78
5.3.3 Radiation from Embedded Fragments .....	80
5.3.4 Genetic Risks .....	81
5.4 Civilian Internal Radiation Exposure.....	82
5.4.1 Civilian Dose .....	82
5.4.2 Cancer Risk.....	83
5.4.3 Genetic Risks.....	84
5.5 External Radiation Effects .....	85
5.5.1 Penetrator External Dose .....	85
5.5.2 Beta Burns and Skin Cancer .....	87
6.0. Validity of Analysis.....	89
6.1 DU Source Terms and Internalized Mass .....	89
6.1.1 In-Vehicle Post-Battle Exposure .....	89
6.1.2 DU Dispersal and Deposition .....	90
6.1.3 Dispersion/Deposition Uncertainty.....	93
6.1.4 Ex-Vehicle Resuspension .....	94
6.2 Biokinetics, Dose, and Risk Coefficients.....	94
6.2.1 Computer Model.....	95
6.2.2 Inhalation Model Data .....	96
6.2.3 Urine Data.....	96
6.2.4 Radiological Risk Coefficients .....	97
6.3 Uncertainty Analysis.....	99
6.4 Comparison with Previous Analyses .....	101
6.4.1 Comparison of Adjusted Predictions .....	101
6.4.2 Summary Comparison of Methods .....	104
6.5 Health Effects Issues .....	106
6.5.1 Birth Defects.....	106
6.5.2 Leukemia .....	108
6.6 Radiological Analysis Validity .....	109
6.6.1 Epidemiological Evidence .....	110
6.6.2 Theory and Research-Based Issues.....	112
6.7 Assessment.....	113
7.0. Conclusions and Recommendations .....	115

7.1 Dispersal/Consequence Methodology.....	115
7.2 Weapons Complex Uranium Guidance.....	115
7.3 DU-Exposed U.S. Veterans.....	116
7.4 DU-Exposed Iraqi Civilians.....	117
References .....	119
Appendix A: Nuclear Basics .....	123
Appendix B: DU Mass Internalized .....	137
Appendix C: DU Biokinetics.....	155
Appendix D: DU Chemical Health Effects .....	169
Appendix E: Radiological Health Effects .....	177
Appendix F: Notation and Glossary .....	191

## Figures

Figure 1. Bradley Fighting Vehicle [6] .....	20
Figure 2. U-235 nuclear fission .....	26
Figure 3. Nuclear decay for U-238.....	27
Figure 4. Specific activity of depleted uranium isotopes as a function of time after processing [1] .....	29
Figure 5. M1A1 tanks [6] .....	31
Figure 6. 120 mm round with DU penetrator [6].....	31
Figure 7. M1A1 with DU armor [6] .....	31
Figure 8. Air Force A-10 aircraft [6].....	31
Figure 9. Principal location of DU munitions use in Iraq and Kuwait [9] .....	32
Figure 10. Possible DU exposure pathways for military personnel .....	33
Figure 11. Possible DU exposure pathways for civilians .....	33
Figure 12. Population densities for regions of Iraq [16].....	39
Figure 13. Geographical zones of Iraq [17].....	40
Figure 14. Geometry assumed for the analysis of DU-puff dispersal following penetrator impact .....	49
Figure 15. Inhaled DU mass and deposited DU areal density vs. x-distance along puff-path centerline (single 120 mm round, single tank, class C conditions).....	50
Figure 16. Assumed geometry for the tank-battle scenario .....	51
Figure 17. Wet deposition $\zeta$ vs. y-distance for 20 targets 20 m apart for a single 120 mm shell impact per target during a tank battle .....	52
Figure 18. Inhaled mass $m$ and deposition $\zeta$ vs. x-distance for 1, 20, and 50 targets ( $D = 20$ m, $y =$ array midpoint, one 120 mm shell per target, wet deposition).....	53
Figure 19. DU mass inhaled and deposited vs. x-distance for the infinite line source model for the very high target density scenario.....	54
Figure 20. Potential human pathways for depleted uranium .....	61
Figure 21. Schematic illustration of overall biokinetic model used in this study.....	63
Figure 22. Percent of inhaled DU in body vs. time after exposure for acute ingestion .....	65
Figure 23. Percent of inhaled DU in major organs vs. time after inhalation for acute ingestion .	66
Figure 24. Time dependence of the percent of DU in the GI tract organs following acute ingestion .....	67
Figure 25. DU mass/g organ vs. time for nominal Level I inhalation for the nominal case.....	68
Figure 26. DU mass/g organ vs. time for Level I inhalation with DU fragments for the nominal case .....	69
Figure 27. DU mass/g of organ vs. time for maximally exposed child at play .....	71

Figure 28. DU mass/g of organ as a function of time for downwind civilian maximum case (puff plus resuspended DU inhalation). .....	71
Figure 29. Grams DU/g kidney as a function of time for Level I veterans for inhalation with and without fragments .....	74
Figure 30. Comparison of lifetime veteran dose from DU exposure with U.S. background dose (50 years) and maximum radiation worker dose (35 Years) .....	78
Figure 31. Lifetime Iraqi civilian effective dose from DU exposure compared to the world-average background dose .....	83
Figure 32. Relative intensity of $\alpha$ , $\beta$ , and $\gamma$ fluxes vs. distance into body .....	86
Figure 33. Whole-body dose rate and incremental fatal cancer risk vs. distance from a DU penetrator (120 mm round) .....	86
Figure 34. Incremental risk of beta-radiation induced skin cancer from direct DU contact.....	87
Figure 35. HPAC prediction of DU deposition for 100 g release in Iraq battlefield for February weather conditions.....	91
Figure 36. Inferred lung cancer relative risk vs. radon concentration for indoor radon and miner radon exposure [42] .....	98
Figure 37. Predicted veteran cancer fatality risk from DU exposure by various studies (data adjusted to make cases comparable).....	102
Figure 38. Lung cancer relative risk for males vs. radon concentration for indoor radon from Cohen study .....	112

## Tables

Table 1. Isotopic compositions for natural uranium, reactor fuel, and depleted uranium; and the half-lives and specific activities for uranium isotopes[7] .....	25
Table 2. Specific activity of several radioactive materials compared to DU .....	27
Table 3. Uranium-238 decay sequence to uranium-234 [8] .....	28
Table 4. U-238 and daughter products Th-234 and Pa-234m radiation characteristics [8].....	29
Table 5. DU munitions used in the 1991 Gulf War [10] .....	32
Table 6. Kidney guidelines for acute uranium intake.....	34
Table 7. ICRP annual radiological exposure guidance (mSv/yr) [15].....	38
Table 8. Method type used to determine internalized DU mass.....	31
Table 9. Methods used to determine internalized DU mass for civilians.....	45
Table 10. Estimated DU aerosol mass released external to vehicle per 120 mm round impact...49	
Table 11. Summary of internalized DU mass for Gulf War veterans .....	59
Table 12. Summary of internalized DU mass for civilians .....	60
Table 13. DU concentrations in kidney for Gulf War veterans and Iraqi civilians .....	74
Table 14. Level I veteran lifetime equivalent doses from DU exposure .....	77
Table 15. Predicted Level I veteran lifetime fatal cancer risks from DU exposure .....	79
Table 16. Predicted incremental fatal cancer risks for veterans from internal DU exposure compared to percentage of all U.S. civilian fatalities from cancer.....	80
Table 17. Incremental risk of serious birth defects for veteran progeny (equilibrium) from DU exposure, compared to U.S. average birth defects / live birth .....	82
Table 18. Lifetime equivalent internal radiation doses for civilians from DU exposure .....	83
Table 19. Iraqi civilian lifetime fatal cancer risks from DU exposure compared to percentage of all U.S. civilian fatalities from cancer .....	84
Table 20. Incremental risk of serious birth defects for civilian progeny (equilibrium) from DU exposure compared to U.S. average birth defects / live birth .....	84
Table 21. Analysis uncertainties for risk multipliers for veterans.....	100
Table 22. Analysis uncertainties for risk multipliers for civilians.....	101

# Executive Summary

The National Security Studies Department at Sandia National Laboratories (SNL) investigates potential terrorist threats and other challenges to U.S. national security. The department also provides independent assessments on topics associated with the nuclear weapons complex. A study of uranium dispersal, exposure, and possible health effects resulting from depleted uranium (DU) munitions use provides a means for assessing our ability to predict the consequences of terrorist use of a radiological dispersal device. In addition, the issue of possible DU health effects is of interest to the department because uranium handling is an integral aspect of the nuclear weapons infrastructure. Given these considerations, an investigation was initiated using DU exposure during the 1991 Gulf War as a case study.

The United States and Great Britain now make extensive use of DU metal in armor-piercing military rounds. DU is a byproduct of the uranium enrichment process and is equivalent to natural uranium with the percentage of uranium-235 (U-235) reduced from 0.72% (for natural uranium) to about 0.2%. Uranium-238 constitutes about 99.8% of the uranium isotopes in a DU penetrator shell. Weapons developers selected DU because of its high density, self-sharpening capability, pyrophoric characteristics, and low cost. However, uranium particulate generated by shell impact with military vehicles may be inhaled or ingested by troops and nearby civilians. During the 1991 Gulf War, some veterans in vehicles accidentally hit by U.S. DU penetrators were wounded by DU fragments, some of which remained embedded in their bodies. Because DU is chemically toxic and weakly radioactive, a number of critics have asserted that wartime use of DU weapons may have resulted in a variety of unintended health consequences. Some critics claim that significant increases in leukemia have been observed in individuals exposed to DU and that increases in the rate of birth defects have been observed in their progeny. These claims are refuted by the U.S. Department of Defense (DoD) as well as a number of independent investigators.

## **Scope**

This study addressed possible health effects from DU exposure for both veterans and Iraqi civilians. Three levels of veteran DU exposure were defined by the DoD. Level I includes veterans occupying vehicles that were accidentally targeted by U.S. tanks. These veterans generally sustained the highest DU inhalation exposures and some retained embedded DU fragments. Level I also includes veterans involved in the rescue of the occupants of targeted vehicles. Level II veterans were involved in post-battle activities associated with DU-damaged vehicles, and Level III includes veterans who experienced brief low-level exposure to DU particulate during or following battle. This study (referred to as the SNL study) investigated possible DU health effects for all three levels of veteran exposure. This investigation also included possible DU health effects on Iraqi civilians. The principal DU exposure scenarios for civilians include civilians downwind of battlefields where DU munitions were used and children playing in or near DU-damaged vehicles. The study also included a comparison of predicted health effects with veteran medical records, epidemiological data, research findings, and health-effect predictions by previous investigators in the United States and Great Britain.

## **Methodology**

The first stage of the analysis provided estimates of the quantities of DU dispersed into the environment and deposited within targeted vehicles. This stage also included estimates of DU intake by inhalation, ingestion, and embedded fragments. For Level I veterans, DU intake by inhalation and fragments was estimated using biokinetic models and measured DU concentrations in the urine of exposed veterans. For veterans working inside a DU-contaminated vehicle, the quantity of DU inhaled was determined from resuspension test data. Resuspension test data were also used to estimate the inhaled DU mass for Iraqi children playing in a DU-contaminated vehicle. Standard models were employed to provide estimates of DU ingestion by hand-to-mouth transfer.

For downwind veterans and civilians, the inhaled mass of DU was determined by using an estimate of the quantity of DU released per shell impact and a Gaussian wind-distribution and deposition model. The model also accounted for the effects on the DU

source distribution resulting from many closely spaced target vehicles. A standard resuspension model provided an estimate for post-battle inhalation of DU deposited external to target vehicles. The low solubility of uranium and uranium oxides and the findings from post-battle monitoring of both the environment and civilian populations suggest that DU intake by ingesting DU-contaminated food and water is negligible.

Standard biokinetics models were implemented to estimate DU deposition within the respiratory system, transport within the respiratory system, blood absorption, redistribution to organs, and elimination in the urine and feces. The rate of blood dissolution for inhaled DU was obtained from extensive test data. Using a straightforward modification of a standard model for blood distribution of uranium, a model was developed for the distribution and organ deposition of dissolved DU from embedded fragments. Standard biokinetic models were also used to analyze the passage of DU through the gastrointestinal (GI) tract following accidental ingestion of DU particulate. Organ radiation doses and health risks were computed based on established calculational methods. The potential for heavy metal kidney damage was assessed using uranium concentration/effect correlations and the calculated time-dependent DU concentrations for the kidney. The health-effect predictions from this study were then compared to veteran medical statistics and the health-effect predictions by previous investigators.

## **Findings for Veterans**

A summary of the radiological risk for veterans is provided in Table ES-1 for internalized DU. The national average in the last column is the U.S. national average for cancer fatalities and the risk of birth defects per live birth. Table ES-1 shows that only a few Level I veterans inhaled sufficient quantities of DU to incur about a 1% risk of radiation-induced lung cancer. (This is the incremental risk, that is, in addition to the risk for someone not exposed to DU.) For comparison, about 7% of all U.S. civilian fatalities result from lung cancer. Because lung cancer is the dominant DU radiological risk, the total radiation-induced cancer risk for these maximally exposed veterans is also about 1%. For perspective, the U.S. national average for all cancer fatalities makes up about 24% of civilian fatalities. Ingested DU did not have a significant impact on the radiological or chemical dose for veterans. Embedded fragments were found to have a

significant effect on some projected cancer risks and genetic risks; however, even when DU fragment contributions are included for the maximum exposure case, the risk of radiation-induced leukemia is only about 0.03%, and the risk of radiation-induced genetic birth defects is also about 0.03%. The predicted risks for most Level I veterans and the risks for other exposed veterans are one-to-several orders of magnitude smaller than those predicted for the maximally exposed Level I veterans. These analysis results are consistent with medical statistics for Gulf War veterans.

**Table ES-1. Veteran lifetime incremental fatal cancer risk and genetic risk from internal DU exposure compared to U.S. average risks\*\***

Health Issue		Level I		Level II		Level III		U.S.* Avg. (%)
		Nom. (%)	Max (%)	Nom. (%)	Max (%)	Nom. (%)	Max (%)	
<b>Lung Cancer</b>		0.085	1.40	0.014	0.210	<0.0001	0.002	7
<b>Leukemia</b>	<i>Inhaled**</i>	0.0004	0.007	0.001	0.001	<0.0001	<0.0001	1
	+ Fragments	0.005	0.03					
<b>Total Fatal Cancer Risk</b>		0.099	1.43	0.014	0.210	<0.0001	0.002	24
<b>Genetic Risk</b>	<i>Inhaled**</i>	0.0004	0.007	<0.0001	0.001	<0.0001	<0.0001	~ 8
	+ Fragments	0.0040	0.028					
<b>Number of Veterans</b>		~150	few	~700	few	Hundreds		

- \* U.S. Avg. = % of all U.S. fatalities or % of live births resulting in birth defects
- \*\* Inhaled = inhalation of DU only; + Fragments = DU inhalation plus embedded DU fragments
- \*\*\* Risks apply to large populations; e.g., if a large population received the maximum Level I radiation dose, 1.43% of that population are predicted to incur a radiation-induced cancer

This study also examined other potential health effects including the effect of the radiological dose at the site of embedded fragments and possible chemically induced health effects. For Level I veterans, the alpha particle dose at the site of embedded fragments is very high. Although some aggressive animal tests indicate that soft-tissue sarcomas are possible at the periphery of imbedded fragments, none have been reported for Level I veterans. For a few maximally exposed Level I veterans, the predicted initial DU kidney concentrations suggest that these veterans may have experienced chemically induced transient kidney damage. Observations from animal testing and veteran monitoring also suggest that neurotoxic and other health effects may result from the

chemical toxicity of DU. Currently, neurotoxic effects cannot be ruled out; however, major neurotoxic effects appear to be unlikely. Evidence for other possible health effects is not well established.

### Findings for Civilians

A summary of the radiological risk from internalized DU for civilians is given in Table ES-2. Risks are compared to the U.S. average because reliable statistics were not found for Iraqi civilians. A nominally exposed child playing in DU-destroyed vehicles for 300 hours and playing outside the vehicle for 700 hours is predicted to incur a nominal radiation-induced lung cancer risk of about 0.04%. The predicted risk of radiation-induced leukemia and colon cancer, for this nominally exposed child, is about 0.0004% and 0.06%, respectively. Thus, the net radiation-induced fatal cancer risk for the nominally exposed child is about 0.1%. The net fatal cancer risk for the maximally exposed child is about 0.3%. Calculations indicate that the DU-related health risks to downwind civilians (including genetic effects) are extremely small (<0.0001%). Furthermore, genetic effects from DU exposure are predicted to be extremely small for civilians.

**Table ES-2. Civilian lifetime incremental fatal cancer and genetic risks from internal DU exposure compared to U.S. average risks**

Health Issue	Child at Play		Downwind		U.S. Avg. (%)
	Nom. (%)	Max (%)	Nom. (%)	Max (%)	
Lung cancer	0.0350	0.140	<0.0001	<0.0001	7
Leukemia	0.0004	0.002	<0.0001	<0.0001	1
Colon Cancer	0.0550	0.160	—	—	3
<b>Total Fatal Cancer Risk</b>	0.092	0.313	<0.0001	<0.0001	24
<b>Genetic Risk</b>	0.0001	0.0004	<0.0001	<0.0001	~ 8

Because of the low specific activity of DU and the small fraction of 1-MeV gamma rays emitted per U-238 decay, the external radiation dose from gamma ray emission should be very low for any realistic scenario. Nonetheless, radiation exposure

from external DU sources (shells, shell fragments, and ground-deposited particulate) was also examined. No beta burns from handling DU are predicted, and the radiological risk from gamma radiation from DU shells was predicted to be very small. The only potential hazard identified for external radiation sources was the possibility of a localized skin cancer if DU metal was held close to the skin in the same location for many years (e.g., DU metal fabricated into earrings).

## **Analysis Validity**

Before drawing conclusions based on findings, the uncertainties and limitations of the analysis methodology must be clearly understood. An uncertainty analysis and a comparison to the predictions from previous studies and veteran medical statistics demonstrated the basic validity of the methodology. A review in this study also found that veteran medical statistics do not support assertions of significant increases in cancers for DU-exposed veterans and that the statistics do not support assertions of significant increase in birth defects for their progeny. Furthermore, the analysis indicates that no significant health risks are posed by normal handling and processing of uranium within the weapons complex, if standard safety guidelines are followed.

## **Conclusions**

- The basic methodology used for this study was determined to be generally valid. The study findings can be used as a benchmark and a guide for evaluating the validity of future radioisotope studies.
- No significant radiological health risks are posed by normal handling and processing of uranium within the weapons complex, if standard safety guidelines are followed.
- Clinical health effects should not result from the chemical toxicity (heavy metal) effect of uranium, if the implicit limit of 3  $\mu\text{g U/g}$  kidney is not exceeded. Although an exposed individual is unlikely to become ill at this maximum permitted kidney burden, transient indicators of renal dysfunction are possible.
- Claims of significant increases in cancers for DU-exposed veterans and significant increases in birth defects for their progeny are not supported by the study findings.

- Only a few veterans are predicted to incur about a 1% lung cancer risk from DU exposure. Also, these veterans may have experienced transient kidney damage.
- Health risks for most DU-exposed veterans are predicted to be very small.
- Soft tissue sarcomas at the location of embedded fragments and chemically induced neurotoxic effects cannot be ruled out; however, major neurotoxic effects are unlikely.
- The highest health risk for civilians was for children playing in DU-contaminated vehicles. The nominal radiation-induced fatal cancer risk for these children was 0.1%.
- Health risks for Iraqi civilians are predicted to be very small, and claims of observable increases in leukemia and birth defects from DU exposure are not supported by this study.
- External radiation doses from DU are generally very small.

### **Recommendations**

- Weapons complex guidelines for chemical toxicity from uranium exposure should be reexamined to determine if they are consistent with recent findings and basic protection standards.
- Screening and treatment should be provided for Level I DU-exposed veterans.
- Monitoring should be continued for veterans who received significant inhalation doses or retain embedded DU fragments.
- Military personnel should be instructed to take reasonable actions when in vehicles hit by DU penetrators (e.g., using the vehicle ventilation system or exiting quickly).
- Children should be discouraged from playing in abandoned military vehicles.
- Basic research on possible chemically induced DU health effects should be continued.
- Post-battle monitoring of the environment and nearby civilians is recommended.

## ACRONYMS

AI	Alveolar-Interstitial
ALL	Acute Lymphoid Leukemia
AMAD	Activity Mean Aerodynamic Diameter
Bb	Bronchiolar
BB	Bronchial
BFV	Bradley Fighting Vehicle
DNA	Deoxyribonucleic Acid
DoD	Department of Defense
DOE	Department of Energy
DU	Depleted Uranium
EPA	Environmental Protection Agency
ET	Extrathoracic
GI	Gastro Intestinal
HPAC	Hazard Prediction and Assessment Capability
ICRP	International Commission on Radiological Protection
KAPL	Knolls Atomic Power Laboratory
LD/50	Lethal Dose to 50% of population receiving dose
LET	Linear Energy Transfer
LI	Large Intestine
LN	Lymph Node
LNT	Linear Nonthreshold
LWR	Light Water-Cooled Reactor
MCNP	Monte Carlo Neutron and Photon Transport
NCRP	National Council on Radiological Protection
OSHA	Occupational Safety and Health Administration
PEL	Permissible Exposure Levels
PNNL	Pacific Northwest National Laboratory
RBE	Relative Biological Effectiveness
RS	Royal Society
seq	Sequestered
SI	Small Intestines
SNL	Sandia National Laboratories
Th	Thoracic
UNEP	United Nations Environmental Program
U.S.	United States
VA	Veterans Administration
WHO	World Health Organization

## **1.0. Basis, Scope, and Approach**

The use of depleted uranium (DU) is relatively new in warfare. The first reported combat use of DU munitions was in the Gulf War in January 1991, in which American and British tanks and aircraft used DU as an armor-piercing penetrator. The United States and Great Britain now make extensive use of DU metal in armor-piercing military rounds because of its high density, self-sharpening capability, pyrophoric characteristics, and low cost. All these properties make DU an outstanding choice for armor-piercing munitions. However, DU is chemically toxic and weakly radioactive. Furthermore, DU aerosols generated during impact can be inhaled or ingested by nearby military personnel or civilian populations, and concerns have been raised that the use of DU munitions may have resulted in serious health effects from DU exposure for both military forces and nearby civilian populations. Among the many allegations are claims of very high incidences of leukemia and birth defects. The U.S. Department of Defense and the World Health Organization [1] dispute these claims.

### **1.1 Basis for Study**

Several scientific studies have been carried out to assess the health risks associated with the use of DU munitions. The first study was initiated by the U.S. Department of Defense (DoD) in the late 1990s and distributed in 2000 [2] (updated in 2003). In 1999, Fetter and von Hippel published the findings from their independent analysis of DU health risks [3]. The British Royal Society carried out a fairly comprehensive study on DU munitions health effects and published its report in 2002 [4]. Pacific Northwest National Laboratory (PNNL) performed extensive DU weapons testing for the DoD Capstone Program to characterize the particulate generated during DU impact with armored vehicles [5]. These data were used to predict possible veteran health effects. The conclusions of these studies clearly did not support assertions of significant and observable increases in cancers as a result of exposure to DU munitions. Based on the continued concern with DU munitions from activist groups and media coverage;

however, these findings appear to have had little effect on widespread concerns over the use of DU munitions.

These four studies were major undertakings that greatly improved understanding of the health effects of DU munitions; however, some topics were not addressed by these studies. The topics not addressed by these studies include (1) the quantitative contribution to organ dose from dissolution of embedded DU fragments, (2) potential health risks for a child playing in a DU-contaminated vehicle, or (3) the risk of birth defects from DU exposure. Furthermore, the most recent data from the Capstone Program were not available for the first three studies, and only Fetter and von Hippel and the Royal Society addressed civilian health effects. An independent study that addresses the limitations of previous studies may provide additional insights, particularly if the reported findings are supplemented by clarifications for the nonscientists.

Although a study that addressed all major topics for DU munitions health effects would be beneficial to scientists, decision makers, and the general public, the decision to undertake a new study in the National Security Studies Department at Sandia National Laboratories was based primarily on department objectives. The National Security Studies Department investigates potential terrorist threats and other challenges to national security. A study of DU exposure and health effects provides a means for assessing our ability to predict the consequences of possible terrorist use of a radiological dispersal device. The department also provides independent assessments on topics associated with the nuclear weapons complex. The issue of possible DU health effects is of interest to the department because uranium handling is an integral aspect of the nuclear weapons infrastructure. Although worker health statistics are available, worker medical statistics have not been quantitatively correlated with uranium exposure (i.e., individual worker exposures were not quantified).

Given these considerations, a study was initiated that compared predictions with observations for a specific case of DU exposure (i.e., the 1991 Gulf War). This study examined possible health effects of DU on U.S. veterans and on Iraqi civilians exposed to DU during and following the war. The 1991 Gulf War was selected as the study focus because (1) DU use was extensive, (2) exposures were significant for some individuals,

(3) medical tests have been carried out for highly exposed veterans, (4) sufficient time has passed to assess some long-term consequences of exposure, (5) exposures include both veterans and civilians, and (6) many issues have been raised specifically about the use of DU during the Gulf War.

## **1.2 Scope and Study Approach**

This study evaluated possible health effects for veterans and Iraqi civilians who were exposed to DU during and after the 1991 Gulf War. Both radiological and chemical health effects were assessed using best estimates of health risks for both nominally and maximally exposed individuals. In this report, a nominally exposed individual refers to the average individual within the group under study. A maximally exposed individual typically refers to an individual in a location where DU concentrations were highest. In addition to “best estimates” of health effects, an uncertainty analysis was used to estimate upper-bound health effects for both nominally and maximally exposed veterans and civilians.

This investigation was not intended to provide a comprehensive assessment of Gulf War DU exposure; nonetheless, the study evaluated the principal exposure scenarios as well as situations that were likely to result in the highest exposures. Greater emphasis was placed on topics that had not been explored in detail in previous studies, such as quantitative health effects from DU-fragment dissolution, health effects from DU exposure for children playing in contaminated vehicles, the effect of multiple target vehicles, and quantitative estimates of the risk of birth defects.

### **1.2.1 Veterans Studied**

The U.S. DoD defines three levels of DU exposure for Gulf War veterans. Level I exposures correspond to friendly fire incidents in which U.S. tanks mistakenly fired DU rounds at other U.S. combat vehicles. Vehicles hit by friendly fire include six occupied U.S. tanks and fourteen Bradley Fighting Vehicles (BFVs; Figure 1). The crews of the targeted vehicles were exposed to aerosolized DU particulate, and some of the crew were wounded by DU fragments. In addition, U.S. troops involved in rescue operations were exposed to potentially high concentrations of aerosolized DU. The DoD has identified

104 surviving U.S. crewmembers of vehicles hit by DU penetrators and 30 to 60 soldiers entering the vehicles to rescue crewmembers immediately following impact. Both the crew and their rescuers are classified in the category of Level I exposures.

The Level II category includes veterans involved in post-combat evaluation of DU-damaged vehicles, removal of equipment, and preparation of vehicles for transport. Level III exposures correspond to short-term, low-level exposures during and following battle. This study examined possible DU health effects for all three levels of veteran exposure and included exposures by inhalation, ingestion, and embedded fragments. Level I veterans were believed to have experienced the most significant exposure to DU, and Level III veterans were expected to have experienced the lowest exposure levels.



**Figure 1. Bradley Fighting Vehicle [6]**

### **1.2.2 Iraqi Civilians Studied**

The types of civilian internal exposures considered in this study include inhalation, direct ingestion (hand-to-mouth transfer), and consumption of food and water contaminated by DU particulate. DU exposure was examined for Iraqi civilians living downwind of the battle zone. However, children playing in DU-contaminated soil and within DU-contaminated vehicles are expected to experience greater DU exposure than downwind populations. As a consequence, this study also addressed health risks to children playing in post-battle zones. Although adults probably explored destroyed

vehicles as well, children are more likely to explore or play in vehicles for extended periods of time. Furthermore, children can exhibit very high hand-to-mouth activity that could result in significant DU ingestion. External radiation effects were also examined for gamma and beta radiation emitted from DU shells, fragments, and particulate.

### **1.2.3 DU Sources Studied**

DU sources included impact-generated particulate and embedded fragments. The inhalation of impact-generated DU particulate suspended in air was assessed for occupants of target vehicles as well as for individuals downwind of the “puff” of DU aerosols released into the environment. The study also included an analysis of the inhaled DU mass from resuspension of deposited DU particulate. For this study, the analysis of inhaled DU focused on impact-generated DU particulate. Although munitions fires also produce DU aerosols, other investigators who studied DU munitions fires [2, 3, 4] concluded that very little DU is converted into respirable aerosols (<0.025%). Even for the enormous Camp Doha fire with 660 damaged rounds, the total quantity of respirable DU released by the fire was less than 1 kg [3]. Furthermore, the principal munitions fire occurred at Camp Doha in Kuwait and did not affect Iraqi civilians. Given these considerations, munitions fires were not investigated in this study.

### **1.2.4 General Approach**

The general approach for this study was to use relatively simple, approximate methods rather than established computer codes. This approach provided a transparent methodology and information specific to the topic of DU exposure from munitions use. Nonetheless, sufficient computational detail was retained to provide reasonable predictive accuracy. When approximations were used, the general trend was to overestimate health risks. Inaccuracies implicit in these approximate methods are judged to be much less than the inaccuracies associated with the uncertainty in the available data used in this analysis.

## 1.3 Report Organization

This document presents the basic methodology, essential data and information, and the principal findings from the study. Section 2 provides general background material to facilitate understanding of the analysis approach, findings, and conclusions from the study.

To assess health effects from DU internalization, it is necessary to estimate the quantity of DU internalized by inhalation, ingestion, and embedded fragments. The quantity inhaled or ingested will depend on the quantity of DU aerosolized during impact and the air concentrations of DU transported by wind external to the vehicle. Furthermore, the amount of DU particulate inhaled after hostilities have ended will depend on the concentration of deposited DU and the concentration in air of DU particulate that has been resuspended by wind or human activity. These considerations are addressed in Section 3.

To assess health effects from DU internalization, it is also necessary to determine how internalized DU is distributed among the various organs of the body and the time-dependence of DU in each organ. These considerations are addressed in Section 4. Using the predicted time-dependent DU organ concentrations, the chemical and radiological health effects can be estimated for DU internalization. Section 5 presents the results of an analysis of both chemical and radiological health risks for veterans and civilians. These risks are compared to typical frequencies for health effects and fatalities for individuals not exposed to DU. Section 5 also discusses the effects of external exposure to DU radiation. One of the principal objectives of this study was to assess the validity of methods used to predict radioisotope dispersion, exposure, and health consequences. Section 6 presents an evaluation of the validity and uncertainty of the analyses. Furthermore, Section 6 compares predictions from this study with veteran health effect predictions from previous studies. The principal issues raised by DU critics are also addressed in Section 6. Finally, Section 7 presents the conclusions and recommendations from the study.

This document is intended to be accessible to scientists and engineers who are not experts in the field. Although the general reader may not have the appropriate background to follow some of the analysis details (particularly the mathematics), the basic findings from this study should be accessible to the nonscientist. Explanatory material has been included for the nonscientist to provide perspective and to assist understanding. Details on methodology, additional background, and other information are provided in appendices. Appendix A is a brief overview of basic nuclear concepts. Appendices B and C discuss the analyses used, respectively, to estimate internalized DU mass and to estimate the time-dependent DU concentrations in the organs of the body. The issue of chemical health effects from DU internalization is explored in Appendix D. The method used to predict radiological health effects is detailed in Appendix E. The discussion of the notation and the glossary in Appendix F should be useful to the nonscientist or nonspecialist.



## 2.0. Background

This section provides general background material to facilitate understanding of the analysis approach, findings, and conclusions from this study. Topics include DU nuclear characteristics, military use of DU, exposure pathways, possible chemical and radiological health effects, and the Iraqi environment.

### 2.1 DU Nuclear Characteristics

The chemical and physical properties of DU are essentially identical to those for natural uranium. Uranium is a naturally occurring heavy metal found in a variety of chemical forms in soil, rock, and water. Naturally occurring isotopes of uranium are weakly radioactive. Table 1 presents a summary of the abundance of naturally occurring uranium isotopes, their half-lives, and their specific activity. DU is almost entirely uranium-238 (U-238) and is obtained as a byproduct of the uranium enrichment process that is used to increase the fraction of the isotope uranium-235 (U-235) for use in nuclear reactors or weapons. The term *depleted uranium* refers to the remaining uranium that is consequently depleted in the isotope U-235. Table 1 also provides a typical isotopic composition for depleted uranium and a typical isotopic composition for light water-cooled reactor (LWR) fuel. DU is about 99.8% U-238. Uranium-236 is present in U.S. enriched and depleted uranium as a result of previous contamination of the enrichment system when spent reactor fuel was once used in the enrichment process. Trace quantities of other actinides are also found in DU.

**Table 1. Isotopic compositions for natural uranium, reactor fuel, and depleted uranium; and the half-lives and specific activities for uranium isotopes [7]**

Uranium Isotope	Natural Abundance (%)	Typical LWR Fuel (%)	Depleted Uranium (%)	Half-life (yr)	Specific Activity (Ci/g)
U-234	0.0054	0.093	0.0009	$2.46 \times 10^5$	$6.24 \times 10^{-3}$
U-235	0.72	3.82	0.20	$7.04 \times 10^8$	$2.16 \times 10^{-6}$
U-236	0.0	1.6	0.0003	$2.34 \times 10^7$	$6.49 \times 10^{-5}$
U-238	99.27	94.49	99.79	$4.47 \times 10^9$	$3.35 \times 10^{-7}$

### 2.1.1 DU Radioactivity

Although uranium is described as weakly radioactive, many people have the mistaken impression that uranium (including DU) is highly radioactive, possibly because of the association of uranium with operating reactors or detonated nuclear weapons. Nuclear reactors and weapons both provide enormous energy as a result of a chain reaction of nuclear fission events. Nuclear fission (the splitting of the atomic nucleus) occurs when the nucleus of certain isotopes (such as U-235) is struck by a neutron introduced into the nuclear fuel by a neutron source. The basic process is illustrated schematically in Figure 2.

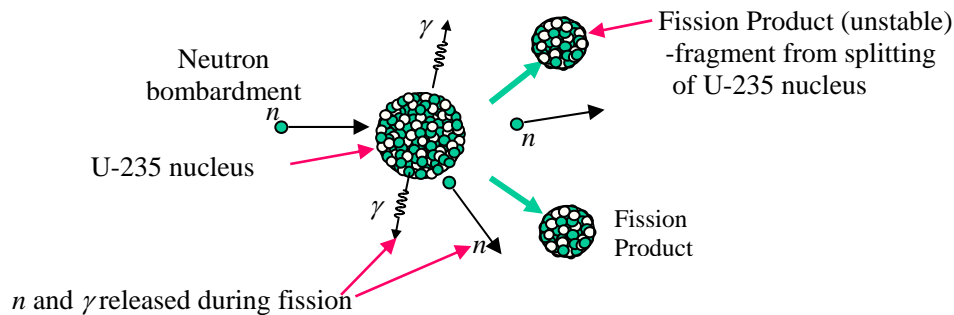


**Figure 2. U-235 nuclear fission**

Energy is released from the nucleus during fission along with two or three neutrons ( $n$ ) and several gamma rays ( $\gamma$ ). (Gamma rays are high-energy electromagnetic radiation.) For each absorbed neutron, the two or three released neutrons can then be absorbed by other nuclei, causing two or more fission events. As a consequence, a chain reaction is initiated, and the number of nuclear fission events can multiply rapidly. Intense radiation is emitted during fission, and the fission product nuclei produced by the splitting of the original nucleus are highly radioactive. These highly radioactive fission products are the principal radiation hazard associated with postulated reactor accidents.

In contrast, radiation emitted by DU results from the slow, natural decay of uranium-238 rather than from the highly radioactive fission products produced by nuclear fission. For radioactive decay of uranium-238, an alpha particle is emitted from the nucleus (Figure 3). An alpha particle is a cluster of two neutrons and two protons; consequently, U-238 loses two neutrons and two protons and is transmuted into the

daughter product thorium-234 (Th-234). The half-life of U-238 is about 4.5 billion years (refer to Appendix A or the Glossary in Appendix F for a discussion of half-life). Because the half-life for U-238 is very long, the specific activity of DU (in curies [Ci] per gram of U-238) is extremely low compared to that of most other radioisotopes (as discussed in Appendix A). Of about 5,000 identified radioisotopes, only 16 are less radioactive than U-238. Table 2 compares the specific activity of U-238 with the specific activities of a few selected radioisotopes.

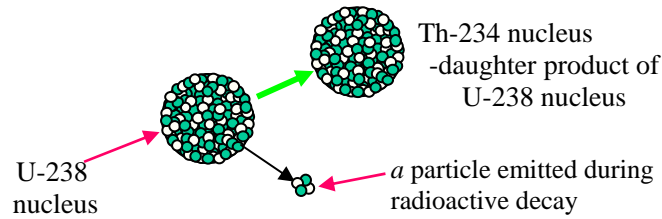


**Figure 3. Nuclear decay for U-238**

**Table 2. Specific activity of several radioactive materials compared to DU**

Isotope	Ci/g	Relative* Specific Activity
U-238 (DU)	$\sim 10^{-6}$	1.0
I-131	$1.24 \times 10^5$	$\sim 10^{11}$
Pu-239	$6.2 \times 10^{-2}$	$\sim 10^5$
Mo-99	$4.8 \times 10^5$	$\sim 10^{11}$
Br-89	$7.3 \times 10^{10}$	$\sim 10^{15}$

\*Relative to the specific activity of DU (U-238 with U-234, Pa-234m, and Th-234)

### 2.1.2 DU Decay Properties

The decay properties for U-238 and the first few decay products are presented in Table 3. Thorium-234, produced by U-238 decay, emits a beta particle (electron) from its nucleus and decays to metastable protactinium-234m (Pa-234m). Protactinium-234m also beta decays and transmutes into U-234. Because the half-lives of Th-234 and Pa-234m are much shorter than those of U-238 and U-234, the decay products Th-234 and Pa-234m achieve secular equilibrium with U-238 over a period of months, as shown in Figure 4. Figure 4 shows the specific activity of DU (activity per gram of DU) as a

function of time following isotope separation. Subsequent isotopes in the series make very little contribution to the activity of DU.

**Table 3. Uranium-238 decay sequence to uranium-234 [8]**

<b>Isotope</b>	<b>Half-life</b>	<b>Decay Mode</b>
<b>U-238</b>	4.47 x 10 <sup>9</sup> years	$\alpha$
Th-234	24 days	$\beta$
Pa-234m	1.17 minutes	$\beta$
<b>U-234</b>	2.4 x 10 <sup>5</sup> years	$\alpha$

Although the 4.2 MeV alpha particle from U-238 is the most significant contribution to internal radiation dose, other isotopes and other forms of radiation also contribute to dose from DU. The alpha decay of U-234 originally present in DU (along with small contributions from U-235 and U-236) makes up about 17% of the activity of the uranium isotopes in DU. Table 4 provides a more detailed summary of the decay characteristics of U-238 and the daughter products Th-234 and Pa-234m. From these tables observe that other potentially significant radiations include one beta particle (electron) emission from the Pa-234m nucleus (2.3 MeV maximum, ~0.82 MeV average). In addition, Pa-234m will emit approximately one 1 MeV gamma-ray for every sixty U-238 disintegrations. For internalized DU, the relatively low-energy 0.09 MeV gamma emission by Th-234 occurs fairly frequently (268 gammas per 1000 U-238 decays) and will make a small contribution to the dose from internalized DU. However, the dose contribution is very small for low-energy gamma rays originating outside the body (e.g., from nearby penetrator round) because very few low-energy gammas will escape the source and penetrate the body.

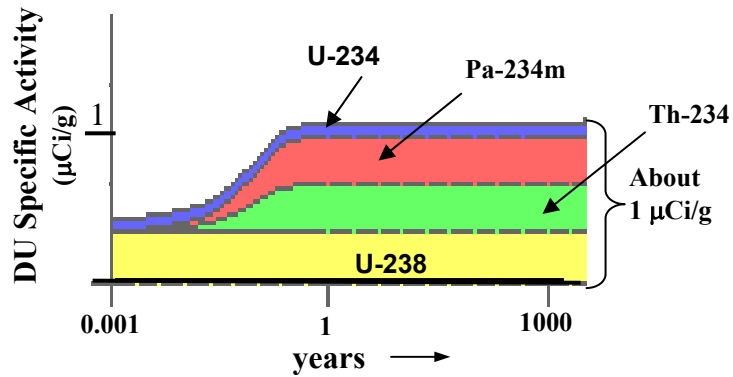


Figure 4. Specific activity of depleted uranium isotopes as a function of time after processing [1]

Table 4. U-238 and daughter products Th-234 and Pa-234m radiation characteristics [8]

Nuclide	Decay Probability (%)	Type	$\alpha$ Energy (MeV)	$\beta$ Energy (MeV) Max / Average	$\gamma$ Energy (MeV)
U-238	79	$\alpha$	<b>4.20</b>	–	–
	20.9	$\alpha, \gamma$	<b>4.15</b>	–	0.05
	0.078	$\alpha, \gamma$	4.04	–	0.11
	0.00005	Fission	–	–	–
Th-234	70.3	$\beta, \gamma$	–	0.20 / 0.05	0.18 (2%)*
	26.8	$\beta, \gamma$	–	0.10 / 0.03	0.09
	0.02	$\beta, \gamma$	–	0.09 / 0.02	0.10
	2.9	$\beta, \gamma$	–	0.08 / 0.02	0.11
Pa-234m	98.20	$\beta$	–	<b>2.29 / 0.82</b>	–
	0.69	$\beta, \gamma$	–	1.49 / 0.50	<b>0.80</b>
	1.01	$\beta, \gamma$	–	1.25 / 0.40	<b>1.04</b>

\* For this decay mode, only 2% of the decays will result in gamma emissions. Thus, the probability for these gamma emissions is 70.3% x 0.02 = 1.4%.

## 2.2 Military Use of DU

Until fairly recently, tungsten alloys were used by the U.S. military as armor-piercing penetrators. However, DU has now become the U.S. material of choice for armor-piercing military rounds and is also being used for armor in military vehicles. For hyper-velocity-penetrator impact ( $\sim 2$  km/s), the penetration depth depends primarily on the length of the penetrator and the relative densities of the penetrator and target [7]. As a consequence, the high density of uranium ( $18.9 \text{ g/cm}^3$ , nearly twice the density of lead) provides a significant advantage both as a penetrator and as armor. The second advantage of DU relates to its self-sharpening characteristics. *Self-sharpening* refers to the continual shearing away of the mushrooming penetrator end formed by impact. Without this shearing-away process, the penetrator tip will blunt and penetration will be inhibited. In addition, because of the pyrophoric nature of DU, impact-generated particulate ignites explosively on impact with an enemy vehicle. The resultant fire and explosive energy can kill or disable the crew and ignite munitions within the vehicle.

### 2.2.1 DU Weapons Used

During the 1991 Gulf War, U.S. M1A1 tanks (Figure 5) used 120 mm DU cannon rounds (Figure 6). The British Challenger tank also used 120 mm DU rounds. U.S. Army M1 tanks and marine M60 tanks employed 105 mm DU rounds. The turret of the M1A1 heavy armor variant of the M1A1 tank is fitted with DU armor, as shown in Figure 7. The most extensive use of DU weapons was by the U.S. Air Force A-10 aircraft (Figure 8). The A-10s fired 30 mm DU rounds from their GAU-8 Gatling guns. Thirty mm DU rounds were used to a limited extent with A-16 aircraft (modified F-16s). The marine AV-8B Harrier jets employed 25 mm DU rounds with their GAU-12 Gatling guns [6]. The DU mass for 120 mm and 30 mm shells are about 4700 g (about 10 pounds) and 280 g (about 0.6 pound), respectively.



Figure 5. M1A1 tanks [6]

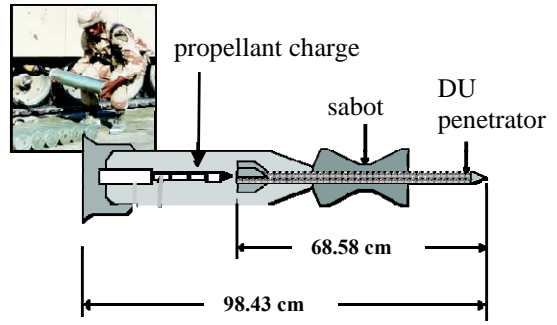


Figure 6. 120 mm round with DU penetrator [6]

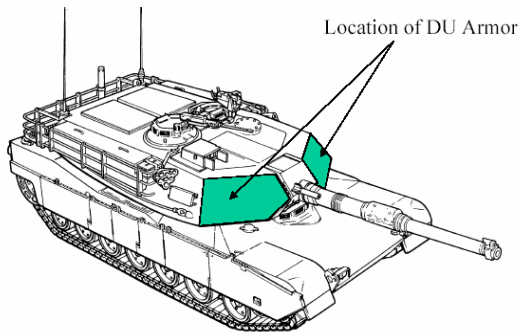


Figure 7. M1A1 with DU armor [6]



Figure 8. Air Force A-10 aircraft [6]

## 2.2.2 Quantity and Locations of DU Weapons Use

The principal battle locations involving DU munitions are presented in Figure 9, and a summary of DU munitions usage in the 1991 Gulf War is presented in Table 5. A total of about 286,000 kg (629,000 pounds or about 315 tons) of DU were used during the Gulf War. Although most of the DU munitions were 30 mm rounds fired from A-10 aircraft, only about 10% of the A-10 DU rounds struck their targets [6]. Furthermore, the DU mass in a 30 mm round is only about 6% of the mass of a 120 mm tank round.

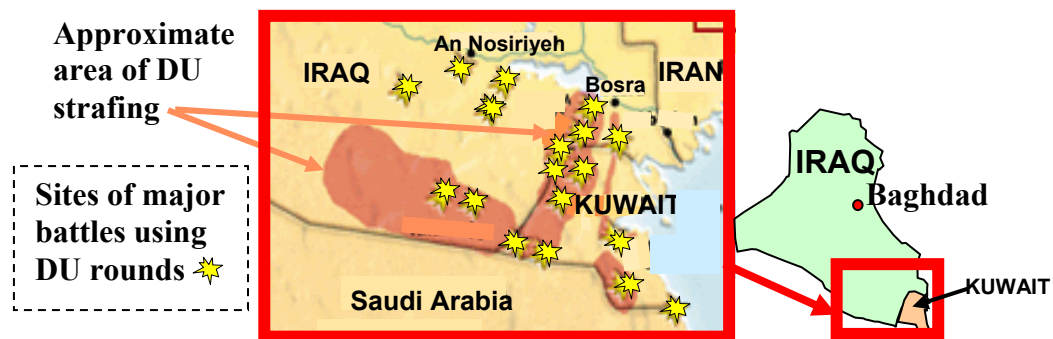


Figure 9. Principal location of DU munitions use in Iraq and Kuwait [9]

Table 5. DU munitions used in the 1991 Gulf War [10]

Branch	Weapon Platform	Ammo Size	Rounds	DU Mass (kg)
U.S. Army	M1 tank	105 mm	504	1,930
	M1A1 tank	120 mm	9,048	37,293
USAF	A-10 aircraft	30 mm	782,514	236,319
	A-16 aircraft	30 mm	1,000	302
U.S. Marine Corps	AV-8B aircraft*	25 mm	67,436	9,881
	M60A3, M1A1	105, 120 mm	?	?
UK Army	Challenger tank	120 mm	88	408
<b>Totals :</b>		<b>Tanks</b>	9,640	39,631
		<b>Aircraft</b>	850,950	246,602
		<b>All</b>	860,590	286,233

\*Harrier jet

## 2.3 Exposure Pathways

Possible DU exposure pathways are illustrated schematically in Figures 10 and 11 for military and civilian populations, respectively. Radiological exposure to DU used in warfare can result from external exposure to radiation emitted from intact munitions or munitions fragments. However, DU particulate generated by hard-target impact can be inhaled or ingested, resulting in more significant exposure than from external DU radiation. Veteran exposures differ from civilian exposures in that some of the veterans inhaled large quantities of DU particulate over short periods of time, and some veterans were wounded by DU shrapnel that remained embedded in their bodies. Iraqi civilians did not inhale large quantities of DU during the time of battle and did not sustain DU shrapnel in their bodies. Nonetheless, some civilians may have experienced prolonged exposure to DU remaining in the environment, and some may have ingested DU-contaminated food and water over a period of years.

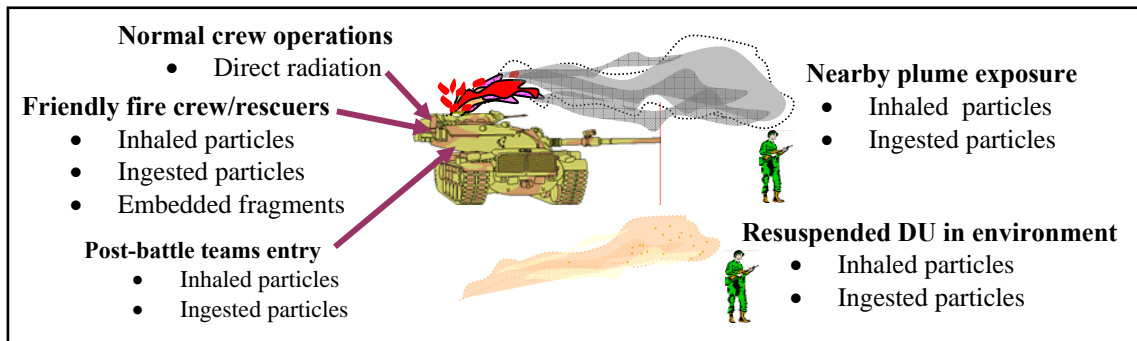


**Figure 10. Possible DU exposure pathways for military personnel**

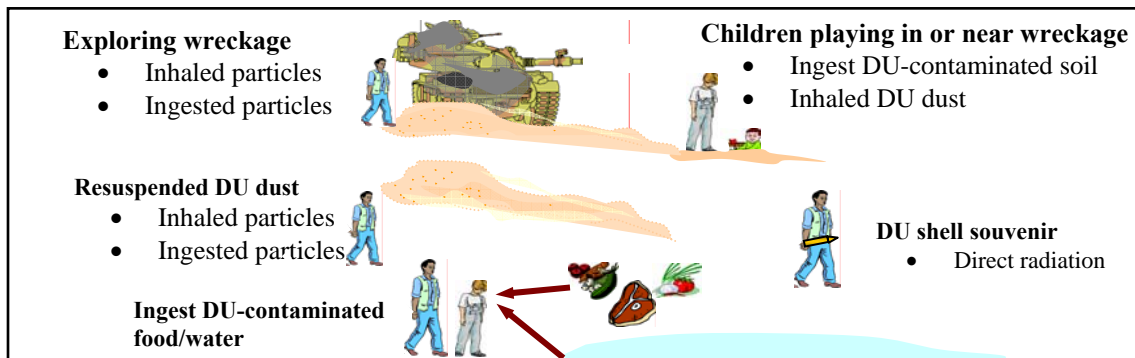


**Figure 11. Possible DU exposure pathways for civilians**

## 2.4. Chemical Health Effects of DU

Uranium is known to exhibit heavy metal toxicity effects. Once DU is dissolved in body fluids, the uranyl ion  $\text{UO}_2^{++}$  is the most common and bioavailable chemical form of uranium. The uranyl ion shares chemical properties with the alkaline earth ions; consequently, some of the absorbed uranium is deposited on the bone. Uranium is also deposited in the kidney, liver, lymph nodes, and other organs in small quantities. Information on the chemical toxicity effects of uranium on humans has been obtained to a large extent by extrapolations from animal testing. Animal test results are buttressed by medical data for uranium workers and by the scarce data available from medical records for workers who accidentally internalized significant quantities of uranium.

The effect of uranium chemical toxicity on the kidney has been clearly identified and is generally considered to be the principal health issue resulting from internalization of significant quantities of uranium. Nephrotoxic effects range from microscopic lesions in the tubular epithelium (for low concentrations) to tubular necrosis (for high concentrations). Symptoms of slight effects on the kidney have been reported for kidney DU concentrations as low as  $0.1 \mu\text{g U/g}$  of kidney for chronic exposures and as low as  $1.0 \mu\text{g U/g}$  of kidney for acute exposures. Protracted kidney damage has been observed for uranium concentrations between 3 and  $10 \mu\text{g U/g}$  of kidney [11: Appendix 1, p. 37]. The traditional (implicit) guideline for limiting uranium intake is a maximum kidney burden of  $3 \mu\text{g}$  of uranium per gram of kidney. The lethal dose to 50% of exposed humans (LD/50) for internalized uranium is estimated at about  $50 \mu\text{g}$  of uranium per gram of kidney [12]. Table 6 provides a summary of the guidelines for internalized uranium health effects on the kidney for acute intake (~ few days or less) and chronic intake (over many days to years).

**Table 6. Kidney guidelines for acute uranium intake**

	$\mu\text{g U/g kidney}$	
	Acute	Chronic
No Effect	< 1	< 0.1
Permitted	< 3	< 3
LD/50*	50	–

\* Without medical intervention

Less conclusive evidence has been reported for other chemical effects associated with uranium internalization. These potential chemical effects include neurocognitive effects, effects on the reproductive system, and chemically induced cancers. Lemercier et al. [13] have shown, using experiments with rats, that internalized uranium can cross the blood-brain barrier. Studies by Benson on female rats with DU implants [14] showed that uranium can cross the placental barrier; however, physical maturation features and reflex behavior of newborn pups did not differ from the control group.

Although the effects identified in this section are usually associated with heavy metal toxicity, research suggests that some of these effects are enhanced by low-level radiological exposure from uranium alpha-particle emission. When both radiological and chemical mechanisms are expected to contribute to a specific health effect, this study did not attempt to identify the relative contributions of each mechanism for most health issues. Some discussion is provided, however, regarding the possibility of a radiological contribution to potential neurocognitive effects typically associated with heavy metal neurotoxicity.

## **2.5 Radiological Health Effects of DU**

Although Gulf War veterans' exposure to DU was over fairly short time periods, internalized DU generally represents a long-term radiological exposure at very low dose rates. Exposure of Iraqi civilians also falls into the category of long-term radiological exposures at low-dose rates. Consequently, in this report, the focus for radiological considerations will be on potential health effects resulting from chronic low-level radiation exposures (i.e., on the potential for cancers and birth defects). Possible health effects from radiation exposure depend on the type of radiation, on the radiation energy, on whether the exposure is external or internal, and on other factors.

### **2.5.1 External vs. Internal Exposure**

DU radiological exposure may result from radiation sources external to the body or from radioactivity internalized within the body. Alpha particles from an external source are unable to penetrate the outermost layer of skin (consisting of dead cells);

consequently, alpha particles do not present an external radiation hazard. Beta radiation can penetrate the skin, and for very high beta exposures, burns and skin cancer induction are possible. As for alpha particles, beta particles cannot reach internal organs from external sources. Gamma rays can penetrate the human body and cause cell damage in internal organs; however, for DU, gamma rays are infrequent and are relatively low energy. Given these considerations, health risks from DU external radiation should be very small.

Internal exposure to DU radiation can result from inhalation of DU dust, from ingestion of DU particulate, from DU fragments embedded in the body, and from DU contamination of wounds. The effects of internal radiation will depend on the path of entry into the body, on the chemical form of the uranium compound, and on a number of other considerations. Although human skin protects internal organs from external sources of alpha radiation, the soft tissues of the lungs and other internal organs are not protected from internal sources of alpha radiation. In fact, for internalized DU, alpha particle radiation is the dominant contributor to radiation dose.

### **2.5.2 Cancers**

Cancers can result from a variety of causes, including ionizing radiation (ionizing radiation is discussed in Appendix A). Radiation damage to the cells of living organisms is primarily associated with damage to DNA molecules. Radiation-induced DNA damage can result from the direct effect of radiation ionization of the DNA molecule or from indirect effects resulting from the production of reactive chemicals that can interact with organic molecules within the cell. DNA damage that is not properly repaired or that does not result in cell death can result in the induction of cancer. A subsequent sequence of events is required, however, for a mutation to develop into cancer. Although the induction of cancers in humans from low radiation doses has not been clearly demonstrated, there does not appear to be a general threshold radiation dose below which the risk of any induced cancers would be zero. For low-level radiation exposure, the standard correlation for the lifetime risk of fatal cancers is 0.04 per person-Sv (whole body dose) for an adult radiation worker and 0.05 per person-Sv for the average population. The risk coefficient is higher for the average population because the average population includes children who are

generally more radiation sensitive than adults. Radiation-induced lung cancer may be possible if significant quantities of insoluble uranium are inhaled and deposited in the lungs. A fraction of the internalized DU will be absorbed by the blood and deposited in other body organs. Because uranium is a bone seeker, leukemia could be considered as a possible health effect from DU exposure. However, the very low specific activity of DU significantly reduces the likelihood of induced leukemia.

### **2.5.3 Birth Defects**

Birth defects can result from mutations in germ cells (spermatozoa or egg) that are passed on to progeny; hence, radiation damage to germ cell DNA may result in genetic effects passed on to the children of an individual receiving germ cell radiation damage. Although in utero effects on the fetus (such as mental impairment) have been found to be statistically significant when pregnant women receive high radiation doses, no clear evidence of radiation-induced genetic birth defects has been observed in humans at any radiation exposure level. The probable reason radiation-induced genetic birth defects have not been observed in humans is that any increase in birth defects from radiation is too small to be detected relative to the spontaneous induction of birth defects. Thus, observation of genetic birth defects from DU exposure is extremely unlikely. The equilibrium genetic risk from radiation exposure is obtained using the risk correlation of 0.008 per person-Sv for workers and 0.013 per person-Sv for the general population.

### **2.5.4 Guidelines**

The International Commission on Radiological Protection (ICRP) and other international and national organizations have established the radiological protection guidance given in Table 7. U.S. guidelines are identical to ICRP guidelines, except that the U.S. five-year average exposure guideline for workers is only 10 mSv/yr, rather than 20 mSv/yr.

**Table 7. ICRP annual radiological exposure guidance (mSv/yr) [15]**

	<b>Occupational</b>	<b>Public</b>
5-year average	20	1
Any single year	50	5
Any organ, skin	500	
Lens of eye	150	

## **2.6 Iraqi Population and Environment**

To facilitate an understanding of possible effects of DU on Iraqi civilians and the local environment, a brief background discussion is provided here on the Iraqi population, terrain, sources of water and food, prevailing weather patterns, and factors potentially affecting veteran and civilian health as a result of the 1991 Gulf War.

### **2.6.1 Population and Terrain**

The total population of Iraq was given as 22,300,000 in a 1997 census. The population distribution of Iraq is shown in Figure 12. About 75% of the population is concentrated in urban areas. The most populous cities are Baghdad (5,605,000), Mosul (1,739,000), Basrah (1,337,000), and Irbil (839,000).

Iraq is often described in terms of four geographic zones: a desert plateau, the northern highlands, the uplands region, and an alluvial plain. These four zones are identified in Figure 13. The desert plateau is part of the Syrian Desert west and southwest of the Euphrates River. The desert plateau covers about 40% of Iraq and is sparsely populated by pastoral nomads. The territory consists of extensive stony plains with scattered sandy areas. Seasonal watercourses flow from the western boundary to the Euphrates River. The desert plateau provides most of Iraq's rangeland grazing and dryland cultivation. The northern highlands are a mountainous region extending to Iran and Turkey. The uplands region is a transition zone between the highlands and the desert plateau. The combined deltas of the Tigris and Euphrates rivers form an alluvial plain. The alluvial plain covers about 30% of Iraq and is the principal region for irrigated agriculture. Large-scale drainage by Iraq and damming and diversion of the Euphrates by Turkey and Syria have severely damaged the once extensive wetlands of this region.

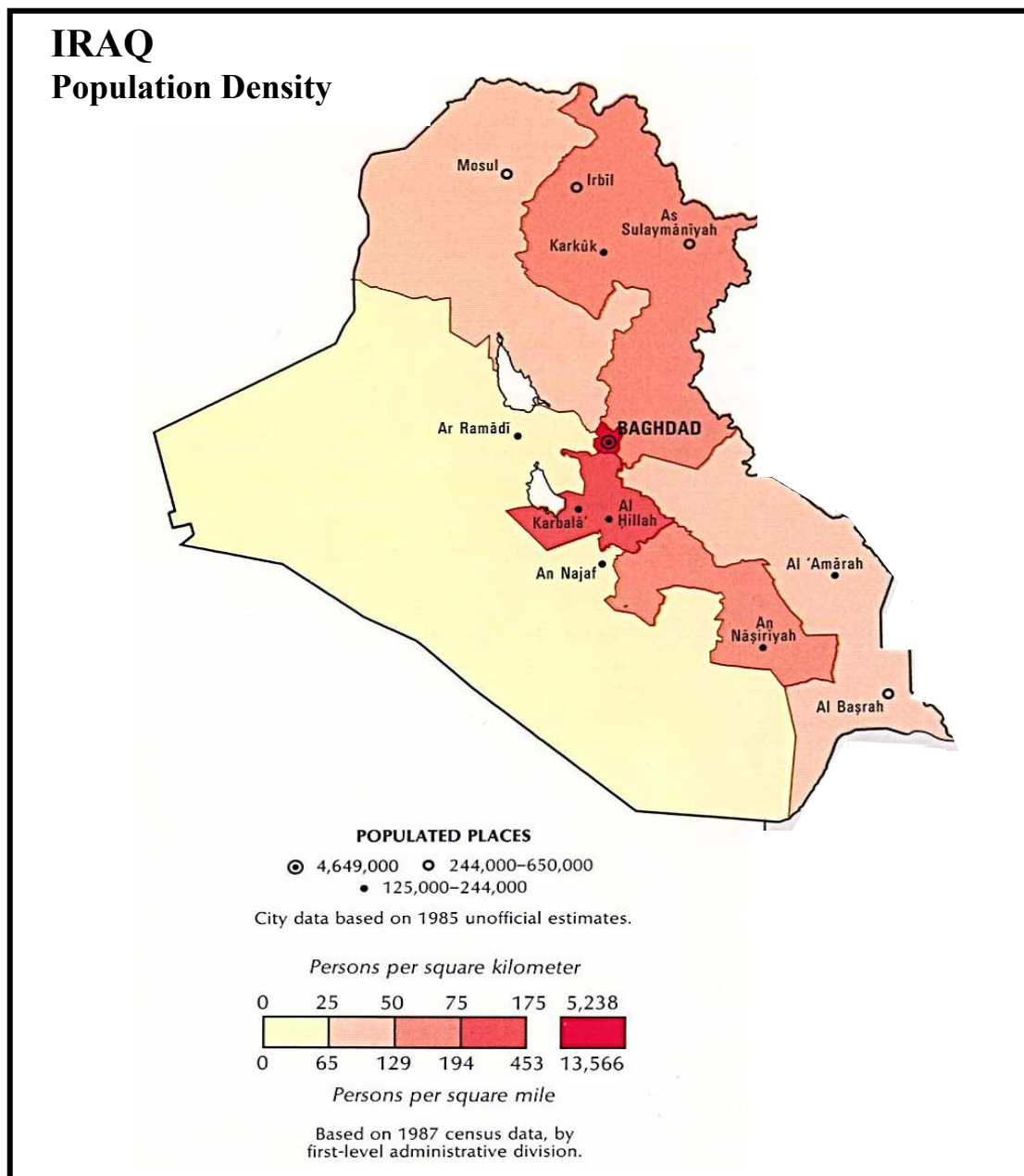


Figure 12. Population densities for regions of Iraq [16]

## 2.6.2 Water and Food Sources

Much of the Iraqi landscape is barren or very sparsely vegetated, especially in the desert plateau where DU munitions were used during the Gulf War [17]. Only 12% of Iraq is arable land, and prior to the Gulf War, Iraq imported roughly 70% of its food. Agriculture in Iraq became more important after the Gulf War; nonetheless, as of 2003,

60% of Iraqis were fully dependent upon government-distributed food rations. The water for about half of Iraq's land area is supplied by the Tigris and Euphrates rivers. Ground water is the principal water source for the remaining (primarily rural) area. Ground water is typically brackish or saline with high mineral concentrations. New watercourses have been constructed in the south.



Figure 13. Geographical zones of Iraq [17]

### **2.6.3 Prevailing Weather**

Most of Iraq has a desert climate with mild winters and hot, dry, cloudless summers. About 90% of the annual rainfall occurs between November and April, mostly between December and March. In the southern and western areas, the average annual rainfall is between 10 and 17 cm. Two prevailing wind patterns are identified for Iraq. The *shari* are southern and southeasterly dry and dusty winds with gusts reaching 80 km/hr. The *shari* occur between April and June and from late September through November. These dusty windstorms can last from one day to several days. The prevailing *shamai* winds are from the north and northwest from mid-June through mid-September.

### **2.6.4 Gulf War Aftermath**

After a war has ended, the resulting devastation may continue to impact the environment and its population. The conduct and environment of warfare may also have unexpected health effects for veterans after hostilities have ended. To provide the proper context for assessing the potential effects of DU on veterans and Iraqi civilians, other factors with potential health consequences must be considered.

In addition to the use of DU, potential toxins, carcinogens, and teratogenic agents were released into the environment. Demolition of chemical weapons stores released chemical agents such as sarin and mustard gas. Oil well fires and oil spills had a significant environmental impact and may have resulted in adverse health effects for both veterans and civilians. In addition, U.S. veterans were given prophylactic drugs, such as pyridostigmine bromide (pb), as well as other medications and vaccines [18]. The possible health effects of these agents, individually and in combination, need to be examined. Before the Gulf War, Iraq had a high standard of living with high levels of education, access to potable water and sanitation, and low infant mortality rates. The standard of living dropped dramatically following the war and the imposition of economic sanctions. Access to food, water, health care, and education deteriorated to substandard levels. Poor post-war sanitation may have contributed to the spread of disease. Chronic malnutrition among children reached 30% by the year 2000.

Malnutrition declined somewhat after 2000 [17]. This drastic change in living conditions must be considered when assessing post-war health effects for Iraqi civilians.

## **3.0. DU Source Terms and Internalized Mass**

To compute organ doses for DU-exposed individuals, it is necessary to determine the DU mass internalized (taken into the body) as a result of particulate inhalation, particulate ingestion, and embedded fragments. This section summarizes the basic methodologies used to estimate internalized DU mass. This section also presents the predicted internalized DU mass for all pathways for both veterans and civilians.

### **3.1 Types of Exposures and Methodologies**

Internalized DU mass was estimated for both veterans and Iraqi civilians. Level I veterans were exposed to potentially high concentrations of aerosolized DU, and some received wounds resulting in embedded DU fragments. Level II and III veterans were not wounded by DU fragments, and their DU-inhalation exposure was generally much lower than that of Level I veterans. A number of veterans also ingested DU particulate by hand-to-mouth contact or by consuming contaminated food.

Civilian DU exposures include civilians downwind of the battle zone and children playing in and around destroyed vehicles following the Gulf War. Although children at play in the battlefield may also live downwind from the battle zone, the exposure of a child at play is much greater than that experienced by downwind civilians. To estimate inhaled DU masses for a child at play, some assumptions were required for the duration of play in the battle zone. Because the durations are difficult to estimate, the exposure times were selected as arbitrary high values. For both the nominal and maximally exposed child, a total of 1000 hours of play is assumed as a conservative best estimate. The in-vehicle exposure time is assumed to be about 1/3 of the total exposure time in the battlefield (i.e., 300 hours of play within the vehicle). Downwind civilians were assumed to spend their entire lives downwind of the battlefield.

A variety of methods can be used to compute the internalized DU mass. The quantity of inhaled DU particulate is typically determined by first computing the aerosolized mass at the time and location of exposure. The aerosolized DU particulate

mass, as well the physical and chemical form of the particulate, is called the source term. The source term data can be used with expected inhalation rates to estimate the time-dependent internalized DU mass. Alternatively, the source term calculation can be skipped, and the inhaled DU mass can be inferred from measured DU concentrations in the urine (assuming urine data are available). Also, measured DU concentrations in urine can be used to determine DU fragment dissolution rates.

To make use of the most reliable data, a variety of methods were utilized in this study to compute the internalized DU mass. Five basic types of methodologies, numbered 1 through 5, were used to compute internalized DU mass for all veteran and civilian exposure scenarios. The methodology type for the cases studied are identified in Table 8, and a brief description of each methodology is provided in Table 9. A more detailed discussion of the source-term analysis is presented in Appendix B.

**Table 8. Method type used to determine internalized DU mass**

Exposure Case		Method Type Identification Number			
		In-vehicle		Ex-vehicle (Downwind)	
		During Battle	Post-battle	During Battle	Post-Battle
Veterans	I	1			
	II		2		
	III		2	3	4
Civilians			2	3	4, 5

**Table 9. Methods used to determine internalized DU mass for civilians**

<b>Method</b>	<b>Pathway</b>	<b>Data/Method Used</b>
<b>1</b>	Inhalation	Inferred inhaled mass from measured DU in urine
	Fragments	Inferred fragment dissolution rate from measured DU in urine
	Ingestion	Typical hand-to-mouth ingestion rates used
<b>2</b>	Inhalation	PNNL post-shot resuspension data, typical inhalation rates used
	Ingestion	Typical hand-to-mouth ingestion rates used
<b>3</b>	Inhalation	PNNL aerosolization data, puff dispersion calculations for DU air concentrations, typical inhalation rates used
<b>4</b>	Inhalation	PNNL aerosolization data, puff DU-deposition and resuspension calculations, typical inhalation rates used
<b>5</b>	Ingestion (food, water)	DU monitoring for civilians (urine, hair, etc.) and environmental data (showing no significant effect)

### **3.2 Method I: During Battle**

The inhaled mass of DU by Level I veterans can be estimated using the aerosolized DU mass released in the vehicle, the vehicle volume, breathing rates, assumptions for local concentrations, and estimates of exposure times. This approach, however, required the use of many assumptions and estimated parameters. Another approach that requires fewer assumptions was used to estimate the inhaled DU mass for Level I veterans. This alternative approach is based on DU concentrations measured in the urine of friendly fire veterans and standard biokinetic models. Using this alternative method, described in Appendix B, the predicted inhaled masses for the nominal and the maximum-exposure cases are 250 mg (about 0.01 oz) and 4 g (about 0.14 oz), respectively.

Fragments of DU munitions embedded in the body from friendly fire DU impact will be mostly unoxidized uranium metal. Uranium metal dissolves very slowly in body fluids; consequently, DU fragments will remain highly immobile, resulting in an appreciable radiation dose at the location of the fragment. As the fragment dissolves, uranium will enter the bloodstream very slowly where it will be reabsorbed by the organs or quickly eliminated in the urine. Dissolution of the DU metal fragment and absorption

of uranium by the blood provides a continuing supply of uranium to the blood and subsequent distribution to the body's organs. The DU fragment dissolution rates for the nominal and maximum exposure cases also were inferred from DU urine-concentration data [19]. As discussed in Appendix B, calculations give the nominal and maximum blood-dissolution rate for DU fragments as 18 and 100  $\mu\text{g}$  DU per day, respectively.

Based on an assessment by the Royal Society [4], a best estimate hand-to-mouth transfer rate of 3 mg of particulate/hr was used as the DU-ingestion rate for adults in a contaminated environment. Assuming that their hands and clothing are covered with DU powder for several hours, a nominal ingested mass of about 15 mg should be reasonably conservative. For the Level I maximum ingestion scenario, a different exposure time was used. For this case, we assume that the vehicle had been hit by a DU penetrator and that the vehicle remains operational. We also assume that the vehicle is subsequently occupied 16 hrs per day for 10 days. Using the hand-to-mouth transfer rate of about 3 mg/hr and 16 hrs x 10 days gives an estimated ingested DU mass of about 0.5 g.

### **3.3 Method 2: Post Battle**

The inhaled mass of DU by Level II veterans is essentially determined by in-vehicle DU exposure from resuspended DU. Most of the inhaled DU for a child at play in the battlefield will also result from in-vehicle DU exposure from resuspended DU. Some Level III veterans are also assumed to explore DU-contaminated vehicles.

#### **3.3.1 Level II Veterans**

From Reference [6: IV, 8], the maximum exposure time for Level II veterans was 100 hours. A nominal exposure time estimate was not found in Reference [6], however, reported Level II exposure times ran from as short as one hour to days. The SNL study used the nominal exposure duration estimate given by the Royal Society [4: p. 42] of 10 hours. The resuspended DU within a vehicle will depend, among other considerations, on the type of vehicle and the number and size of DU rounds striking the vehicle.

The recent Capstone test program [5], discussed in Appendix B, yielded a wealth of excellent data on DU particulate generated by the impact of DU-weapons with

armored vehicles. Using the Capstone test data, a maximum worker-resuspended DU mass density of  $2 \text{ mg/m}^3$  was obtained (Appendix B). This DU concentration is equivalent to a resuspended DU concentration for a tank struck by at least two 120 mm shells. This maximum DU concentration of  $2 \text{ mg/m}^3$  was used for both the nominal and maximally exposed Level II cases. Elevated breathing rates of  $2 \text{ m}^3/\text{hr}$  and  $3 \text{ m}^3/\text{hr}$  were assumed for nominal exposure and maximum exposure, respectively. Thus, the nominal and maximum inhaled DU masses were 0.04 g and 0.60 g, respectively. As for the Level I computation, a hand-to-mouth transfer rate of 3 mg/hr was used for estimating the mass of ingested DU. Using the estimated exposure times, the ingested DU mass for the nominal and maximum exposure cases are 0.03 and 0.30 g, respectively.

### **3.3.2 Level III Veterans**

It would be very difficult to place a bound on the time spent exploring damaged vehicles by Level III veterans. Consequently, we take the approach of guessing that a maximally exposed veteran spends about one hour inside DU-contaminated vehicles. If the DU exposure is small, then the accuracy of the time estimate is of little consequence. We also assumed that three 120 mm DU shells hit the destroyed vehicle, and the veteran breathing rate was somewhat elevated at  $2 \text{ m}^3/\text{hr}$ . Using the previously discussed methodology for in-vehicle resuspension, the inhaled DU mass for in-vehicle activities was computed to be 0.006 g. Also, for an in-vehicle exposure time of one hour, the ingested DU mass for the maximum exposure case is 0.003 g.

### **3.3.3 Child at Play**

It is assumed that an Iraqi child will play within the vehicle intermittently over a period of 10 years. If a number of vehicles are entered over this period, some of the vehicles may not have been hit by DU penetrators, some may have been hit by one or more 30 mm shells, and some may have been hit by one or more 120 mm shells. Thus, both nominal and maximum in-vehicle particulate mass estimates represent averages over many vehicles containing different quantities of DU. Using the Capstone data, we assume that the nominal and maximum DU concentrations in air are 0.5 and  $2 \text{ mg/m}^3$ , respectively. The nominal-exposure DU air concentration corresponds to an average

resuspended DU air density (average of all PNNL resuspension test data) for a child playing in vehicles struck by one 120 mm shell. The maximum-exposure DU air concentration was obtained by multiplying the maximum resuspended-DU air concentration per 120 mm shell ( $1 \text{ mg/m}^3$ ) by two (equivalent to vehicles hit by two 120 mm shells). With a breathing rate of  $0.36 \text{ m}^3/\text{hr}$  for a child, the in-vehicle inhaled DU mass was 54 mg and 216 mg for the nominal and maximum-exposure cases, respectively. For DU ingestion by a child at play, the nominal and maximum hand-to-mouth transfer rates of 10 and 30 mg/hr were assumed (an order of magnitude higher than for adults [4: Annex B, p. 9]). Using the estimated in-vehicle exposure time of 300 hours, the ingested DU mass for the nominal and maximum exposure cases are 3 g and 9 g, respectively.

### **3.4 Aerosol Generation and Dispersal (1 Target)**

For Methods 3 and 4, the masses of DU particulate generated by impact must be known to quantify the amount of DU suspended in the air external to the vehicle. To compute DU air concentrations, it is necessary to determine the fraction of aerosolized DU released internal to the vehicle and the fraction released external to the vehicle. The possible exposure of individuals downwind from the impact can be assessed by estimating the wind-dispersed concentrations of DU suspended in air (puff) at various positions as a function of time after penetrator impact. In addition, calculations must include the contribution of dispersed DU deposited on the ground and subsequently resuspended and inhaled many days after hostilities have ceased. This section discusses aerosol generation, dispersal, resuspension, and inhalation for a single target vehicle.

#### **3.4.1 DU Particulate Masses Generated**

Appendix B provides the method used to estimate the quantity of DU aerosolized by impact of a 120 mm round with an armored vehicle. The estimated DU aerosol masses released within and external to the target vehicle are presented in Table 10, which also provides estimates of the total percentage of DU that is aerosolized during impact. As explained in Appendix B, the mass of DU released external to the vehicle is assumed to approximately equal to the DU mass released internal to the vehicle. The masses

presented in Table 10 apply to both U.S. and Iraqi vehicles. The light-vehicle classification includes BFVs.

**Table 10. Estimated DU aerosol mass released external to vehicle per 120 mm round impact**

Target	Shell (mm)	DU Mass (g)		Total Aerosolized (%)
		Internal or External	Total	
Tank (U.S., Iraqi)	105, 120	100	200	4.3
Light Vehicle (BFV, etc.)	120	30	60	1.3

### 3.4.2 Atmospheric Dispersal

Here we examine the dispersal of DU following the impact of a 120 mm DU shell against a single tank. From Table 10, the mass released external to the vehicle is approximately 100 g (about 0.22 pound or 3.5 oz). The basic geometry is illustrated in Figure 14. Although lofting of particulate can result in an effective source height greater than the release height, the location of the source is assumed to equal the penetrator exit height (= impact height =  $H \approx 2 \text{ m} \approx 6.56 \text{ ft}$ ). The decision to set the source height equal to the impact height is discussed in Appendix B.

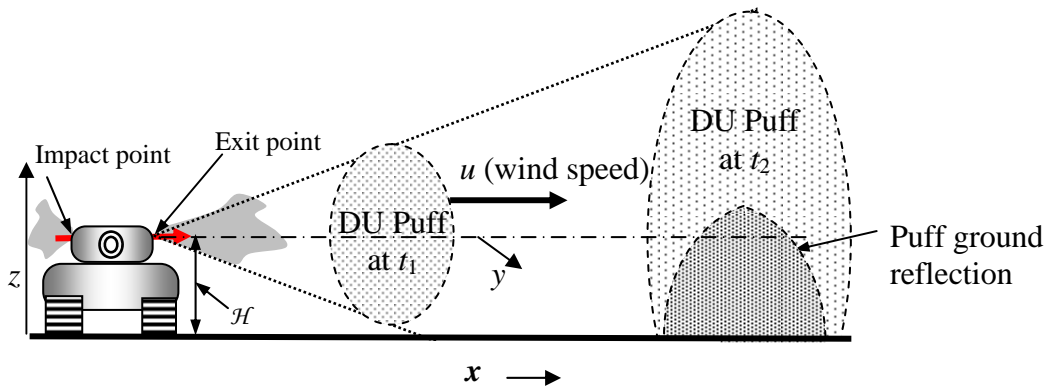


**Figure 14. Geometry assumed for the analysis of DU-puff dispersal following penetrator impact**

The dispersion of DU particulate following impact was estimated using the Gaussian puff model described in Appendix B. The dispersal and deposition of DU at the

battle location will depend on the atmospheric conditions at the time of the battle. Wind speeds between 2 and 15 m/s and frequent thunderstorms occurred during many of the battles involving DU munitions [20]. To estimate aerosol densities and surface depositions from DU impact with hard targets, calculations were performed assuming both wet and dry deposition, low and high wind speeds, and a range of weather conditions categorized by atmospheric stability classes A through G (see Appendix B).

Based on the study discussed in Appendix B, the largest integrated air concentrations and the greatest DU deposition densities resulted from wet deposition for class E weather conditions and a wind speed  $u$  of 2 m/s. For the best estimate prediction, a mid-range stability class was selected (class C, slightly unstable) at an intermediate wind speed of 8 m/s. Because the dominant deposition mechanism (wet or dry) was not identified for all battles, wet deposition was selected as the more conservative assumption (yields higher DU areal densities). The deposited DU areal density  $\zeta$  (g/m<sup>2</sup>) and the time-integrated inhaled DU mass  $m$  (assuming a breathing rate  $R_b$  of 1 m<sup>3</sup>/hr) were calculated for these conditions and are presented in Figure 15 as a function of downwind distance  $x$  at cross-wind distance  $y = 0$  (i.e., along the centerline of the puff). For a single target vehicle, Figure 15 shows that the inhaled DU mass and deposited DU densities decrease very rapidly with downwind distance from the vehicle.

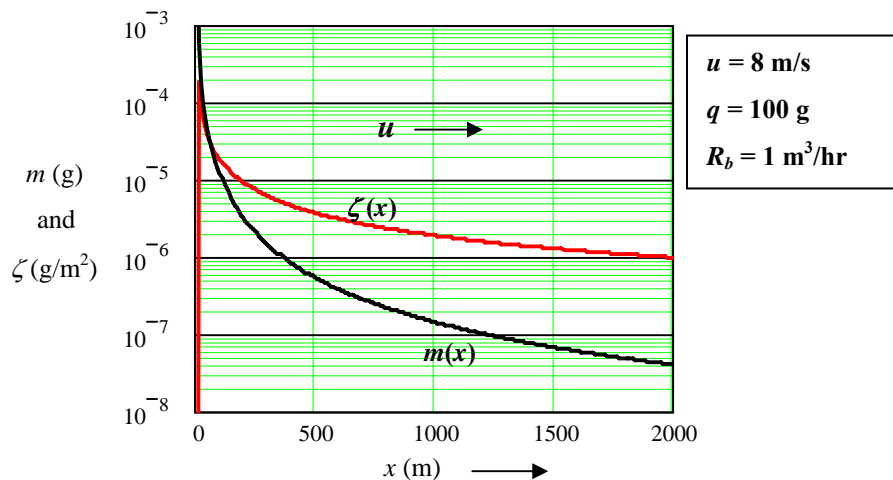


**Figure 15. Inhaled DU mass and deposited DU areal density vs. x-distance along puff-path centerline (single 120 mm round, single tank, class C conditions)**

### 3.5 Aerosol Generation and Dispersal (Multi-Target)

Although the preceding model is reasonable for estimating dispersion resulting from impact against a single tank, DU aerosols resulting from multiple-target impacts will provide multiple source terms. Calculations of DU air concentrations and deposition densities at larger distances must account for the combined effect of multiple targets. Two types of multiple targets were assessed in this study:

- (1) an array of tanks in a tank battle and
- (2) a long column of densely packed, light target vehicles struck by 30 mm DU rounds.

#### 3.5.1 Tank Battle Array

The analytic model assumes that the battlefield target vehicles are deployed in a column of regularly spaced vehicles, separated by distance  $\mathcal{D}$ . Appendix B provides the equations used to predict DU deposition for an array of targets. Figure 16 illustrates the scenario that was used to develop an analytical model for predicting DU dispersion and deposition during a tank battle. The analysis assumed a separation between tanks  $\mathcal{D}$  of 20 m, class C weather conditions, a wind speed of 8 m/s, and wet deposition. The 20 m separation estimate was based on photographs of destroyed Iraqi tanks and discussions with veterans. The analysis is performed assuming that each target vehicle is struck by a single 120 mm DU tank round, releasing 100 g of DU aerosols. Thus, the predictions are made on a per shell impact basis.

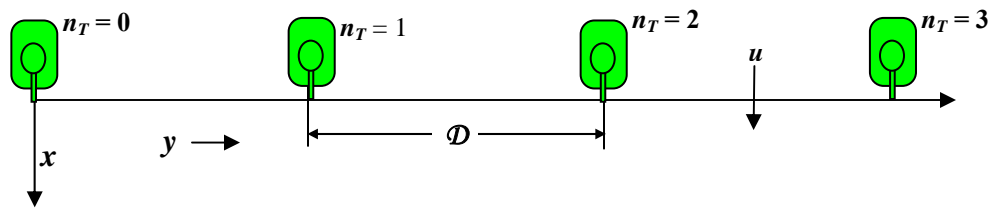
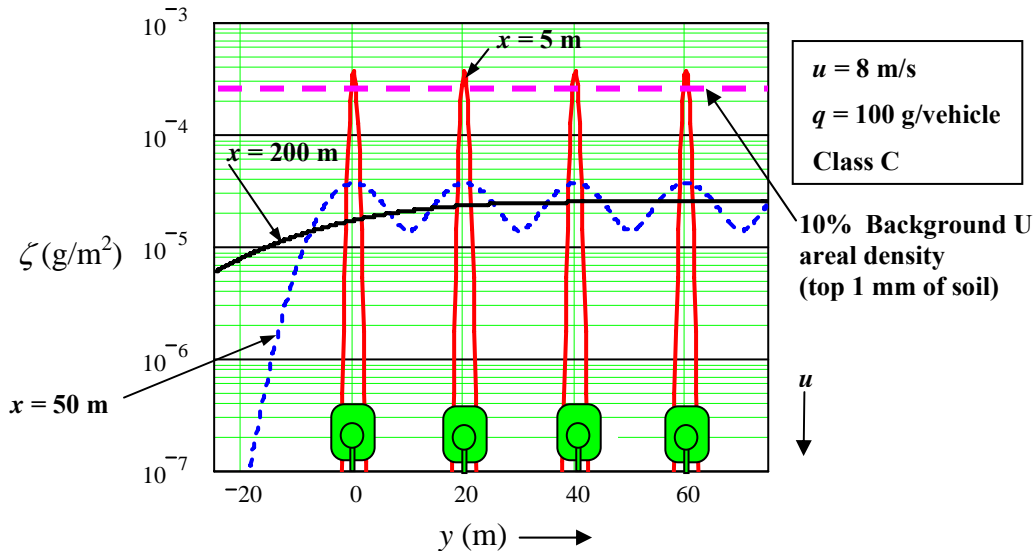


Figure 16. Assumed geometry for the tank-battle scenario

The estimated DU deposition is presented in Figure 17 as a function of transverse distance ( $y$ ) for several different downwind distances ( $x$ ). At distances close to the target (e.g., at  $x = 5$  m) DU from neighboring vehicles have little effect on the local deposition.

At 50 m, the effect of DU from neighboring vehicles contributes to the local deposition. By 200 m, the effect of DU from neighboring vehicles effectively removes the y-dependence of the deposited DU for locations in front of the column. Figure 17 also shows that the deposition decreases beyond the edge of the column. For comparison, the figure also includes the uranium areal density equal to 10% of the natural background areal density for the top 1 mm of soil (magenta dashed line).



**Figure 17. Wet deposition  $\zeta$  vs.  $y$ -distance for 20 targets 20 m apart for a single 120 mm shell impact per target during a tank battle**

The estimated DU deposition is presented in Figure 18 as a function of downwind distance for a column of 1, 20, and 50 target vehicles. For the column of 20 target vehicles, the deposition changes very slowly with distance beyond 100 m; however, the deposited DU density is very low compared to the natural background. Furthermore, natural uranium in the soil is only a small contribution to the background radiation dose from all natural radiation sources. Thus, the effects of deposited DU should be very small. The inhaled mass as a function of downwind distance, assuming a breathing rate of 1 m<sup>3</sup>/hr, is also presented in Figure 18. The inhaled DU mass calculation assumes that an individual remains at downwind location for the brief period of time required for the puff to pass through location  $x$ . The closeness or overlap of the deposition curve for one target vehicle with the inhalation curve is accidental. A different choice of units for deposition (e.g., g/cm<sup>2</sup>) would not show this overlap. The curves in Figure 18 also show that the

assumption of more than 20 target vehicles did not significantly affect the deposition density of DU. Increasing the number of targets has the effect of increasing the distance the DU is carried rather than increasing the maximum deposition density or inhaled mass.

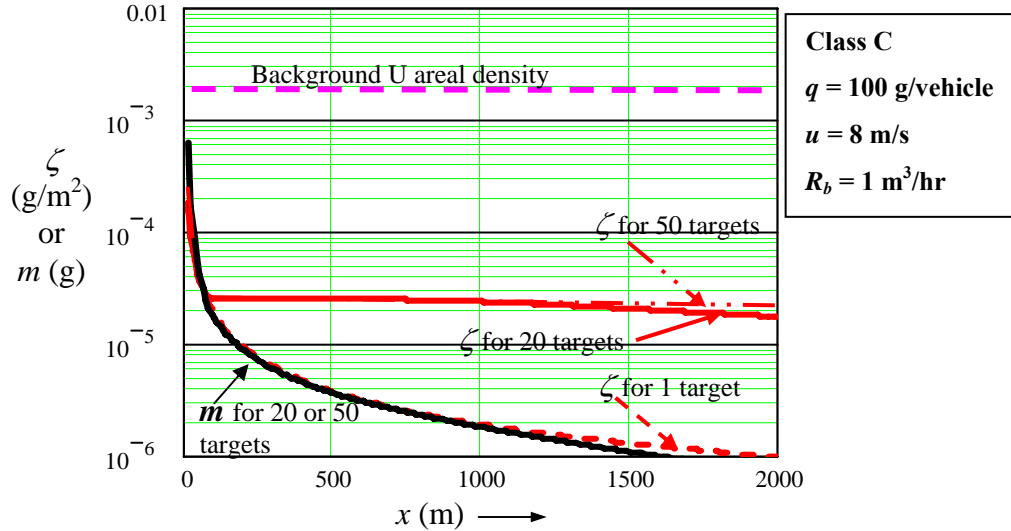


**Figure 18. Inhaled mass  $m$  and deposition  $\zeta$  vs.  $x$ -distance for 1, 20, and 50 targets ( $\phi = 20$  m,  $y =$  array midpoint, one 120 mm shell per target, wet deposition)**

### 3.5.2 Very High Density of Targets

For this case, we consider very high target-density battlefields such as the so-called Highway of Death. For simplicity, we assume an infinitely long battlefield with many targets per km of transverse ( $y$ ) distance. For high-density battlefields of the type considered here, most of the enemy vehicles were light vehicles destroyed by either non-DU weapons (releasing no DU) or by 30 mm DU penetrators fired from A-10 “tank-killers” and other aircraft. As discussed in Appendix B, the SNL study assumes an infinitely long line source releasing 15 g of DU per m of column.

The method for computing the deposition density and integrated inhaled DU mass for a line source is presented in Appendix B. Other assumptions for this calculation include a wind speed of 8 m/s, class C weather conditions, wet deposition, and a breathing rate of 1 m<sup>3</sup>/hr. The calculated deposition density and the inhaled DU mass are presented in Figure 19 as a function of  $x$ -distance. For an infinite line source and wet deposition, the deposition density reduction with distance results from vertical dispersion

and the very small effect of puff depletion (i.e., depletion of DU from the puff because of DU ground deposition). Thus, the deposition density is almost constant at about  $7 \times 10^{-5} \text{ g/m}^2$  over a 20 km (12.44 miles) distance. For the inhaled DU mass, however, the concentration drops appreciably with downwind distance.

At long distances, the effect of puff reflection by an atmospheric temperature inversion layer may become important. Puff reflection refers to the downward reflection of the vertically expanding cloud of DU aerosols by a layer of higher temperature air, such that the puff remains trapped between the ground surface and the temperature inversion layer (ceiling). In order to examine this potential effect, calculations were performed assuming both (1) no inversion layer reflection and (2) assuming a relatively low ceiling height of 150 m. The inhaled mass as a function of distance is shown in Figure 19 for these cases. Observe that inversion layer reflection has the effect of maintaining the inhaled DU mass at a nearly constant value beyond about 2 km. The deposited DU areal density is the same with and without reflection by a temperature inversion layer.

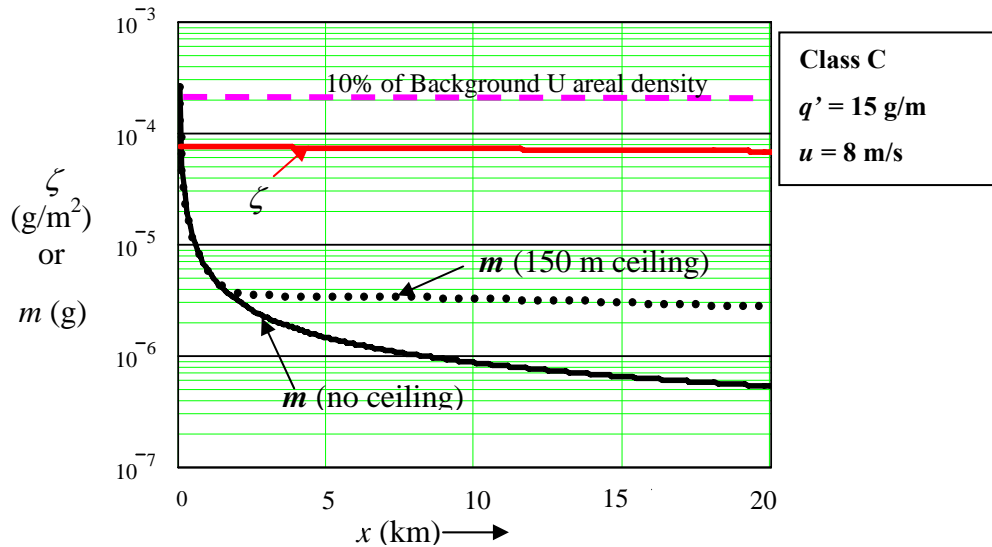


**Figure 19. DU mass inhaled and deposited vs. x-distance for the infinite line source model for the very high target density scenario**

## 3.6 Methods 3 and 4: Ex-Vehicle

Methods 3 and 4 apply to Level III veterans, downwind civilians, and a child playing outside a vehicle struck by a DU penetrator.

### 3.6.1 Level III Veteran

A Level III veteran downwind from a vehicle struck by a DU shell is unlikely to be closer than 100 m from the vehicle during the battle. Figures 18 and 19 show that the maximum deposition and inhaled dose is determined by the very high target density case rather than by the multi-target case, even if we assume that the tank battle scenario involved four shell impacts per target and much more than 20 targets. At about a hundred meters from the battle zone, the time-integrated inhaled DU mass is about  $10^{-4}$  g, and the deposited DU areal density is essentially position-independent at about  $10^{-4}$  g/m<sup>2</sup>. These values are selected for the areal density and inhaled masses for maximum exposure Level III veterans. Figure 19 shows that the areal density and ceiling-reflected inhaled mass decrease very slowly with distance from the battle; however, the slow decline effect is exhibited only after the quantity of DU drops to very low levels (a few percent of the natural uranium soil concentration). For nominal exposure of downwind veterans, the inhaled DU mass and deposition density at about 3 km was obtained from the line-source calculation (Figure 19). The inhaled mass from a puff at 3 km is about  $3 \times 10^{-6}$  g, and the deposited areal density is about  $7 \times 10^{-5}$  g/m<sup>2</sup>. The battlefield exposure times for the nominal and maximum cases were assumed to be 30 days and 90 days for the nominal and maximum exposure cases, respectively. The inhaled DU masses from resuspended DU were found to be  $10^{-6}$  g and  $3 \times 10^{-6}$  g for the nominal and maximum cases, respectively. The total inhaled mass for the nominal and maximum exposure cases were, respectively,  $4 \times 10^{-6}$  and 0.0061 g.

### 3.6.2 Downwind Civilian

Figures 18 and 19 also provide source term data for downwind civilian populations. The nominal and maximum inhaled DU mass from a puff for downwind civilians are the same as for Level III veterans. Because the exposure times and the areal

densities are the same for both the nominal and maximum cases for civilians, the inhaled DU mass from resuspension are the same ( $3 \times 10^{-6}$  g) for both cases.

### 3.6.3 Child at Play

Near the target, the typical Gaussian methods used for estimating atmospheric dispersal and deposition do not account for gravitational deposition of larger particles and explosive deposition of DU particulate. To estimate this effect for the maximum exposure case, Capstone test data were used. The maximum-recorded DU particulate deposition from the Capstone tests was about  $15 \text{ g/m}^2$  [5: Attach. 1, p. 5.37] (using the reported tray surface area of 160 cm), and the average over all tests was about  $1 \text{ g/m}^2$ . Assuming that the maximally exposed child plays habitually in the zones closest to the damaged vehicles over the 10-year period, the average initial DU aerial density near the vehicles of  $1 \text{ g/m}^2$  was assumed. The uncertainty analysis presented in Section 6 will examine the effect of assuming the highest aerial density of  $15 \text{ g/m}^2$ . From Figures 17 through 19, we observe that the initial DU deposition density beyond a few meters is less than  $0.001 \text{ g/m}^2$ , even for multiple targets. For the nominally exposed child, the average initial DU areal density of  $0.001 \text{ g/m}^2$  will be used. The inhaled DU mass from activities external to the vehicle was found to be  $10^{-5}$  g and 0.010 g for the nominal and maximally exposed child, respectively.

## 3.7 Method 5: Food/Water Contamination

DU may be ingested by civilians as a result of eating contaminated food, drinking contaminated water, or by hand-to-mouth contact if their hands are contaminated with DU particulate. In general, however, none of these exposure mechanisms are likely to contribute to significant internalization of DU by downwind civilians. The deposited downwind DU concentrations are much less than the natural uranium concentrations in the soil. According to a study of environmental consequences of DU in Iraq and the Balkans by Bleise et al. [21]:

*[Depleted uranium] transfer to drinking water or locally produced food has little potential to lead to significant exposures to DU. Since poor solubility of uranium*

*compounds and a lack of information on speciation precludes the use of radioecological models for exposure assessment, biomonitoring has to be used for assessing exposed persons. Urine, feces, hair and nails record recent exposures to DU. With the exception of crews of military vehicles having been hit by DU penetrators, no body burdens above the range of values for natural uranium have been found. Therefore, observable health effects are not expected and residual cancer risk estimates have to be based on theoretical considerations. They appear to be very minor for all post-conflict situations; i.e., a fraction of those expected from natural radiation.*

The long-term effects of tons of sand-buried DU munitions must be considered as well. Bem and Bou-Rabe [22] carried out environmental monitoring in areas of Kuwait where DU munitions were used. Bem and Bou-Rabe state the following:

*Systematic measurements of water samples from the only underground source in the Rawdathein area did not show any increase of total alpha activity, and the mean concentration was  $1.2 \mu\text{g}\cdot\text{dm}^{-3}$ ... [dm = 0.1 m] Slowly reacting metallic uranium deposited in the humid ground, in long term perspective (over several hundred years) can cause the increase in some local wells (underground water), but only in exceptional cases can it exceed the US EPA limit of  $30 \mu\text{g}\cdot\text{dm}^{-3}$ ....Comprehensive environmental radioactive measurements in Kuwait in the years 1992-1994 do not confirm significant contamination over the territory of this country, which may lead to exceeding the current hygiene or safety standards.*

The Royal Society [11: p. 25] points out that DU contamination of ground water did not occur at either the Aberdeen proving ground or the Yuma test site. The Royal Society also notes that because of the low solubility of uranium, DU uptake by vegetation roots is very low. Bleise et al. state that uranium transfer from soil to pasture grass is low. Thus, the intake of DU by grazing animals will be very small. Furthermore blood absorption of ingested uranium is very small for both animals and humans. Given these

considerations, the health effect from DU ingestion by human consumption of grazing animals or their milk should be extremely small. A UNEP report [23: p. 8] concluded as follows:

*In Kosovo, the mission did not find any widespread contamination of the soil or ground surface, though some localized points of contamination were identified at some of the sites where the use of DU had been reported. The major part of the ground contamination was found in the upper 10-20 cm directly below the penetrator. No DU contamination of water or domestic cow milk was found during the mission or subsequent laboratory testing, and there was no evidence to suggest immediate health problems.*

However, this same report found some detectable DU contamination of drinking water and in several air samples in Serbia/Montenegro. The authors point out that the detected levels remained below international safety limits. They conclude,

*In terms of groundwater contamination arising from DU at contamination points or from more widespread ground contamination, the consequences in Serbia and Montenegro were insignificant.*

From these observations, we conclude (1) mathematical estimates of DU transport to water and food supplies are unlikely to be highly reliable; (2) ground-deposited DU particulate downwind of the battlefield is only a small fraction of the natural uranium soil concentrations; (3) because of the low solubility of uranium metal, significant DU contamination of food and water from buried munitions is unlikely; and (4) no significant DU contamination of the environment was observed in Kosovo, Kuwait, or DU test areas in the United States. Given these observations, the exposure of downwind civilians to DU from contaminated food and water is considered to be insignificant, and a mathematical analysis will not be undertaken for this potential pathway.

### 3.8 Summary of Internalized DU Mass

A summary of the internalized DU masses for veterans is presented in Table 11. The mass given for fragments is the total mass dissolved in the blood over a 50-year period, assuming a constant dissolution rate over the entire 50-year span. The actual embedded DU mass may be greater than the quantity dissolved in the blood, and the quantity present in the blood at any moment will be much less than the total dissolved mass. It is possible that the entire embedded fragment will have dissolved before the end of the 50-year period. In this case, the mass for fragments in Table 11 will be overestimated. Note that the health effect per gram of internalized DU depends on the internalization pathway (e.g., inhalation of DU presents a greater health risk than ingesting the same quantity of DU).

**Table 11. Summary of internalized DU mass for Gulf War veterans**

Case		Internalized DU Mass (g)	
		Nominal Exposure	Maximum Exposure
<b>Level I</b>	<b>Inhaled</b>	0.250	4.00
	<b>Fragments*</b>	0.330	1.80
	<b>Ingested</b>	0.015	0.50
<b>Level II</b>	<b>Inhaled</b>	0.040	0.60
	<b>Ingested</b>	0.03	0.30
<b>Level III</b>	<b>Inhaled</b>		
	<i>In-vehicle</i>	0.00	0.006
	<i>Puff</i>	0.000003	0.0001
	<i>Resuspended</i>	0.000001	0.000003
	<b>Total Inhaled</b>	0.000004	0.0061
	<b>Ingested</b>	0.0	0.0030

\* The estimated fragment mass is the total DU mass from fragments dissolved in the blood over a 50-year period.

A summary of the civilian internalized DU masses is presented in Table 12. Observe that the internalized DU mass for a child at play is much higher than for downwind civilians. Also, for the assumed hand-to-mouth transfer rates and occupation times, the ingested DU for a child is much higher than for veterans. The total internalized DU for downwind civilians is extremely small.

**Table 12. Summary of internalized DU mass for civilians**

Case	Internalized DU Mass (g)	
	Nominal Exposure	Maximum Exposure
<b>Child at Play</b>		
<b>Inhaled</b> <i>In-vehicle</i>	0.0540	0.216
<i>Ex-vehicle</i>	0.00001	0.010
<b>Total Inhaled</b>	0.0540	0.226
<b>Ingested</b>	3.00	9.00
<b>Downwind Civilians</b>		
<b>Inhaled</b> <i>Puff</i>	0.000003	0.0001
<i>Resuspended</i>	0.000003	0.000003
<b>Total Inhaled</b>	0.000006	0.0001

## 4.0. Biokinetic Analysis

A biokinetic analysis is used to trace the path of internalized DU within the human body. The basic pathways within the human body are shown in Figure 20. The principal path for DU internalization is by inhalation. Roughly half the inhaled DU will be exhaled. Depending on particle size, the remaining DU will be deposited in the various regions of the respiratory system. Much of the deposited DU will be transported out of the respiratory region and into the throat by the movement of hair-like cells called cilia. DU entering the throat will either be expelled (e.g., spit out) or swallowed. The swallowed DU will then pass through the GI tract, and most will be eliminated in the feces. In addition to ciliary action, DU is cleared from the respiratory system by dissolution and absorption by the blood. The absorbed DU is either eliminated in the urine, or it is deposited in various organs, such as the bone, soft tissues, or the liver. Some of the deposited DU will be transported by macrophage uptake to the lymph nodes, and DU in the lymph nodes will eventually be removed by blood absorption.

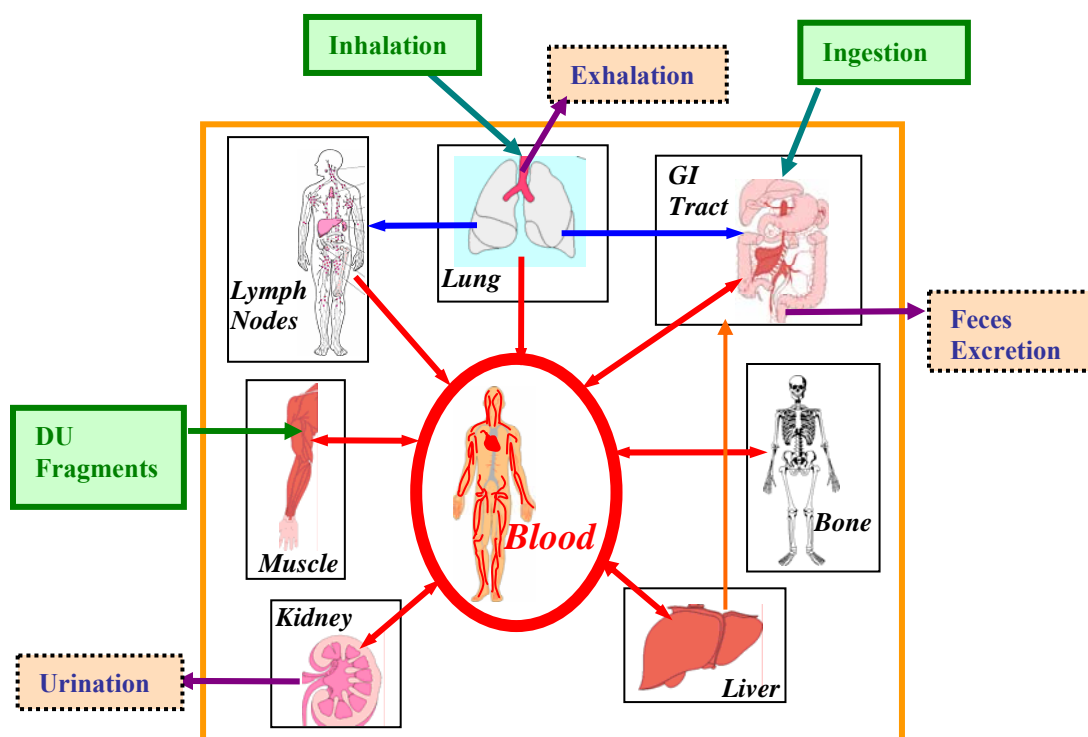


Figure 20. Potential human pathways for depleted uranium

Ingested DU moves through the GI system and is eliminated by muscular contraction (peristalsis) of digestive organs. A small fraction of the ingested DU is absorbed by the blood in the small intestines. As for inhaled DU, once it has entered the blood stream it will be either quickly eliminated in the urine or deposited in various organs. For the situation in which DU shrapnel is embedded in muscle (friendly fire scenario), the fragment will slowly dissolve, and DU will be absorbed by the blood. Again, DU in the blood stream will either be eliminated in the urine or deposited in various organs. DU deposited in the various body organs will be gradually reabsorbed by the blood, where it can be either eliminated in the urine or redeposited among the organs.

## 4.1 Biokinetic Model

The biokinetic analysis is based on the established biokinetic models developed by the ICRP [15, 24, 25, 26]. The overall biokinetic model is illustrated schematically in Figure 21. As noted in the preceding paragraphs, inhaled DU is deposited in various regions of the respiratory system. The model for cilia transport of DU between compartments within the respiratory system is also illustrated schematically in Figure 21. The figure legend identifies the organs and organ compartments with the symbols in the figure. Figure 21 also shows the detailed pathways for DU transport through the body organs. Note that the target organs are generally represented by more than one compartment, labeled compartments 1 and 2. The most recent applicable ICRP model [26] uses more than two compartments for the soft tissues, and the transport of uranium between the bone compartments is more complex than in the model adopted for this study. A discussion of these simplifications and a more detailed discussion of the biokinetic model are presented in Appendix C.

The biokinetic model permits a detailed time-dependent analysis of the passage of DU through the various organs of the body. The ICRP models are the product of an extensive long-term effort by an international group of scientists, and they are based on detailed research and theoretical considerations. The models use sets of differential equations along with basic input data, such as the internalized DU mass, the dissolution rates for uranium, and organ region-dependent particle transport rates. Some of these data

have been furnished with the basic ICRP models. Other data depend on the specific case under investigation. Some of the important case-dependent data include

- the amount of DU taken into the body
- the time dependence of DU intake (acute or chronic intake rate)
- the mode of entrance into the body
  - inhalation
  - ingestion
  - embedded fragments or contaminated wounds
- the size of particulate and fragments
- the dissolution rate of DU in body fluids (depends on chemical form)
- the elapsed time following DU exposure.

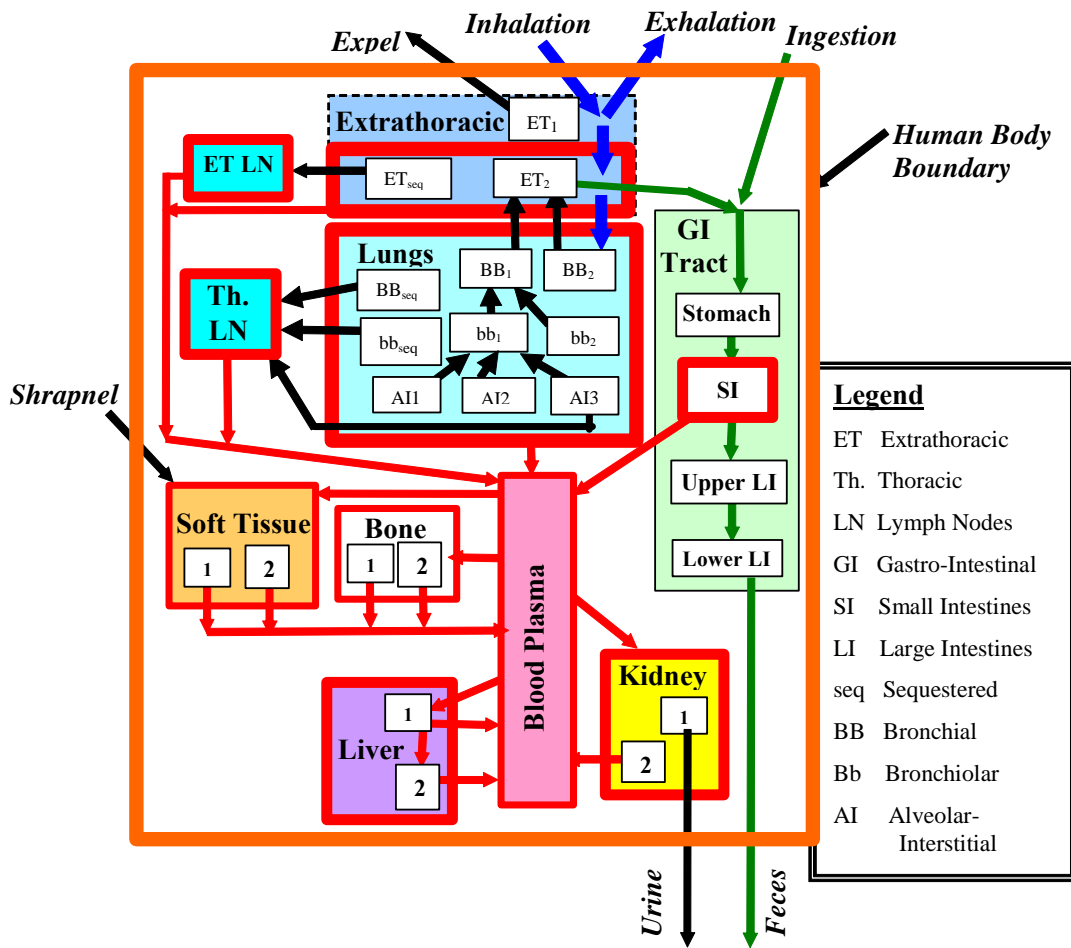


Figure 21. Schematic illustration of overall biokinetic model used in this study

## 4.2 Acute Inhalation and Ingestion

The transport of DU within the human body for the cases of acute inhalation and acute ingestion is described in this section to illustrate the general biokinetic behavior of internalized DU.

### 4.2.1 Acute Inhalation

Acute inhalation applies to all veterans and to civilian populations downwind from aerosolized DU during the time of battle. One of the principal particulate parameters required for the inhalation dose analysis is the Activity Median Aerodynamic Diameter (AMAD). The AMAD is the diameter in an aerodynamic particle size distribution for which the activity of particles having greater diameters make up 50% of the total activity. However, the Capstone data suggest that the particulate size distribution is bimodal rather than a simple lognormal distribution characterized by an AMAD. For this study, impact-generated aerosols were found to be reasonably characterized by assuming a bimodal distribution with peaks at about 0.5  $\mu\text{m}$  and 5  $\mu\text{m}$  [5: Attach. 1, p. 6.42].

The chemical composition of DU particulate generated by impact and chemical reaction with the air is typically the insoluble oxide  $\text{U}_3\text{O}_8$ . A small fraction of the particulate also includes the more soluble oxide  $\text{UO}_3$  [5: Attach. 1, p. ix]. A review of data from the Capstone report suggests a slowly soluble fraction of about 0.80 with a dissolution rate of about  $0.004 \text{ d}^{-1}$  ( $\text{d} = \text{days}$ ) and a rapidly soluble fraction of 0.20 with a dissolution rate of about  $8 \text{ d}^{-1}$ . Appendix B discusses the selection of the particulate parameters.

The time dependence of inhaled DU remaining in the body (plotted in Figure 22 for all organs) was calculated using the equations developed in Appendix C. Observe that all but about 10% of the inhaled DU is either exhaled or rapidly cleared ( $\sim 1$  day) by ciliary action or blood absorption. Most of the 10% of DU remaining in the lung after one day will eventually be absorbed by the blood, and all but about 1/3 of the DU absorbed by the blood will be rapidly excreted in the urine. Thus, about 3% of the inhaled DU will be redeposited in the kidney, bones, and other organs. The DU deposited in these other target organs will be eventually reabsorbed by the blood and excreted in the urine or

redeposited again among various organs. Within less than two years, only 1% of the inhaled DU is retained.

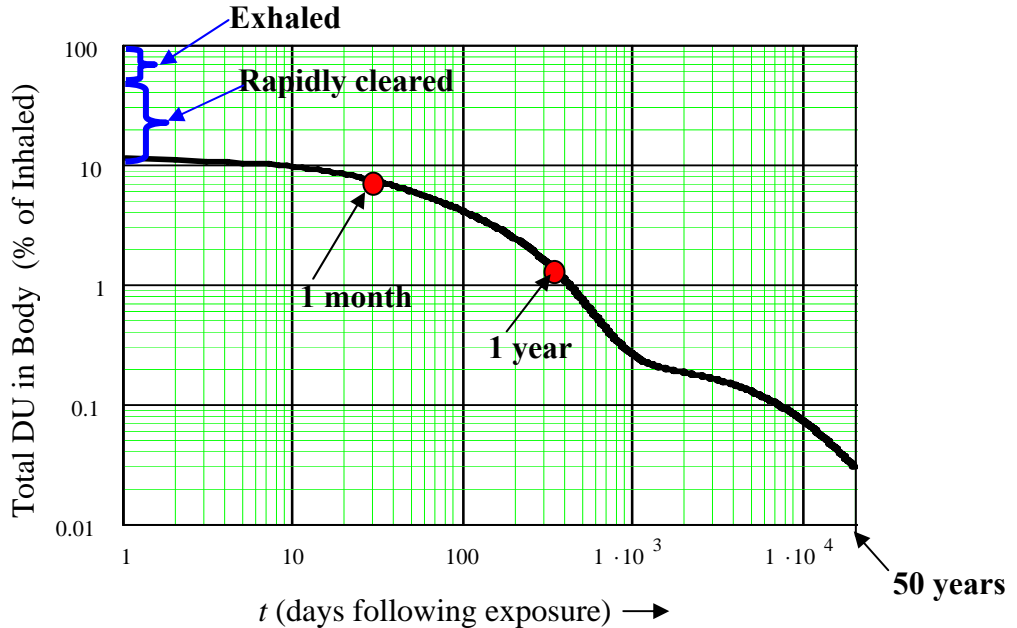


**Figure 22. Percent of inhaled DU in body vs. time after exposure for acute ingestion**

The time-dependent percentages of the inhaled DU in the principal organs are presented in Figure 23. As noted above, a significant fraction of the inhaled DU is cleared by ciliary action. Most of the cleared DU is swallowed and enters the GI tract where it is rapidly excreted. Only a small percentage of the DU entering the GI tract is absorbed by the blood. The amount of inhaled DU entering the blood stream via the GI tract is only about 0.4%. Although the lung is cleared of DU more quickly than for other organs shown in the figure, the initial concentration of DU in the lung is significantly greater than the maximum DU concentrations in other organs. DU buildup by blood deposition in organs occurs in less than one day; consequently, the buildup is not observable in the logarithmic plots in Figures 23 (origin for plot is one day). Although the DU concentration in the kidney drops more quickly than for the bone and soft tissue, the maximum DU kidney concentration at one-to-two days is the more important concern for assessing potential heavy metal toxicity. By forty to fifty years following exposure, the largest percentage of the remaining inhaled DU is predicted to be found in the bone and the soft tissues. However, the quantity of DU in the bone and soft tissue is very small.

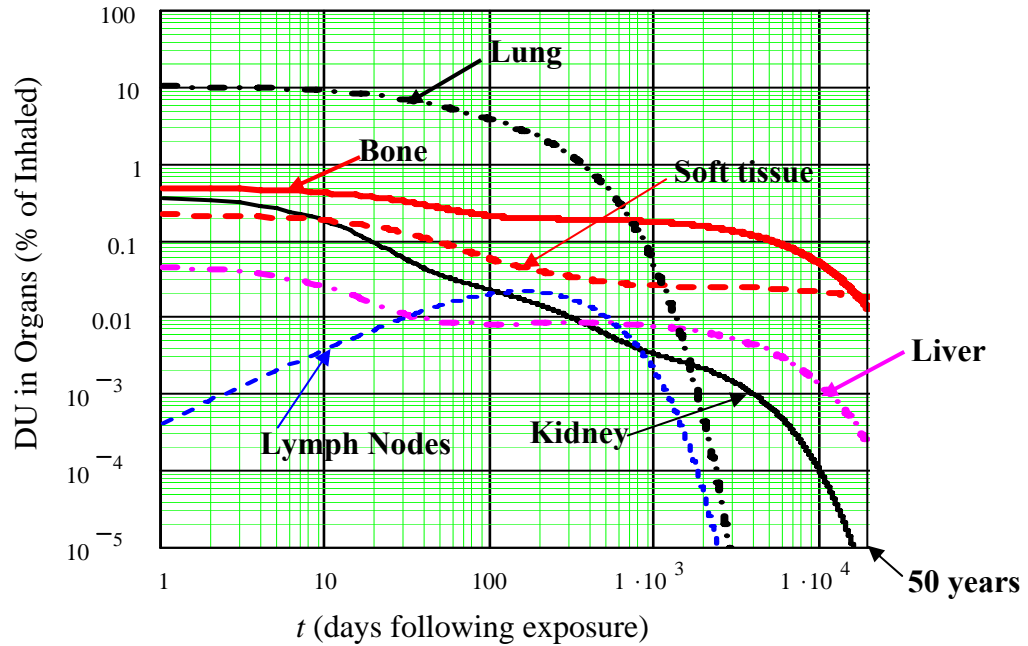


**Figure 23. Percent of inhaled DU in major organs vs. time after inhalation for acute ingestion**

#### 4.2.2 Acute Ingestion

Acute ingestion of DU applies primarily to military personnel. For friendly fire veterans, ingested DU will result from either clearing of inhaled DU particles from the lungs and swallowing, from hand-to-mouth contact with DU-contaminated hands, and in some cases from contaminated food or water. It is generally assumed that for the GI tract, all of the absorption by the blood takes place in the small intestines. The fraction of the ingested DU absorbed by the blood is about 1.4%. For the case of acute ingestion, the equations for the time-dependent fractions of DU in the GI system organs are developed in Appendix C. Using these equations, the DU concentrations in the GI system organs were calculated and plotted in Figure 24. As can be seen, ingested DU does not remain very long in the GI tract.

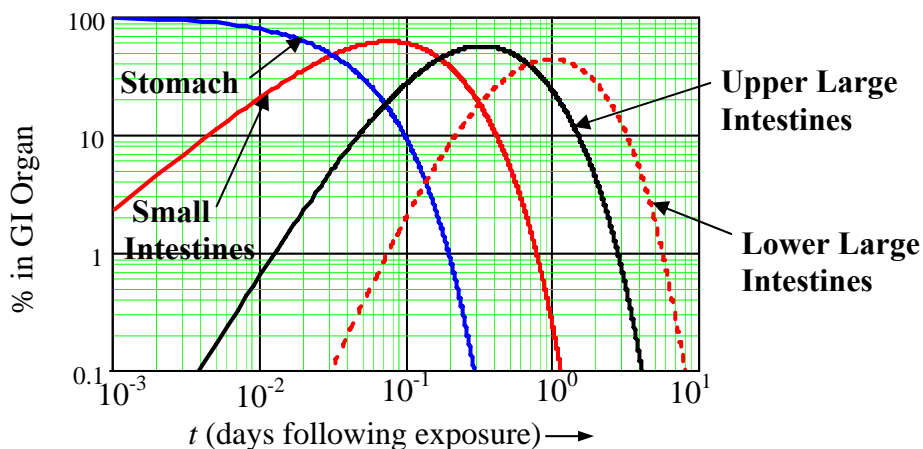


**Figure 24. Time dependence of the percent of DU in the GI tract organs following acute ingestion**

### 4.3 Biokinetics for Veterans

Level I veterans were exposed to DU by inhalation of DU aerosols, imbedded fragments, wound contamination, and ingestion of particulate. The DU internalized mass for Level II and III veterans was generally less significant than for Level I, does not include embedded fragments, and can be estimated using the basic biokinetic models developed for Level I veterans. Given these considerations, the following discussion focuses primarily on the biokinetics for Level I veterans.

#### 4.3.1 Level I

The DU mass deposited in the lungs, absorbed by the blood, and redeposited in other organs was computed using the acute-inhalation biokinetic model. The time-dependent DU mass per gram of organ for the inhalation of 250 mg of DU (from Table 13) is presented in Figure 25. The basic approach to determine DU deposition in target organs from dissolution of DU fragments was similar to the approach used for blood distribution of DU to target organs from inhalation. For the fragment case, however, a constant fragment dissolution rate was assumed, as discussed in Appendix C. The combined effect of DU inhalation and fragments on DU concentrations in various organs is presented in Figure 26. When fragments are included, it is seen that the concentrations of DU in the kidney, bone, and liver do not decline appreciably after 100 days, and the DU concentrations in the soft tissues increase after a few years. Thus, the effect of

fragments must be considered when assessing the radiological and chemical toxicity of DU. A reliable method for quantifying wound contamination has not been identified; however, the effect of wound contamination by DU particulate is expected to be small compared to the effect of fragments. Thus, exclusion of the effect of wound contamination should not alter the conclusions of this study.

For the estimated ingested masses for Level I veterans, the time-dependent DU mass to the GI tract and other organs was assessed using the standard ICRP biokinetic model described in Appendix C. This study found that for Level I veterans, the small quantity of ingested DU did not produce a significant dose to organs in the GI tract, and the effect on other organs was insignificant relative to the effects of inhaled DU.

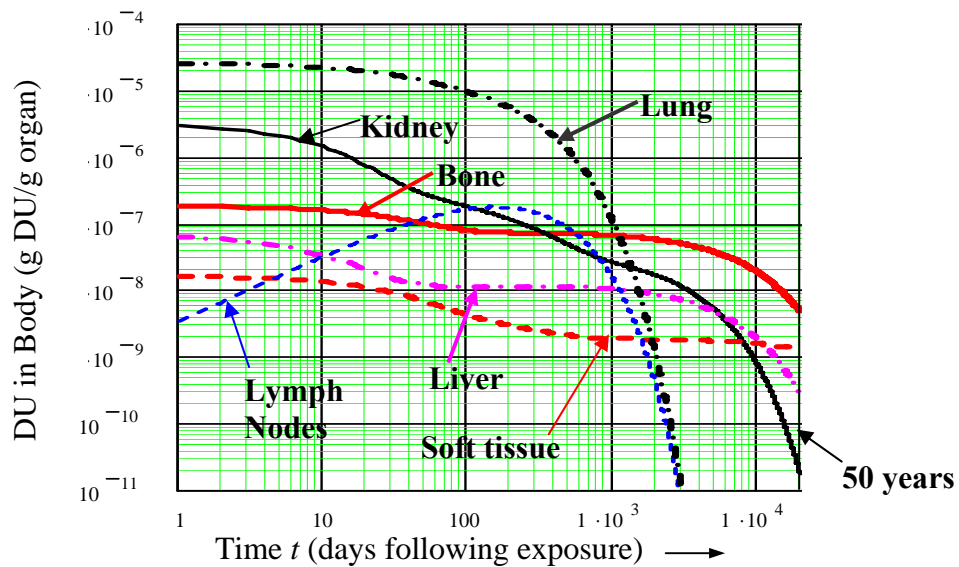


**Figure 25. DU mass/g organ vs. time for nominal Level I inhalation for the nominal case**

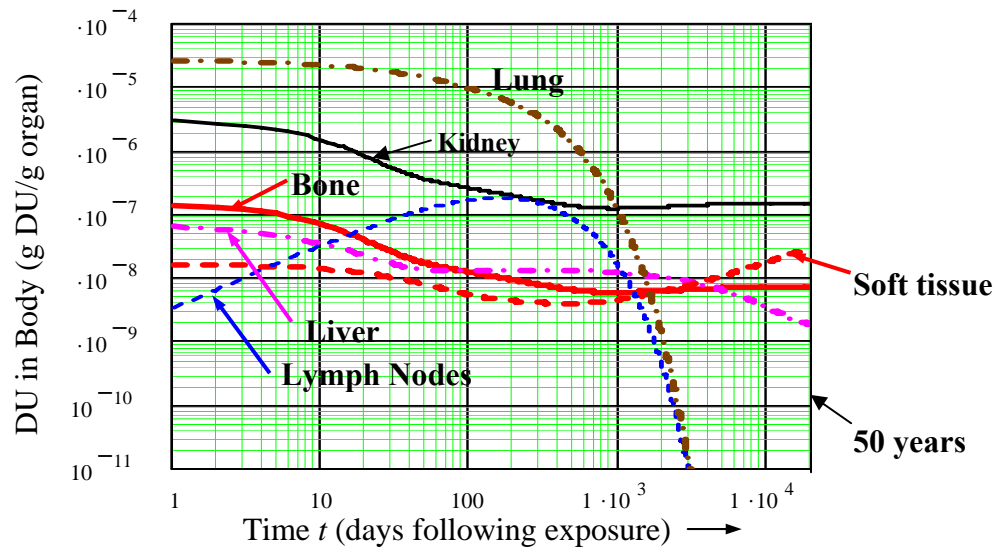


**Figure 26. DU mass/g organ vs. time for Level I inhalation with DU fragments for the nominal case**

### 4.3.2 Levels II and III

DU inhalation for Level II and III veterans occurred over relatively brief time periods. As a consequence, the biokinetic behavior for these cases can be modeled using the acute inhalation model, and the calculated biokinetic behavior shown in Figure 25 approximates the relative DU behavior in the body for Levels II and III veteran DU inhalation. The absolute value for DU concentrations in the organs (g DU/g organ) can be obtained by simply scaling the Level I organ concentrations by the inhaled DU masses for Levels II and III relative to the inhaled DU mass for Level I veterans.

## 4.4 Biokinetics for Civilians

Biokinetic models for civilians are essentially the same as those used for veterans. The principal difference in the biokinetic analysis for civilians, relative to veterans, is that civilian exposure is chronic rather than acute. For children, the breathing rate and organ masses will differ as well. In addition, the estimated high-ingestion intake for children playing in the post-battle zone required an analysis of the time-dependent concentrations of DU in the GI tract.

#### **4.4.1 Child at Play**

A child playing in or near vehicles destroyed by DU munitions may inhale or ingest significant quantities of DU. Depleted uranium inhalation was examined for both the nominally and maximally exposed child playing both inside and outside DU-contaminated vehicles over a period of 10 years. The model used to estimate the resulting DU masses in civilian internal organs for this scenario differs from the Level I veteran model in that it permits chronic exposure to DU for 10 years followed by 40 years with no DU exposure. Using this chronic exposure model for a maximally exposed child, the time-dependent DU masses in organs were computed and are presented in Figure 27 as a function of time. The calculated DU concentrations in Figure 27 include both inhalation and ingestion resulting from play within a contaminated vehicle and in contaminated soil external to the vehicle. From the study of veteran exposures, it was found that DU in the lymph nodes does not present a significant cancer risk; consequently, no calculations were made for lymph node DU concentrations for civilians. The significant hand-to-mouth activity and extended-duration battle-zone play assumed for these children resulted in substantial chronic ingestion of DU particulate. Thus, chronic ingestion had an appreciable effect on radiological exposure for the GI tract (GI tract organ concentrations not shown in Figure 27) for children playing in the battle zone.

#### **4.4.2 Downwind Civilians**

Civilians living downwind from a battlefield may inhale battle-generated DU particulate that becomes entrained in the air and carried by wind. Civilians may also inhale DU that has been deposited on the ground and subsequently resuspended by wind and human or animal activity. As discussed in Section 2, DU intake from contaminated crops and water does not appear to be significant. Using the model for chronic inhalation exposure, time-dependent DU masses in the body organs were computed for downwind civilians. The total DU mass in the various organs for downwind civilians is the sum of the contributions from the DU cloud (puff) produced by impact and the contribution from resuspended DU. The time-dependent total DU organ masses for downwind civilians are shown in Figure 28. Note that the DU concentrations in the major organs for downwind

civilians (shown in Figure 28) are several orders of magnitude smaller than the values for Level I veterans shown in Figures 25 and 26.

The time-dependent DU concentrations in various organs, discussed in this section, can now be used to assess possible heavy metal toxicity effects and the organ doses and risks from internal radiation. DU-related health risks are discussed in Section 5.

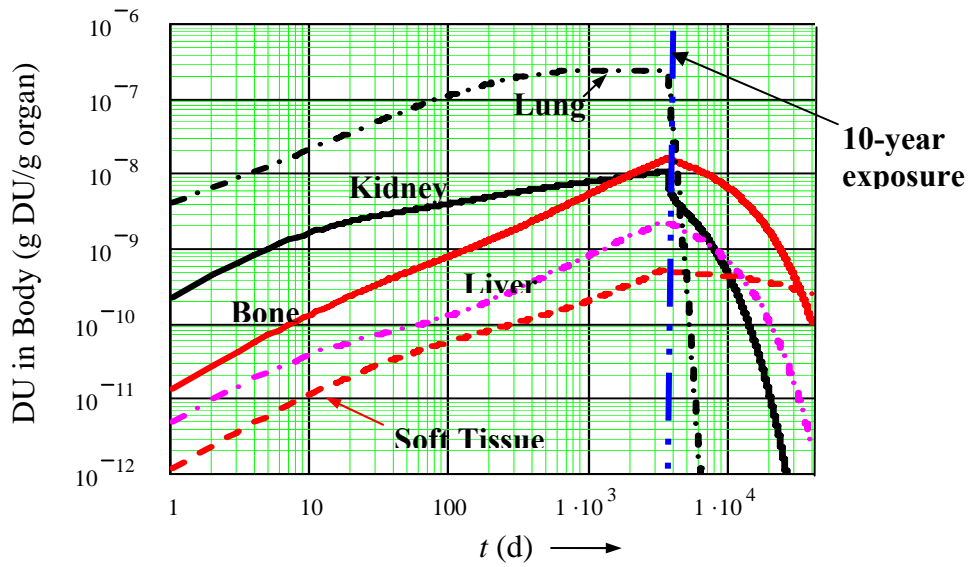


Figure 27. DU mass/g of organ vs. time for maximally exposed child at play

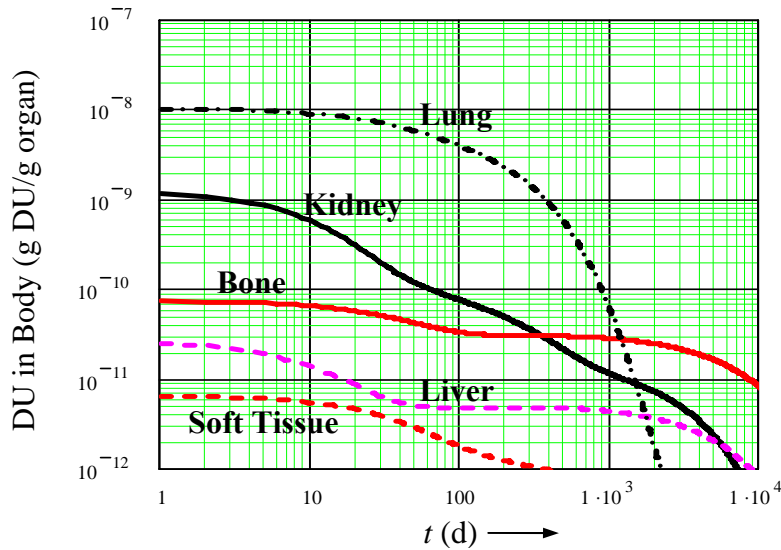


Figure 28. DU mass/g of organ as a function of time for downwind civilian. Maximum case (puff plus resuspended DU inhalation).



## 5.0. Health Effect Estimates

Potential health effects from DU exposure include both chemical and radiologically induced effects. Chemical effects relate to the heavy-metal toxicity of uranium, such as the potential for kidney damage or neurotoxic effects. Potential radiological effects include cancers and genetic effects. Appendix D provides a more detailed discussion of uranium properties and chemical health effects from internalized DU. Radiological dose concepts and calculations are discussed in Appendices A and E, respectively.

### 5.1 Kidney Heavy Metal Effect

The principal health effects from DU exposure considerations relate to heavy-metal effects on the kidney. The heavy-metal effect on the kidney from internalized uranium can be addressed by comparing the estimated uranium concentrations in the kidney with the uranium effects guideline in Table 6.

#### 5.1.1 Estimated Concentrations vs. Guidelines

The uranium concentrations in the kidney for Level I veterans are presented in Figure 29 as a function of time after exposure. DU concentrations are provided for the nominal and maximum exposure cases for both inhalation-only and inhalation plus fragments. The peak concentration for the nominal case is, coincidentally, essentially at the 3- $\mu\text{g}$  U/g kidney worker limit. The estimated peak DU concentration for the maximum inhalation case is very high and is, also coincidentally, approximately equal to the LD/50 concentration. Uncertainties in kidney/heavy-metal dose/effect correlations and variability among individual responses do not permit conclusive comparisons of estimates with medical test results.

Figure 27 shows that for the maximally exposed child at play, chronic exposures are less than 0.01  $\mu\text{g}$  DU/g. This very low exposure is below the minimal value reported for adverse kidney effects from chronic exposure. A similar calculation for the nominally exposed child gave an estimated chronic dose of only  $\sim 0.001$   $\mu\text{g}$  DU/g kidney. For

downwind civilian populations, the estimated kidney concentration is insignificant for both the exposure to a DU puff during battle and exposure to resuspended DU. A summary of the kidney exposures for all cases studied is provided in Table 13.

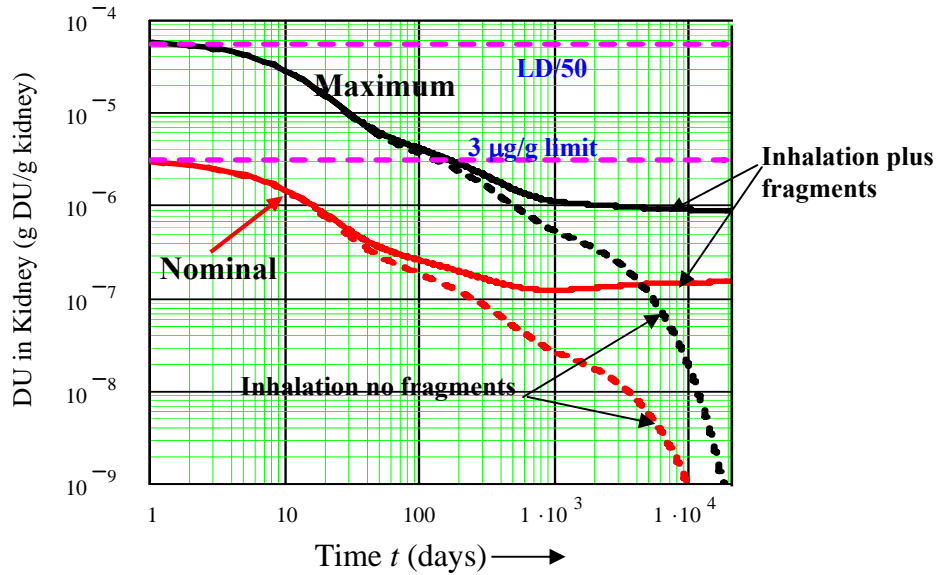


**Figure 29. Grams DU/g kidney as a function of time for Level I veterans for inhalation with and without fragments**

**Table 13. DU concentrations in kidney for Gulf War veterans and Iraqi civilians**

Case	Exposure	( $\mu\text{g/g kidney}$ )	
		Acute	Chronic
Level I Veterans	Nominal	3	$\sim 0.1$
	Maximum	53	$\sim 1.0$
Level II Veterans	Nominal	0.5	$\sim 0.01$
	Maximum	8	$\sim 0.1$
Level III Veterans	Nominal	negligible	negligible
	Maximum	0.08	$\sim 0.001$
Child at Play	Nominal	–	$\sim 0.001$
	Maximum	–	$\sim 0.01$
Downwind Civilian	Nominal	negligible	negligible
	Maximum	0.0005	negligible

### **5.1.2 Kidney Health Effects Assessment**

Although adverse kidney health effects have not been reported for Level I veterans, maximally exposed veterans may have experienced undiagnosed transient kidney effects associated with high concentrations of DU in the kidney. Our current understanding suggests no long-term effects on the kidney; nonetheless, the potentially significant kidney damage predicted for some Level I veterans merits careful consideration and continued monitoring. The fact that no kidney failure fatalities or hospitalization has been reported for Level I veterans suggests that exposures significantly higher than the estimated values are unlikely.

The analysis in Appendix E estimates the uncertainty in the calculated DU kidney concentration for a child at play is about a factor of three. For the downwind civilians, the uncertainty of the estimated DU kidney concentration is within an order of magnitude. Thus, the calculations for all civilians show low uranium concentrations in the kidney, even when uncertainties are included. These results suggest that no adverse kidney effects will result for Iraqi civilians.

## **5.2 Other Heavy Metal Effects**

Some evidence has been reported for the possibility of other chemical effects associated with uranium internalization (see Appendix D). Because uranium is a heavy metal, it may be associated with neurotoxic effects. Pellmar et al. [27] studied rats implanted with DU pellets. Although Pellmar found that excitability of neurons in the hippocampus was reduced for rats with significant internalized DU, no behavioral differences were observed from a battery of behavioral tests. Among the tested veterans, McDiarmid's team observed a statistically lower score in one type of neurocognitive test for veterans with high uranium concentrations in their urine. However, the slight neurocognitive effects did not appear to affect normal functioning; and the measured effect appears to be declining [19]. Lewis conducted uranium inhalation tests on rats to determine whether or not inhaled DU particulate can enter the brain directly through the nasal cavity without crossing the blood-brain barrier [28]. Preliminary results show that uranium passed directly to the brain and appears to be preferentially deposited in the

substantia nigra area of the brain. These preliminary observations do not provide sufficient evidence to support or refute a possible linkage between DU exposure and adverse neurocognitive effects. Although significant cognitive impairment has not been observed, further study of this topic is warranted.

Veteran, animal, and in vitro testing suggests that a few other chemically induced health effects are possible, such as reproductive effects and chemically induced cancers. However, epidemiological data for humans with exposure to elevated levels of uranium particulate do not show an increase in health effects of any type, relative to the general population (refer to Appendix D). The evidence for other chemically induced DU effects is not, at present, well established.

## **5.3 Veteran Internal Radiation Exposure**

Both internal and external radiation effects are considered in this study. Internal radiological exposures result from internalization of radioactive materials. For DU, internal radiation is far more important than external radiation. Internal radiation for veterans was examined for inhalation and ingestion of DU particulate as well as DU deposited in organs from dissolution of DU fragments embedded in the body.

### **5.3.1 Veteran Doses**

The doses to various organs were calculated using the estimated time-dependent DU mass in the principal target organs (discussed in Section 3, and the methodology for computing dose is described in Appendix E). Almost the entire equivalent internal dose (~99%) is from alpha particle emission; the remainder is primarily from gamma and beta activity from Th-234 and Pa-234m. The activity from the uranium isotopes U-234, U-235, and U-236 makes up about 17% of the total DU alpha particle activity. The dose from trace actinides (e.g., Pu) is less than 1%. Thus, internal dose contributions from other uranium isotopes, from trace actinides, and from daughter products (Th-234 and Pa-234m) were accounted for by increasing the calculated dose from U-238 alpha decay by 20% (refer to Appendix E).

For Level I veterans, the doses and risks presented in Table 14 were computed for a period of 50 years following exposure. Equivalent doses are given for nominal and maximum exposures assuming DU inhalation with and without imbedded fragments. The effective dose was obtained as the sum of the weighted organ doses. Radiation health risks are readily determined by multiplying equivalent organ doses by risk coefficients.

**Table 14. Level I veteran lifetime equivalent doses from DU exposure**

<b>Organ</b>	<b>Inhalation-Only (Sv)</b>		<b>Inhalation + Fragment (Sv)</b>	
	<b>Nominal</b>	<b>Maximum</b>	<b>Nominal</b>	<b>Maximum</b>
Lung	0.125	2.0	0.125	2.0
Bone surface	$8.7 \times 10^{-3}$	0.14	0.104	0.69
Bone marrow	$1.1 \times 10^{-3}$	0.017	0.012	0.083
Lymph nodes	0.02	0.31	0.02	0.31
Kidney	$3.0 \times 10^{-3}$	0.048	0.046	0.30
Liver	$1.1 \times 10^{-3}$	0.018	$1.6 \times 10^{-3}$	0.021
Soft tissue	0.0005	0.008	0.005	0.035
Effective Dose	0.015	0.25	0.019	0.265

To provide perspective, the effective dose for DU-exposed veterans is compared to the average U.S. background dose and the maximum permitted dose for radiation workers in Figure 30. The maximum permitted radiation worker dose does not include the exposure contribution from background radiation. About 85% of the U.S. background dose is from natural sources, such as radon gas and cosmic radiation. The remainder of the background dose is mostly from medical procedures, such as x-rays. For this comparison, standard exposure lifetimes were assumed. A 50-year post-exposure duration was assumed for both the veteran exposures and the U.S. background dose. For radiation workers, a 35-year exposure period was used. As can be seen, even for the maximum case, the accumulated dose for a DU-exposed veteran is less than the allowed accumulated dose for a radiation worker. For all other cases, the dose from DU exposure is less than the background exposure dose. The dose for Level III veterans is calculated to be extremely small.

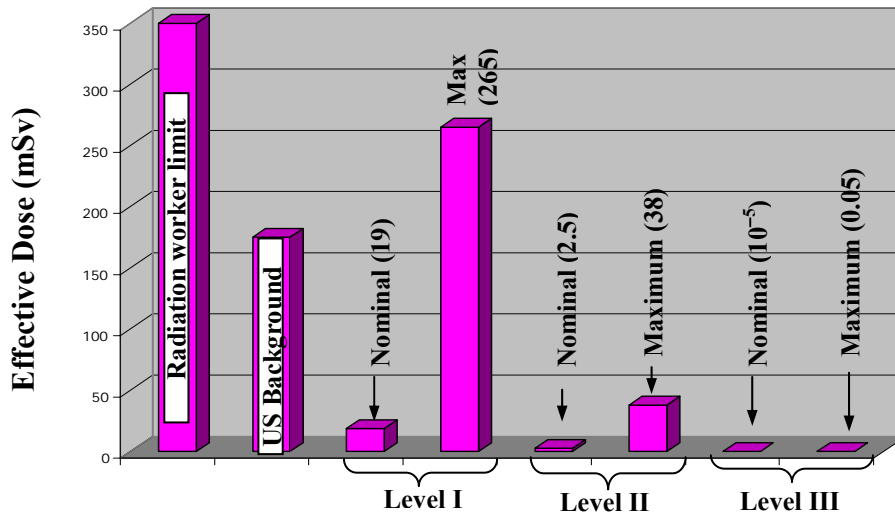


**Figure 30. Comparison of lifetime veteran dose from DU exposure with U.S. background dose (50 years) and maximum radiation worker dose (35 years)**

### 5.3.2 Cancer Risks

Estimated cancer risks for Level I veterans are presented in Table 15. Predicted risks are given for inhalation with and without embedded fragments for both the nominal and maximum cases. As can be seen, the risk of lung cancer is 0.014 (1.4%) for the maximally exposed Level I veteran. DU fragments are predicted to increase non-respiratory system cancer risks. However, even for the maximum case with fragments included, the risks for all other cancer types are very small. For the maximally exposed Level I veteran with fragments, the risk of leukemia is only 0.0003 (0.03%). No evidence has been found for radiation-induced brain cancer below the very high exposure of 1 Gy [29: pp. 122-125] (20 Sv for alpha particles). The brain (categorized as a soft tissue) is predicted in Table 16 to receive a maximum dose of only 0.035 Sv; consequently, the risk of radiation-induced brain cancer was dropped from further consideration. Similarly, the risk of radiation-induced lymph cancer is extremely small, and lymph cancer was not included in the analysis of other exposure scenarios.

**Table 15. Predicted Level I veteran lifetime fatal cancer risks from DU exposure**

<b>Cancer</b>	<b>Inhalation-Only Risk</b>		<b>Inhalation + Fragment Risk</b>	
	<b>Nominal</b>	<b>Maximum</b>	<b>Nominal</b>	<b>Maximum</b>
Lung	$8.5 \times 10^{-4}$	0.014	$8.5 \times 10^{-4}$	0.014
Bone tumor	$3.5 \times 10^{-6}$	$5.6 \times 10^{-5}$	$4.1 \times 10^{-5}$	$2.8 \times 10^{-4}$
Leukemia	$4.2 \times 10^{-6}$	$6.7 \times 10^{-5}$	$5.0 \times 10^{-5}$	$3.3 \times 10^{-4}$
Lymph Nodes	$9.0 \times 10^{-8}$	$1.4 \times 10^{-6}$	$9.0 \times 10^{-8}$	$1.4 \times 10^{-6}$
Kidney	$3.0 \times 10^{-6}$	$4.8 \times 10^{-5}$	$4.6 \times 10^{-5}$	$3.0 \times 10^{-4}$
Liver	$1.3 \times 10^{-6}$	$2.2 \times 10^{-5}$	$1.9 \times 10^{-6}$	$2.5 \times 10^{-5}$
Total	$6.2 \times 10^{-4}$	0.014	$9.9 \times 10^{-4}$	0.0143

Similar calculations were performed for Level II and III veterans. The best-estimate risk of DU-induced fatal lung cancer, leukemia, and the total DU-induced fatal cancer risk for all exposed veterans is summarized in Table 16. The upper bound for all predictions is obtained by multiplying the risk prediction by the multiplier  $\mathcal{M}_c$  given in the bottom row for each column. The risk multiplier is based on the uncertainty analysis described in Section 6 and is defined in the Glossary in Appendix F.

To provide a more intuitive understanding of projected risks, Table 16 presents risk as a percent rather than a fraction. Table 16 also provides the national average of fatal cancer risks for comparison. The risk of fatal lung cancer for the U.S. national average is about 7%, and the lifetime risk of fatal leukemia for the general population is about 1%. The risk of fatal lung cancer for nonsmokers is very small; however, the national average for lung cancer (which includes a mixture of smokers and nonsmokers) is about 7%. For the general population, the percent of all fatalities from all cancers is about 24% [30]. Only a few Level I veterans inhaled sufficiently large quantities of DU to incur a 1.4% risk of lung cancer (3.5% upper bound). The cancer risks for most veterans are much smaller than for a maximally exposed Level I veteran.

**Table 16. Predicted incremental fatal cancer risks for veterans from internal DU exposure compared to percentage of all U.S. civilian fatalities from cancer**

Cancer Type		Level I		Level II		Level III		U.S. Avg. (%)
		Nom. (%)	Max (%)	Nom. (%)	Max (%)	Nom. (%)	Max (%)	
Lung		0.085	1.40	0.014	0.210	10 <sup>-6</sup>	0.002	7
Leukemia	<i>Inhaled*</i>	0.0004	0.007	0.0001	0.001	10 <sup>-8</sup>	10 <sup>-5</sup>	1
	<i>+ Fragments</i>	0.005	0.03					
<b>Total Fatal Cancer Risk</b>		0.099	1.43	0.014	0.210	10 <sup>-6</sup>	0.002	24
<b>Number of Veterans</b>		~150	few	~700	few	Hundreds		
<b>Multiplier <math>\mathcal{M}_c</math></b>		~2.5		~2.5		~14		

Risk projections are properly understood in terms of large populations rather than as a risk projection for an individual. For example, if we look at a sample of 10,000 people from the U.S. population, Table 16 predicts for the U.S. average that 2,400 will eventually die from cancers and the rest will die from other causes. If all 10,000 people received the nominal Level II exposure to DU, Table 16 predicts one or two DU radiation-induced fatal cancers in addition to the 2,400 cancers from spontaneous causes.

### 5.3.3 Radiation from Embedded Fragments

Although the foregoing discussion included the effect of dissolution of DU fragments and uranium deposition in organs, the discussion did not address the effect of alpha particle bombardment of tissue near the surface of embedded fragments. The radiation doses at these locations are very high and may result in localized cancer risks greater than those predicted using standard ICRP models. The local alpha particle dose, however, will mostly induce cell killing rather than nonfatal DNA damage to the cell. Nonetheless, cancers may be induced in the less intense radiation field near the boundary of the alpha particle range. The contribution of beta particles to the local dose must be considered as well. Furthermore, recent studies have suggested a so-called bystander effect in cancer induction. These studies indicate that cancers may be induced in cells that have not been radiation damaged but are in close proximity to radiation-damaged cells.

Tests on rats by Hahn et al. [31] showed the development of soft-tissue sarcomas at the location of large surgically implanted squares. Although the DU implant size is comparable to the size of DU fragments remaining in the bodies of some Level I veterans, the body mass of a veteran is roughly 100 times greater than the body mass for the rats used in the experiments. Hahn observed a DU-fragment surface area dependence wherein 1 x 2 mm pellets did not induce tumors, 2.5 x 2.5 x 1.5 mm squares induced tumors in 6% of the test rats, and 5 x 5 x 1.5 mm squares induced tumors in 18% of the test rats. Leggett and Pellmar [32] conducted similar tests and also found that 1 x 2-mm pellets did not induce tumors. Hahn points out that rats are more implant-sensitive and more radiation-sensitive than humans. For many materials, tissue reactions that have been observed in rats do not occur for humans. Although sarcomas in the vicinity of embedded fragments have not been reported in the literature for veterans, these animal tests suggest further study and continued monitoring of veterans with embedded fragments.

#### **5.3.4 Genetic Risks**

The incremental risk of DU-induced birth defects for veterans is estimated by multiplying the equivalent dose to the gonads by 0.008 per person-Sv. This risk estimate applies to equilibrium conditions (i.e., the genetic effect established after several generations). The genetic risk for first-generation birth defects is at least five times smaller than for equilibrium conditions. Table 19 provides the genetic risk for veterans for the nominal and maximum cases. These predictions are compared to the U.S. average of ~8% of live births resulting in serious birth defects [29: pp. 56-61]. Some sources estimate birth defects incidences appreciably greater than 8% per live birth [29: pp. 56-61, 33]. The U.S. average for all serious birth defects includes both genetic and nongenetic effects and includes birth defects recognized over a period of about one to two years following birth. Only about one-third of all birth defects are recognized at birth [29: p. 56, 33]. Genetic effects appear to comprise a bit more than half of all birth defects [29: p. 57].

From Table 17, we observe that the predicted risk of radiation-induced birth defects is extremely small and should not result in an observable increase in birth defects. Assertions of DU-induced birth defects apply to first-generation births, yet first-

generation genetic risk factors are at least five times smaller than equilibrium values. Thus, the findings from this analysis do not support the claim that the children of U.S. Gulf War veterans were born with serious birth defects at a rate that significantly exceeds projected incidents for unexposed veterans. Furthermore, as discussed in Appendix E, Gulf War veteran health statistics do not support claims of significant increases in birth defects for children of Gulf War veterans.

**Table 17. Incremental risk of serious birth defects for veteran progeny (equilibrium) from DU exposure, compared to U.S. average birth defects / live birth**

	Level I		Level II		Level III		U.S. Avg. (%)
	Nom. (%)	Max (%)	Nom. (%)	Max (%)	Nom. (%)	Max (%)	
<i>Inhaled</i>	0.0004	0.007	$6 \times 10^{-5}$	0.001	$6 \times 10^{-9}$	$10^{-5}$	~8
+ <i>Fragments</i>	0.0040	0.028					
<b>Number of Veterans</b>	~150	few	~700	few	Hundreds		
<b>Multiplier <math>\mathcal{M}_g</math></b>	~3		~3		~14		

## 5.4 Civilian Internal Radiation Exposure

The basic method used to predict the radiation dose for Iraqi civilians is the same as for veterans.

### 5.4.1 Civilian Dose

The dose to the major organs for both nominally and maximally exposed children is presented in Table 18. For the prolonged high-ingestion intake of DU assumed for a child at play, the radiation dose to the organs of the large intestines is comparable to the lung dose. The equivalent doses for a civilian downwind of the battle zone were computed for inhaled DU entrained in the air during battle (puff) and DU that was resuspended subsequent to battle. The doses to downwind civilians are also presented in Table 18. All radiological organ doses to downwind civilians resulting from inhaled DU are observed to be extremely small.

**Table 18. Lifetime equivalent internal radiation doses for civilians from DU exposure**

Organ	Battle Zone –Child (Sv)		Downwind Civilian (Sv)	
	Nominal	Maximum	Nominal	Maximum
Lung	0.041	0.164	$3.3 \times 10^{-6}$	$5.3 \times 10^{-5}$
Bone surface	$6.1 \times 10^{-3}$	0.024	$2.2 \times 10^{-7}$	$3.6 \times 10^{-6}$
Bone marrow	$7.3 \times 10^{-4}$	$3.0 \times 10^{-3}$	$2.7 \times 10^{-8}$	$4.4 \times 10^{-7}$
Stomach	0.002	0.006	–	–
Small intestines	0.0015	0.004	–	–
Large Intestines	0.064	0.19	–	–
Soft tissue	$3.4 \times 10^{-4}$	$1.3 \times 10^{-3}$	–	–
Effective Dose	0.013	0.044	$4.1 \times 10^{-6}$	$6.5 \times 10^{-6}$

Figure 31 compares the doses for a child playing in DU contaminated vehicles and for downwind Iraqi civilians with the world-average background dose. As for veterans, the civilian and background doses are for a 50-year post-exposure duration. Observe that even for the maximum-exposure case of child at play, the effective dose is much smaller than the world-average background dose. For downwind civilians, the dose is extremely small.

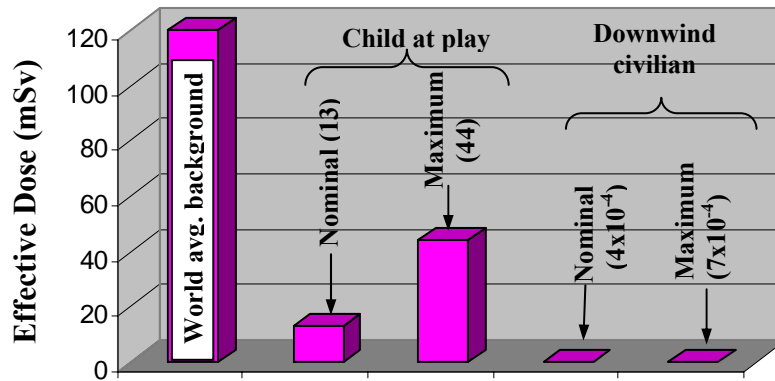


**Figure 31. Lifetime Iraqi civilian effective dose from DU exposure compared to the world-average background dose**

### 5.4.2 Cancer Risk

The predicted cancer risks (%) for civilians are compared to U.S. national averages in Table 19 (reliable Iraqi statistics were not found). A maximally exposed child playing in DU-destroyed vehicles for 300 hours and playing outside the vehicle for 700

hours is predicted to incur a maximum lung cancer risk of about 0.14%. The predicted risks of leukemia and colon cancer, for this maximally exposed child, are about 0.002% and 0.16%, respectively. For downwind civilians, the risk of cancer is very small.

**Table 19. Iraqi civilian lifetime fatal cancer risks from DU exposure compared to percentage of all U.S. civilian fatalities from cancer**

Cancer Type	Child at Play		Downwind		U.S. Avg. (%)
	Nom. (%)	Max (%)	Nom. (%)	Max (%)	
Lung	0.0350	0.140	$4 \times 10^{-6}$	$7 \times 10^{-5}$	7
Leukemia	0.0004	0.002	$4 \times 10^{-8}$	$10^{-6}$	1
Colon	0.0550	0.160	–	–	3
Total Fatal Cancer Risk	0.092	0.313	$3 \times 10^{-6}$	$5 \times 10^{-5}$	24
Multiplier $\mathcal{M}_c$	~3.5		~14		

### 5.4.3 Genetic Risks

The incremental risk of DU-induced birth defects for civilians is estimated by multiplying the equivalent dose to the gonads by 0.013 per person-Sv. Table 20 provides the incremental genetic risk for Iraqi civilians. No data were found for the national average of birth defects in Iraq; however, malnutrition, disease, and chemical toxins released into the environment may have resulted in an increase in Iraqi birth defects following the Gulf War. Table 20 shows that the risk of DU-induced birth defects for Iraqi civilians is predicted to be far too small to have resulted in observable increases in birth defects.

**Table 20. Incremental risk of serious birth defects for civilian progeny (equilibrium) from DU exposure compared to U.S. average birth defects / live birth**

	Child at Play		Downwind		U.S. Avg. (%)
	Nom. (%)	Max (%)	Nom. (%)	Max (%)	
Genetic Risk	0.0004	0.002	$10^{-8}$	$10^{-7}$	~8
Multiplier $\mathcal{M}_g$	~3.5		~14		

## 5.5 External Radiation Effects

Radiological exposures can also result from radiation emission from external sources, including undamaged DU penetrators, fragments, and particulates. External radiation effects were briefly studied for veterans and civilians. Figure 32 illustrates the relative intensities of the  $\alpha$ ,  $\beta$ , and  $\gamma$  fluxes as a function of distance into the body. The energies of the  $\alpha$ ,  $\beta$ , and  $\gamma$  particles assumed for Figure 32 are consistent with the radiations emitted by DU. As can be seen, external alpha particles do not penetrate the dead skin layer of the body; consequently, external alpha particle radiation does not present a health hazard to humans. Although the lens of the eye is not protected by a dead skin layer, credible exposures of the eye are not significant for alpha particle radiation from DU. External radiation by beta particles from DU can penetrate the dead skin layer, but cannot reach internal organs. Thus, beta particles from external sources may cause skin burns or increase the risk of skin cancer, but will not contribute to the cancer risk for internal organs. External gamma radiation, however, can penetrate through the body and reach internal organs.

### 5.5.1 Penetrator External Dose

The external dose rate from an unburied 120 mm DU penetrator was computed as a function of distance, as discussed in Appendix E. Figure 33 presents the gamma dose rate and the incremental whole-body fatal cancer risk from an intact DU penetrator as a function of distance from the penetrator for 100, 1000, and 10,000 hours of exposure. The incremental fatal cancer risk from gamma radiation is observed to be very small, even at close proximity for 10,000 hours.

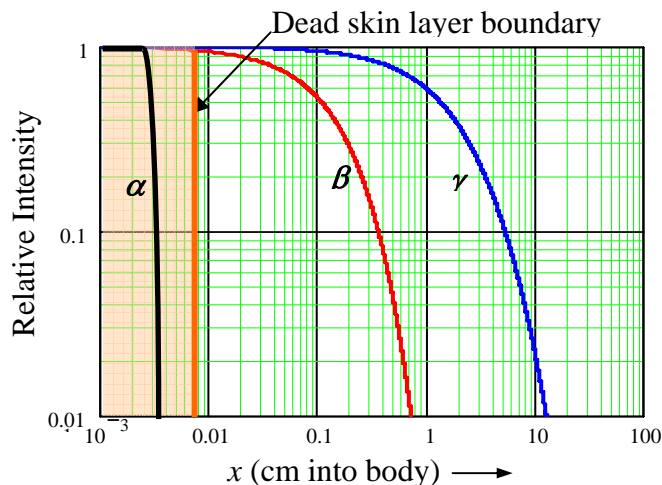


**Figure 32. Relative intensity of  $\alpha$ ,  $\beta$ , and  $\gamma$  fluxes vs. distance into body**

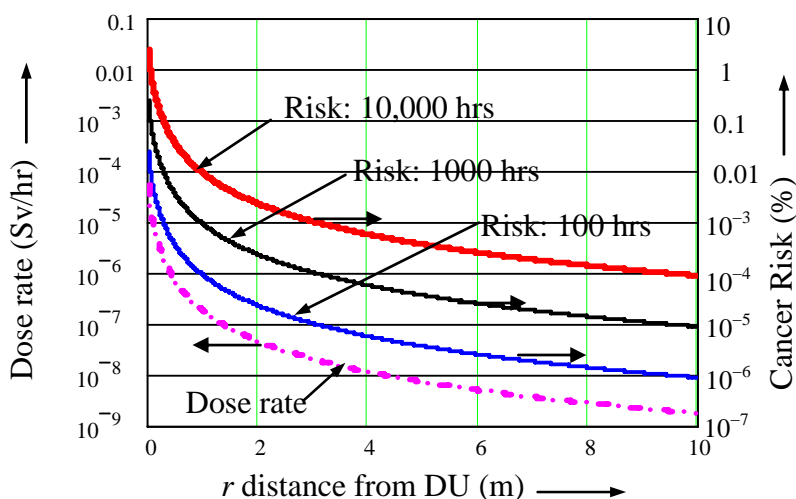


**Figure 33. Whole-body dose rate and incremental fatal cancer risk vs. distance from a DU penetrator (120 mm round)**

The U.S. DoD measured dose rates of  $<0.002$  mSv/hr to the occupants of an Abrams tank containing a full load of DU penetrator rounds [2: p. 136]. Based on this measured dose rate, the tank crew could occupy the vehicle 24 hours a day 365 days a year without exceeding international radiation worker guidelines. Fetter and von Hippel have estimated that the ground shine from a distribution of  $1 \text{ g DU/m}^2$  would be only  $0.01 \text{ mSv/yr}$  [3]. From Section 3, we found that the typical DU areal density is much lower than  $1 \text{ g DU/m}^2$ ; consequently, the dose from ground shine is insignificant.

## 5.5.2 Beta Burns and Skin Cancer

The beta radiation from DU exposure is very low, and an evaluation of the effect of long-term contact with the skin indicates that beta radiation burns should not result (as shown in Appendix E). However, long-term contact with a DU fragment or shell might result in a beta radiation-induced local skin cancer. The estimated risk of skin cancer as a function of exposure time is presented in Figure 34 for continuous exposure and for an average contact time of about 15 minutes a day (~1%). These predictions suggest that continuous direct-contact exposure for decades could significantly increase the risk of localized skin cancer (for example, a DU souvenir worn as a pendant). As shown in Appendix E, gamma radiation from the pendant is insignificant.

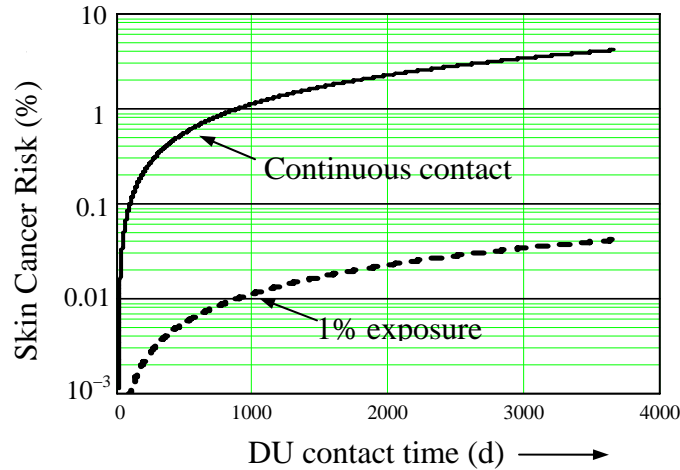


**Figure 34. Incremental risk of beta-radiation induced skin cancer from direct DU contact**



## **6.0. Validity of Analysis**

This section addresses the validity of the analysis methodology used to predict radioactive material dispersal and consequent health effects associated with exposure to the dispersed materials. Uncertainties in the data and models used in the study are estimated, and these uncertainties are used in an uncertainty analysis to estimate an upper bound for projected health effects. In addition, a number of issues are addressed that directly or indirectly challenge the standard methodology used to estimate dispersion and radiological health effects.

### **6.1 DU Source Terms and Internalized Mass**

With the exception of inhalation DU exposure and embedded DU fragments for Level I veterans, the accuracy of DU mass predictions directly affects the accuracy of the DU health-effect estimates for internalized DU. As mentioned in Section 3, a variety of methods were used to estimate DU source terms and internalized DU mass.

#### **6.1.1 In-Vehicle Post-Battle Exposure**

DU inhalation masses were estimated for veterans working in DU-contaminated vehicles and for children playing in DU-contaminated vehicles. For both of these cases, the inhaled DU mass was based on resuspension data from the Capstone study. For veteran in-vehicle-resuspension calculations, the measured maximum DU air concentration per shell was used in the analysis; consequently, no upper-bound allowance is required for resuspended air concentration uncertainty. Fairly long occupation periods were assumed. Nonetheless, a factor-of-two allowance will be made for the in-vehicle occupation duration. Although high hand-to-mouth ingestion rates were used in this study, the Capstone study estimated hand-to-mouth ingestion rates that were three times higher [5: p. 4.8]. Consequently, a factor of three will be used to provide an upper bound for veteran ingestion rates.

Very high ingestion rates were also assumed for Iraqi children (ten times the ingestion rate assumed for veterans). Nonetheless, soil-pica may result in even higher

ingestion rates. Soil pica is the recurrent ingestion of unusually high amount of soil typically observed in children six years old and younger. The Agency for Toxic Substances and Disease Registry suggests an upper bound of 5 g of soil per day when soil pica is assumed [34]. Several points are noteworthy: (1) the agency acknowledges that 5 g per day is too high, (2) the high soil consumption rate is not typically exhibited on a daily basis, and (3) we have assumed that the in-vehicle play occurs periodically over a 10 year period (the child will be older than six years of age for most of the exposure period). Given these considerations, the 10-year average of the soil ingestion rate for soil pica is probably no more than 25% of the maximum 5 g per day. Assuming an eight hour day for ingestion, we obtain an upper-bound soil ingestion rate of about 150 mg/hr. Thus, the upper bound ingestion rate is about a factor of five greater than the best estimate value used for the maximally exposed case. In addition, a factor-of-two allowance will be made for the in-vehicle occupation duration.

### **6.1.2 DU Dispersal and Deposition**

The DU air concentrations and ground deposition following penetrator impact will depend on the quantity of material generated by impact, the fraction released into the environment, the characteristics of wind dispersal, and conditions affecting ground deposition. The accuracy of these predictions depends on both the accuracy of the data and the validity of the calculational models. Unfortunately, neither the data nor the models used to predict dispersion and deposition can be characterized as highly reliable. On the other hand, the predicted exposures to individuals downwind of the battle zone are so low that the conclusions are unaffected when generous uncertainty bounds are included.

The release of DU particulate into the environment is discussed in Appendix B. The inferred DU particulate masses released into a tank during turret crossing shots, presented in Figure B-2, show surprising consistency among the various test shots. Although some conservatism was used in estimating the released DU mass for hard target impact with tanks, we have not validated the assumption that equal quantities of DU are released internal and external to the vehicle. A generous uncertainty bound of a factor of three will be used to account for the uncertainty resulting from this assumption. For the

line source calculation, both the mass of DU released for a 30 mm shell and the number of hard target hits per m of column are uncertain. Thus, for the line source calculation, a very large uncertainty limit equal to an order of magnitude was assumed.

Because the dispersion/deposition model used in this study is fairly crude, a check on the predictive accuracy was made using the Hazard Prediction and Assessment Capability (HPAC) calculational tool [35]. HPAC is a detailed dispersion/deposition model developed by the U.S. Defense Threat Reduction Agency to predict the effects of hazardous material releases into the atmosphere. The test case used for the model check was for a 100 g release from a single target impact during heavy rainfall. For the HPAC calculation, the actual terrain and historic weather patterns were used at the time and approximate location of the battlefields in southern Iraq. Figure 35 shows that HPAC predicts a deposition density of  $10^{-5}$  g DU/m<sup>2</sup> at 70 m from the point of release, compared to the simple model prediction of  $2.6 \times 10^{-5}$  g DU/m<sup>2</sup>. Given the simplicity of the model used in the current study, the agreement is good.

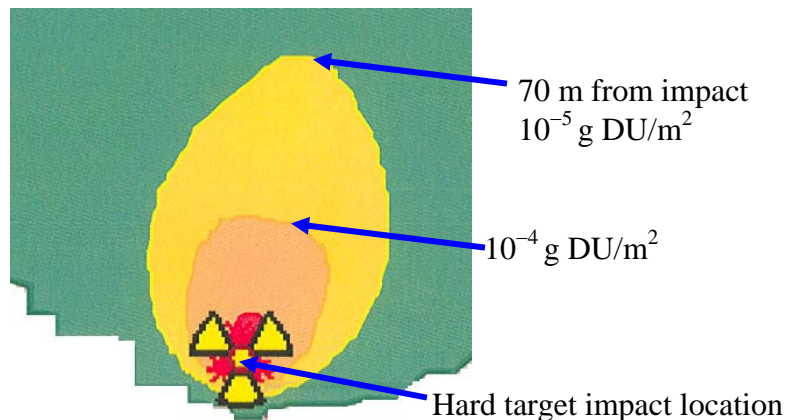


**Figure 35. HPAC prediction of DU deposition for 100 g release in Iraq battlefield for February weather conditions**

A concern has been raised by Dietz [36] that DU will be transported much farther than generally assumed. This concern was based on the finding of DU particulate in filters at distances up to 42 km from their source at Colonie, NY, which appears to contradict official claims that DU particulate will only travel short distances when airborne. However, the concern that DU will travel further than generally believed is not

an issue because the “official comment” Dietz referred to is not relevant to the calculational methods typically used to predict health effects downwind from toxic material release. The dispersal analysis used in this report and in previous DU studies suggests that high concentrations of DU are only found within a few meters of the point of impact, but trace quantities will be present many km from the source.

The case suggested by Dietz relates to the release of DU particulate from the National Lead plant at Colonie, NY, and the finding of DU particulate in the air filters at the Knolls Atomic Power Laboratory (KAPL) 16 km from National Lead. DU was also found in a few filters 42 km from the National Lead plant. Dietz points out that National Lead exceeded the allowed monthly limit corresponding to about 387 g of DU per month. Another document reports that the highest stack releases during the period 1979–1984 were 54,000 times greater than the maximum allowed [37: p. 9]. The amount of DU released when the measurements were made (1979) is unknown. If we assume that the amount released was 10% of the maximum, the release rate would be about 0.8 g/s. The uncertainty on the release rate is about an order of magnitude for the upper bound, and several orders of magnitude for the lower bound (a value for the lower bound cannot be determined from the available data).

Reference [38] provides plots of particulate concentration vs. downwind distance for continuous (plume) releases. The plume model is the continuous release version of the basic model used in this study for puff releases. Assuming a wind speed of about 4 m/s, and a release rate of 0.8 g/s, Figures 2.9 A-F in Reference [38] give an air concentration at distances of 15–50 km in the range between about  $5 \times 10^{-9}$  and  $5 \times 10^{-7}$  g/m<sup>3</sup>. This large range results because weather conditions, effective stack height, wind speed, and the possible existence and location of a temperature inversion layer are unknown. The logarithmic mid-range DU concentration at 16 to 42 km from National Lead is about 50 ng DU/m<sup>3</sup>. With the very large uncertainty estimates for the release rate and the factor of 10 uncertainty in the model parameters, the DU air concentration at KAPL could be less than 0.001 ng DU/m<sup>3</sup> or as high as 700 ng DU/m<sup>3</sup>.

The measured DU content and the volume of air sampled by each KAPL filter were provided in Table VI.b of Reference [39]. From these data, the approximate DU air concentrations at KAPL are predicted to range between 0.02 and 0.25 ng DU/m<sup>3</sup>. Thus, the inferred DU concentrations from the filters fall within the very large range of possible concentrations predicted by the model. Furthermore, the mid-range value inferred from the filter data (~0.1 ng DU/m<sup>3</sup>) is considerably less than the mid-range prediction of 50 ng DU/m<sup>3</sup>. Hence, the assertion that DU transport will be severely underestimated by predictive tools cannot be supported by the available data.

### **6.1.3 Dispersion/Deposition Uncertainty**

Although the comparison of our simple model to the more detailed HPAC model was encouraging, the accuracy of HPAC was not determined. Furthermore, the range of uncertainty in the parameters was far too large to assess the model accuracy from the National Lead/KAPL analysis. Reported estimates of model accuracy must be used. Reference [38: pp. 2.13-2.15] suggests that model uncertainties could range between a factor of two to almost an order of magnitude, depending on the situation. For this study, the use of multiple sources and separate accounting for the uncertainty in wind speed and weather conditions should reduce some of these uncertainties. Nonetheless, to assure that exposures are not underestimated, the highest suggested range (factor of 10) will be used for the uncertainty inherent in the basic model.

Sensitivity studies were performed for the possible range in wind speeds, weather conditions, release heights, and ceiling heights. The analysis showed that the uncertainties in downwind DU concentrations because of the range of possible wind speeds and weather conditions were a factor of three and a factor of two, respectively. The release height did not have a significant effect on downwind DU concentrations. The uncertainty for downwind DU concentrations because of the assumed temperature inversion layer ceiling height was about a factor of two. Wet deposition was assumed with a high washout constant. Wet deposition was found to result in considerably greater deposition densities than dry deposition; consequently, the deposition used should represent an upper bound value. Furthermore, for the limiting case, the analysis was made

assuming no puff depletion from deposition. Thus, different deposition assumptions will not increase the downwind DU concentrations relative to the best-estimate values.

For the analysis of the inhalation dose for a child playing in the soil outside of a DU-contaminated vehicle, an initial average DU areal density of  $1 \text{ g/m}^2$  was used. From the Capstone study, local deposited DU densities up to  $15 \text{ g/m}^2$  were observed. Thus, the uncertainty analysis should include the possibility that a child plays habitually in the location of the highest DU areal density. Including this possibility, however, had no effect on the inhaled dose because the in-vehicle inhalation exposure for resuspended DU particulate is several orders of magnitude greater than for ex-vehicle inhalation.

### **6.1.4 Ex-Vehicle Resuspension**

As discussed in Appendix B, a condition-dependent scale factor  $R_{scale}$  was used to determine the air concentration of resuspended DU. Although a very high scale factor of 100 was used, some data suggest that heavy vehicular traffic in the area may result in a scale factor of almost 1000 [11: Annex B, p. 4]. Consequently, an order-of-magnitude uncertainty for resuspension will be used to assure that the upper bound is not underestimated.

## **6.2 Biokinetics, Dose, and Risk Coefficients**

The biokinetic models used in this study were based on the most recent ICRP models [15: pp. 24–26]. The inhalation model was developed using ICRP 66, and the ingestion model was mostly obtained from ICRP 69. The model for blood-deposition of inhaled and ingested DU in other organs and the time dependence of DU in these organs was based mostly on ICRP 69 along with information from ICRP 30. The basic ICRP 69 model was also used to estimate the time dependence of DU in the body from dissolution of embedded fragments. Leggett and Pellmar [32] carried out studies using rats with surgically implanted DU pellets. Their findings indicate that the use of this model for fragments is appropriate:

*The comparisons indicate that the biokinetics of U migrating from embedded DU fragments is similar to that of commonly studied forms of U with regard to long-term accumulation in kidneys, bone, and liver.*

The accuracy of the basic model for this study refers to the equations and most of the standard data used to predict the biokinetic behavior of uranium. The model accuracy does not include considerations of the uranium dissolution rate in the lungs or particle size uncertainties for the respiratory tract model. For embedded fragments, the fragment dissolution rate uncertainty is not included in the model accuracy. A review of the literature did not yield a clear uncertainty estimate for the basic models as defined here. However, based on this review, the models appear to be reasonably accurate, and for the limited scope of the model definition, a modeling uncertainty of about 50% was judged to be a reasonable estimate.

### **6.2.1 Computer Model**

This study used the basic approach for biokinetic calculations suggested by the ICRP, with some simplifications, and the calculations were carried out using the Mathcad calculational tool [40]. Even with simplifications, the computer model was complex and included many calculational steps. To verify the reliability of the computer model, two check-calculations were performed. For the first check calculation, the example calculation for respiratory tract doses presented in the ICRP 66 report [25: pp. 102–106] was carried out using the Mathcad-based biokinetic computer model developed for this study. The Mathcad model predicted doses to all respiratory tract organ compartments and lymph nodes that were in essentially exact agreement with the results presented in the report.

For the second check, the Level II inhalation calculational results presented in the Royal Society report were compared to the Mathcad calculation using very similar input data. An exact comparison was not possible because of the limitations of the simple Mathcad model. Nonetheless, agreement was generally good for both the respiratory tract and other target organs (such as the bone surface). The whole-body dose predicted using this simple model was within 12% of the value reported by the Royal Society. The largest

deviation from the Royal Society calculations for an individual organ was for the thoracic lymph node, for which the Mathcad model predicted a dose 27% lower than that predicted by the Royal Society.

### **6.2.2 Inhalation Model Data**

The principal case-dependent data used in the model include the dissolution rate in the lung, the particle size, the DU mass inhaled, and whether the individual was a nose breather or a mouth breather. The mass uncertainty was discussed in Section 6.1. The uncertainties in the dissolution rates and fractions (rapid and slow) were determined by using the range of dissolution data from the Capstone study in the biokinetic model. The dissolution rate uncertainty resulted in a lung dose uncertainty of  $\pm 50\%$ , and a bone marrow and testes dose uncertainty of  $-75\%$  to  $0\%$ .

The uncertainty in the particle size distributions was also obtained from the Capstone study [5: Attach. 1, p. 6.42]. Calculations exploring the range in particle size distributions resulted in a maximum uncertainty of  $\pm 50\%$  for the lung dose and no significant effect for the bone marrow or testes. The particle size uncertainty for the peak concentration for DU in the kidney was  $\pm 15\%$ . The uncertainty associated with breathing type was examined by using depositions for just-nose breathers and just-mouth breathers. The uncertainty associated with this consideration was  $\pm 25\%$  for the lung dose. Nose vs. mouth breathing had no significant effect on the bone marrow or testes dose or on the peak concentration of DU in the kidney.

### **6.2.3 Urine Data**

For Level I, the inhaled DU mass and the DU dissolution rate for fragments were obtained by using the measured DU mass per g creatinine in the urine of DU-exposed veterans, using an excretion rate of 1.7 g of creatinine per day, and using the standard value of 63% for the amount of uranium entering the bloodstream that is rapidly excreted in the urine. The uncertainty in the quantity of uranium rapidly excreted (63%) should be small. Based on Reference [41], the uncertainty in the mass of creatinine excreted per day is about 35%. The fragment analysis also assumes that the DU dissolution rate is roughly

constant over the lifespan of the individual. As shown in Appendix B, the latter assumption is probably conservative.

## **6.2.4 Radiological Risk Coefficients**

Radiological risk coefficients used in this study were obtained from ICRP 60 for cancers and birth defects [15]. Risk coefficient uncertainties for lung cancer, leukemia, and whole body exposure cancer induction were examined by the U.S. Environmental Protection Agency (EPA). The risk coefficient uncertainty for genetic effects was estimated from the range in the values for the coefficient obtained from a number of recent studies.

Enhanced risk of lung cancer has been demonstrated from the study of groups exposed to significant doses of ionizing radiation. The increased incidence of lung cancers for uranium miners may appear to be of particular significance to this study; however, the radiological dose resulting from the release of radon gas in mines greatly exceeds the radiological contribution from uranium itself. Consequently, the dose from uranium for this group is insignificant by comparison and does not provide any information specific to uranium radiological exposure. Nonetheless, miner statistics have been used to study the relationship of alpha and beta particle radiation from radon and radon daughter products to lung cancer. Residential radon statistics and data from atom bomb survivors have been used as well. As for all studies of low-dose rate exposures, the uncertainty is large, and the relationships of dose to cancer induction vary considerably from study to study.

A detailed uncertainty analysis carried out by the U.S. EPA determined that the actual lung cancer risk correlation could be a factor of two higher or a factor of five lower [42: p. 26]. Their analysis included possible dosimetry errors, diagnostic misclassification, sampling variation, extrapolations to low dose, and other considerations. Figure 36 shows the composite results of a number of studies used on the relative risk of lung cancer from indoor exposure to radon gas as a function of radon concentration [43: p. 175]. Each data point in Figure 36 represents dose/risk correlations compiled from statistics typically involving thousands of individuals. The dashed line in

Figure 36 is the relative risk of lung cancer obtained from a study of miners exposed to radon gas. Despite the large uncertainty bands, common to low-level dose-effect analysis, a meta-analysis from the indoor radon gas studies yielded a relative risk of about 1.14, which is in close agreement with the relative risk of 1.13 from the miner study. The relative risks from the radon studies are consistent with the lung cancer risk coefficients in Table E-6. The data and data uncertainty bars in Figure 36 provide a sense of the uncertainty in the risk correlations at low doses.

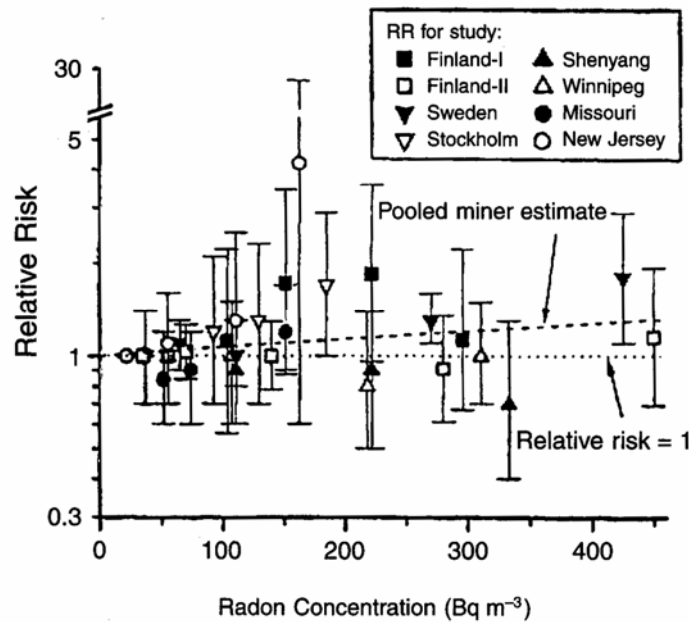


**Figure 36. Inferred lung cancer relative risk vs. radon concentration for indoor radon and miner radon exposure [43]**

The EPA cites evidence that the radiation weighting factor for alpha particle-induced leukemia should be 1.0 rather than 20 [42: p. 16], and the National Council On Radiological Protection (NCRP) [43: p. 198] reports that atom-bomb survivor statistics show no apparent leukemia risk for doses below 0.2 Sv. However, the use of a reduced coefficient or a zero coefficient is not widely accepted and will not be implemented in this assessment for leukemia risk estimates. As a consequence, the EPA estimate of a factor of 1.7 higher and a factor of three lower health effect correlations will be used to estimate the leukemia uncertainty bounds [42: p. 29]. The EPA also provided a whole-

body risk correlation uncertainty of only 10%. Here, for simplicity, we will assume that the upper bound uncertainty in the cancer risk correlation for each organ is represented by the largest calculated uncertainty equal to a factor of two. A similar analysis was carried out by the NCRP, which recommends an uncertainty bound of about a factor of two [44].

For genetic effects, the uncertainty was estimated from the range of recent estimates of incidence rates for radiation-induced genetic disease. The upper end of the range from the BEIR V study [45, 29: p. 60] was roughly three times greater than the value recommended by the ICRP that was used in this study. Thus, a factor of three applied to the nominal genetic risk coefficient will be used to represent the uncertainty upper bound.

### 6.3 Uncertainty Analysis

In this section, a simple uncertainty analysis is presented that was used to obtain an upper bound for health risk estimates. Sections 6.1 and 6.2 discussed the effect of parameter and methodology uncertainties on health effects predictions. The effects of these uncertainties on DU-induced cancer or birth defect predictions are summarized in Table 21 for veterans. Assuming that the uncertainty associated with various aspects of the analysis are independent, the net uncertainties were computed as the square root of the sum of the squares of the component uncertainties. From Table 21, a cancer risk multiplier  $\mathcal{M}_c$  of 2.5 was obtained for Level I and II veteran risks. The multiplier is used to obtain the upper-bound cancer risk for Level I and II veterans by multiplying the best-estimate risk given in the table by  $\mathcal{M}_c$ . The risk multiplier for genetic effects  $\mathcal{M}_g$  is slightly higher (i.e., about 3.0). For Level III veterans, the net risk multiplier is about a factor of 14.

The effects of uncertainties on health effect predictions for civilians are presented in Table 22. For a child at play, risks are dominated by colon and lung cancer. The risk multipliers in Table 22 and projected risks for lung and colon cancer were used to obtain a net cancer risk multiplier of about 3.5. The risk multiplier for genetic effects is also about 3.5, and the multiplier for downwind civilians is the same as for Level III veterans.

**Table 21. Analysis uncertainties for risk multipliers for veterans**

	<b>Level I</b>	<b>Level II</b>	<b>Level III</b>
<b>Urine Data Use</b>	35%	–	–
<b>Vehicle Occupation Time</b>	–	100%	–
<b>Dispersion</b>	DU Release	–	900%
	Dispersion/Deposition		900%
	Wind Speed		200%
	Weather Class		100%
	Ceiling Height		100%
	Target Density		200%
	Resuspension		~0%
<b>Biokinetic Model</b>	50%		
<b>Dissolution Rate*</b>	50%		
<b>Particle Size*</b>	50%		
<b>Nose/Mouth*</b>	25%		
<b>Cancer Risk Coefficient</b>	100%		
<b>Genetic Risk Coefficient</b>	200%		
<b>Lung Cancer Net</b>	140%	165%	1300%
<b>Leukemia Net</b>	120%	150%	1300%
<b>Genetic Net</b>	210%	230%	1300%
<b>Cancer Risk Multiplier <math>\mathcal{M}_c</math></b>	2.5	2.5	14
<b>Genetic Risk Multiplier <math>\mathcal{M}_g</math></b>	3.0	3.0	14

\*Effect on lung cancer. Effect on bone marrow and testes is insignificant.

**Table 22. Analysis uncertainties for risk multipliers for civilians**

	<b>Child</b>	<b>Downwind</b>
<b>Ingestion Rate</b>	400%	–
<b>Vehicle Occupation Time</b>	100%	–
<b>Dispersion</b>	DU Release	900%
	Dispersion/Deposition	900%
	Wind Speed	200%
	Weather Class	100%
	Ceiling Height	100%
	Target Density	200%
	Resuspension	~0%
<b>Biokinetic Model</b>	50%	
<b>Dissolution Rate*</b>	50%	
<b>Particle Size*</b>	50%	
<b>Nose/Mouth*</b>	25%	
<b>Cancer Risk Coefficient</b>	100%	
<b>Genetic Risk Coefficient</b>	200%	
<b>Lung Cancer Net</b>	165%	1300%
<b>Leukemia Net</b>	150%	1300%
<b>Colon Cancer Net</b>	430%	–
<b>Genetic Net</b>	230%	1300%
<b>Cancer Risk Multiplier <math>\mathcal{M}_c</math></b>	3.5	14
<b>Genetic Risk Multiplier <math>\mathcal{M}_g</math></b>	3.5	14

\*Effect on lung cancer. Effect on bone marrow and testes is insignificant.

## 6.4 Comparison with Previous Analyses

Estimated veteran cancer risks from previous studies [4, 6, 46, 47] are compared to risk estimates from the current study in Figure 37. Comparable predictions for civilian risks were not generally available from previous studies. Finding comparable risk predictions from previous studies for veterans also presented some problems. To make a more consistent comparison, the results from previous studies were adjusted to obtain the risk estimates shown in Figure 37. Uncertainty bounds for the current study (SNL) are also shown in the figure. Note that the lower uncertainty bound is much larger than the upper uncertainty bound.

### 6.4.1 Comparison of Adjusted Predictions

Whenever previous studies provided only dose estimates, risk estimates in Figure 37 were obtained by multiplying the reported doses by the appropriate risk coefficient.

With the exception of the risk for the maximally exposed Level I veteran, the Fetter and von Hippel study [3] did not, in general, provide predictions in a form that could be easily compared to the predictions from this study (e.g., collective doses and risks); consequently, no comparison was made to their predictions in Figure 37. Fetter and von Hippel’s predicted dose/risk for maximally exposed Level I veterans was approximately the same as the prediction by the DoD study. The Royal Society [4] upper-bound case included upper-bound assumptions in their maximum exposure predictions, while the maximum case for the SNL study was a best estimate for the maximally exposed veteran. Here, the Royal Society maximum risks were divided by the appropriate approximate uncertainty multipliers (estimated for the current SNL study) to put the Royal Society estimates on approximately the same “best-estimate” basis used in the SNL study.

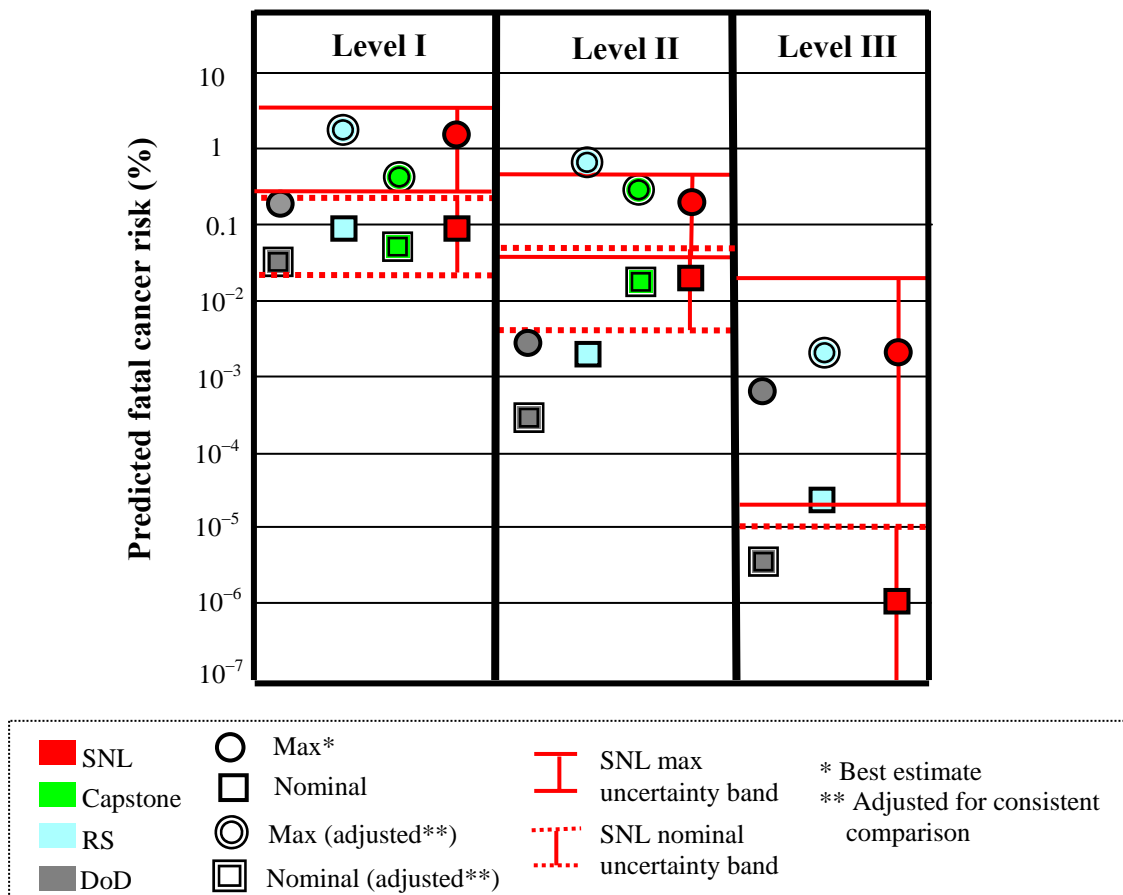


**Figure 37. Predicted veteran cancer fatality risk from DU exposure by various studies (data adjusted to make cases comparable)**

For Level I, the Capstone study [46] provided risk projections for a range of scenarios assuming that one DU shell struck the target; thus, their maximum exposures did not account for multiple hits by DU penetrators. Hence, the Level I risk projection from the Capstone study was multiplied by three to account for the possibility of multiple DU penetrator hits (as assumed in the DoD study). For Level II, the Capstone report only provided dose rates for a variety of exposure scenarios; consequently, the nominal and maximum dose rates were multiplied by the risk coefficient and by 10 hours and 100 hours, respectively, to be consistent with the exposure durations used in the SNL study. The nominal and maximum Capstone dose rates for Level II were approximated as the average dose rate and maximum dose rate, respectively, for all Level II scenarios. The Capstone study did not examine downwind inhalation for Level III. As a consequence, no comparable Level III data were available for comparison.

The nominal Level I value for the DoD study [6] was estimated using the average of the minimum and maximum doses (without the factor of three for multiple hits). The nominal and maximum dose rates for Level II were approximated as the average dose rate and maximum dose rate with exposure durations of 10 and 100 hours, respectively. For the Level III DoD nominal case, 5 hours of exposure and no vehicle entry were assumed. For the maximum Level III DoD case, vehicle entry was included and 100 hours of exposure were assumed.

For Level I, the nominal risk of 0.09% from the current study is in agreement with the Royal Society prediction, and the Capstone and DoD predictions are within the SNL uncertainty bounds. The maximum value of 1.4% from this study is in reasonably good agreement with the Capstone [46] and Royal Society's adjusted predictions, but the DoD's 2003 prediction [6] is just below the uncertainty bound for the maximum case. The Level II nominal and maximal risk predictions from the current study are in good agreement with the Capstone prediction (using the same exposure durations). However, all Royal Society and DoD predictions fall outside the SNL uncertainty bands.

For Level III, previous studies examined a broad range of scenarios and often used very conservative assumptions. Furthermore, dispersion, deposition, and

resuspension predictions contain large inherent modeling and data uncertainties. Despite these limitations and uncertainties, the Level III maximal-exposure risk prediction is in surprisingly good agreement with the DoD prediction and the adjusted Royal Society prediction. The DoD Level III nominal case risk projection is in reasonable agreement with the SNL prediction, and the Royal Society prediction is a bit above the upper SNL uncertainty bound.

Given the complexity, uncertainty in exposure durations and environments, and the different approaches taken by the various studies, the agreement among these studies is reassuring that the projected fatal cancer risks are not significantly in error. The comparisons suggest that the nominal and maximum Level I risks are on the order of 0.1% and 1%, respectively. For Level II, the nominal risk is about 0.01% or less, and the maximum is a few tenths of a percent. For Level III, the maximum cancer risk is on the order of 0.001%, and the nominal risk is in the range between  $10^{-6}$  % and about  $10^{-5}$  %. A similar comparison was made for the maximum concentration of DU in the kidney for Level I veterans. The comparison of DU kidney concentrations predicted by the various studies follows the same trends observed for the cancer prediction comparison. Although the Capstone study did not explore all scenarios and issues, its analysis for Level I and II veterans was based on exhaustive testing and analysis and may represent the most reliable predictions for these cases.

#### **6.4.2 Summary Comparison of Methods**

The SNL inhaled DU mass predictions for Level I veterans presented in Table 11 are in surprisingly good agreement with the Royal Society predictions. Both studies predict an inhaled DU mass of 250 mg for nominal Level I veterans. For the maximally exposed Level I veteran, the SNL inhaled mass is 4 g compared to the Royal Society's predicted inhaled mass of 5 g. To predict the inhaled DU mass, the Royal Society used estimates of the fraction of DU aerosolized per shell impact, inhalation rates, particle sizes, and the expected in-vehicle duration for Level I veterans. Their estimate of about 100 g of DU aerosolized within the vehicle [4: Annex C, p. 3-4] was in good agreement with the value estimated in the SNL study (but not used for the SNL Level I estimates) based on Capstone test data. The Royal Society estimate for the time-dependent decrease

in the DU air concentration was also in good agreement with the Capstone test data. For their worst-case estimate, however, the Royal Society simply assumed a ten-fold increase in the DU air concentration. This assumption and other upper bound assumptions resulted in a high inhaled mass for their Level I worst-case estimate.

The Royal Society was also limited by pre-Capstone dissolution rate data for its prediction of the biokinetic behavior of inhaled DU. As a consequence, the essentially exact agreement of the SNL and Royal Society inhaled DU mass for the nominal Level I case did not result in exact agreement for the doses and risks. Although the SNL study used a method similar to that of Fetter and von Hippel's for Level I veterans, SNL's use of the more recent Capstone data resulted in a much higher risk estimate than that by Fetter and von Hippel.

Some of the methodology used for the DoD study was not clear; consequently, a discussion of the DoD methodology will not be provided here. The Capstone analysis had the advantage of excellent test data and a detailed mathematical analysis. Nonetheless, their analysis required some assumptions for exposure time, the number of shells striking the target, the state of the ventilation system, and individual breathing rates. For Level II, the principal difference among the studies was that the Royal Society did not have the most recent resuspension and particulate characteristics data (provided by the Capstone test program) that were used for both the Capstone and SNL studies.

For the central estimate for Level III, the Royal Society made the simple assumption of exposure to 1 kg of DU released 100 m upwind, 10 kg of DU released 1 km upwind, and 100 kg of DU released 10 km upwind of Level III veterans [4: p. 65]. The worst-case estimate was obtained by increasing the DU mass released for each case by a factor of ten. Relatively standard dispersion calculations were used to estimate exposures downwind of the releases. For the resuspension inhaled dose calculation, the Royal Society assumed a deposition density of 1 g/m<sup>2</sup>, and performed resuspension calculations using both the Garland resuspension method and the dust loading approach [4: Annex C, pp. 17-23]. As for Levels I and II, the Royal Society was limited by pre-

Capstone dissolution rate data for their prediction of the biokinetic behavior of inhaled DU.

## 6.5 Health Effects Issues

Two noteworthy claims relating to possible DU health effects include the assertion that DU exposure has resulted in very high incidences of birth defects in the offspring of Gulf War veterans and the assertion of high incidences of leukemia among DU-exposed veterans. In addition, criticisms have been raised regarding the general methodology used to estimate radiation-induced health effects. The claims and criticisms relating to radiation health effects predictions and observations are numerous, and no attempt was made to examine all possible concerns. In this section, a few of the more important claims and concerns are briefly reviewed.

### 6.5.1 Birth Defects

In a 1994 article in *The Nation* [48], Laura Flanders wrote the following:

*...Susie Spear, a health writer for the Clarion-Ledger in Jackson, Mississippi, reported that among her local unit of the National Guard severe birth defects affected thirteen of fifteen babies conceived by veterans or their spouses since the end of the war. Since then, a Veterans Administration survey of 251 parents state-wide has revealed that 67% of their children conceived since the war are afflicted with illnesses rated severe or have birth defects including missing eyes and ears, blood infections, respiratory problems, and fused fingers”.*

Although the article states that “Birth defects would be consistent with radiation from depleted uranium,” other possible causes are mentioned (sand-fly borne infection and vaccines). Subsequent writers have focused on DU as the cause of the birth defects, and some have generalized the statement to imply that 67% of all children of Gulf War veterans suffered severe birth defects. If the article were correct that a significant increase in birth defects did result from Gulf War exposures, it would be impossible to draw conclusions as to which potential teratogen was responsible. Given that radiation-induced birth defects have never been clearly observed in humans at any dose, the likelihood of

significant increases in birth defects from the very modest DU radiation exposure is improbable to the extreme.

Using the conservative risk correlations for radiation-induced genetic effects, we calculate that each veteran would need to inhale about 34 kg (75 pounds) of DU to result in an equilibrium birth defect incidence of 60% (with spontaneous birth defects the total is about 67%). This estimate, however, is for equilibrium conditions established after many generations. First-generation genetic effect induction is about five times smaller [29: p. 60]. Viewed from another perspective, we find that to induce 60% birth defects in the first generation, each veteran would need to inhale more than 40,000 times the amount of DU that is expected to result in a chemically induced kidney failure fatality.

We must also examine the claim that a significant increase in birth defects for post-war-conceived children actually occurred among Gulf War veterans. The article by Laura Flanders provided no references to support any of the statements in the article, and no Veterans Administration (VA) report was found to support her claim. On the other hand, two government-funded studies, conducted in 1994 and 1996, examined the statistics for the two Mississippi National Guard units referred to in the article. The studies found that of a total of 55 births, five children were born with birth defects [49]. These studies concluded that “The rate of birth defects of all types in children born to this group of veterans is similar to that expected for the general population.” In addition, the frequencies of premature births and low birth weight children were similar to those of the general population.

A number of other birth defect studies were performed for children of other Gulf War veterans, with similar conclusions. In one study of 75,000 births, 7.45% of the Gulf War veteran children were born with birth defects, compared to 7.59% for children of veterans not deployed in the Gulf [50]. In another study, where statistically significant excesses were found for a few specific types of birth defects out of 46 birth-defect categories (i.e., tricuspid valve insufficiency, aortic valve stenosis, and renal agenesis). The authors concluded, “We did not have the ability to determine if the excess was

caused by inherited or environmental factors, or was due to chance because of myriad reasons, including multiple comparisons.” [18]

Claims have been made that significant increases in birth defects were also observed in Iraqi children following the Gulf War. These claims have not been verified, and if true, any increase in birth defects cannot be ascribed unambiguously to a particular cause. In addition to DU exposure, both civilians and veterans may have been exposed to chemicals, such as sarin gas and mustard gas released during demolition of chemical weapon supplies. Furthermore, severe malnutrition (common among post-war Iraqi civilians) can be a major cause of birth defects.

### **6.5.2 Leukemia**

Although DU-induced leukemia has been raised as a concern for Gulf War veterans and Iraqi civilians, the principal evidence cited for DU-induced leukemia was for Italian Balkan War veterans [51]. During the Balkan War, U.S. aircraft fired 30 mm DU rounds at enemy targets. As for the Gulf War, DU particulate was generated by impact with armored vehicles. Italian and other allied ground troops moving through the battlefield may have been exposed to wind-borne DU puffs or resuspended DU particulate. Because only 30 mm rounds were used and very high target densities have not been reported for the Balkan War, exposure levels for Italian ground troops should be less than the exposure for Gulf War Level III veterans. Nonetheless, we can make the conservative assumption that Balkan War exposures and leukemia risks are roughly comparable to those for Gulf War Level III exposures and risks. From Table 18, the nominal risk for DU-induced leukemia was  $10^{-6}$  %. Assuming about a factor of ten uncertainty, the upper bound for DU-induced leukemia is  $10^{-5}$  %.

About 1% of all U.S. civilian fatalities (nation-wide) result from spontaneous incidences of leukemia (based on Reference [29: p. 113]). If the natural incidence of leukemia for Italian soldiers is approximately the same as for U.S. civilians, the leukemia fatality risk from DU exposure for Italian troops is at least 100,000 times smaller than the risk of dying from spontaneous leukemia fatalities. The spontaneous incidence of leukemia for a population of young adult men is only about ~0.005% per year. This risk

of natural incidences for leukemia over the two year period of the Italian study is at least 1,000 times greater than the lifetime risk of a leukemia fatality from DU exposure. A review of cancer incidents was carried out by the Investigative Commission established by the Italian Ministry of Defense [52]. The commission identified a total of two cases of Acute Lymphatic Leukemia (ALL) among the 39,450 Italian personnel (84.5% from the army) in the Balkan theater. When a one-year latency period was assumed, the number of cases was one, compared to an expected (spontaneous) number of cases of 0.48 for this particular form of leukemia. This deviation from expectations was not statistically significant.

The Italian Investigative Commission also examined Non-Hodgkin's lymphoma, Hodgkin's lymphoma, and solid tumors. As for leukemia, all deviations from expectations were not statistically significant. The sum of all of the observed cancers was lower than the expected number of cancers, possibly because of a bias resulting from the physical fitness of the military personnel.

The U.S. presidential Advisory Committee also reviewed the U.S. Veterans Administration's medical records of the first 52,216 Gulf War veterans completing physical examinations in the VA's Persian Gulf Health Registry. The VA found no apparent increase in cancers of any type relative to the age-matched U.S. population [53]. Although the current study predicts that lung cancer is the principal cancer risk from veteran DU exposure, the latency period for lung cancer is at least 20 years; consequently, current Gulf War veteran statistics for lung cancer are not yet relevant.

## **6.6 Radiological Analysis Validity**

Two general types of criticisms are defined regarding the validity of the radiological analysis methods used to predict DU health effects. The first type is based on claims that the current methodology is not supported by epidemiological data. The second type of criticism is that the methodology is inconsistent with research findings and theoretical developments.

### 6.6.1 Epidemiological Evidence

An early study reported an excess of infant leukemia fatalities near the Sellafield nuclear reprocessing plant in the U.K. (e.g., [54]). Similar claims have been made for the Dounreay reprocessing plant in the U.K. Counterarguments to these claims point out that the results are biased by the selection of population groups and time periods for study that yield clusters of increased leukemia, while a different selection of population grouping and time periods in the same area do not. Counterarguments also point out that for some cases, the number of illnesses cited is too small to be statistically significant. In addition, the original studies did not look at other nuclear facilities to determine if the observations were common to most nuclear facilities. One interesting study examined six sites that had been considered for nuclear facilities, but were never used for that purpose. Incidences of leukemia and Hodgkin's disease were higher than expected for these non-nuclear areas, suggesting probable statistical variations or confounding factors [29: p. 97]. The Cancer Institute of the United States carried out a very extensive study of nuclear facilities. The Cancer Institute concluded in its three-volume report that it found no evidence of a cause-and-effect relationship between nuclear facilities and cancer occurrences [29, 55].

Other epidemiological arguments have been used to challenge standard radiological health effects methodologies, and counterarguments have refuted these arguments. More in-depth analyses of epidemiological data are provided by Mettler [29: pp. 90–105] and the NCRP [43: pp. 131–201]. Some of the limitations and pitfalls of various types of epidemiological studies are discussed in Reference [43: p. 131–137]. An interesting example of an *ecological* epidemiological study is shown in Figure 38 for lung cancer mortality vs. indoor radon concentration in U.S. homes [43: pp. 174–177]. The study shows a negative slope for lung cancer; in other words, the results show a cancer reduction benefit from increased radiation exposure (hormesis). Although the consistently downward trend of the plot and the small error bands are impressive, the NCRP rejects the findings of this study on the grounds that the authors did not have available county-by-county information on smoking frequency and were forced to use crude surrogate frequencies. In addition, the NCRP points out that the downward trends are not consistent with other indoor radon gas studies. In general, it is often difficult to

draw firm conclusions on the effects of low-level radiation from epidemiological studies. The suggested approach for interpreting findings from low dose rate epidemiological studies is to consider the weight of evidence from a number of independent studies, rather than drawing conclusions based on the results of one or two studies.

Unexpectedly high incidences of thyroid cancer have been observed in children downwind of the Chernobyl reactor accident (several times higher than predicted incidences using standard risk coefficients for radiation-induced thyroid cancers) [56]. The finding of unexpectedly high incidences of thyroid cancer appears to be strongly associated with exposure to radioactive iodine released during the accident. This result may indicate that the thyroid risk coefficient used for inhaled radioactive iodine is too low. Radioactive iodine is generated as a fission product during reactor operation and is not present in DU. Nonetheless, the underestimate of thyroid cancer cases should instill a measure of caution when making predictions of health effects. On the other hand, significant data have been accumulated from miner and indoor-radon-gas studies that provide some confirmation that incidences of lung cancer are unlikely to deviate significantly from predictions. Furthermore, no increase in leukemia was found for exposed populations following the Chernobyl accident (the standard methodology predicted increased incidences of Leukemia) [56]. The low incidence of leukemia is consistent with statements by the EPA and others that standard methods for risk projections may significantly overestimate the predicted incidences of leukemia from internalized alpha emitters.

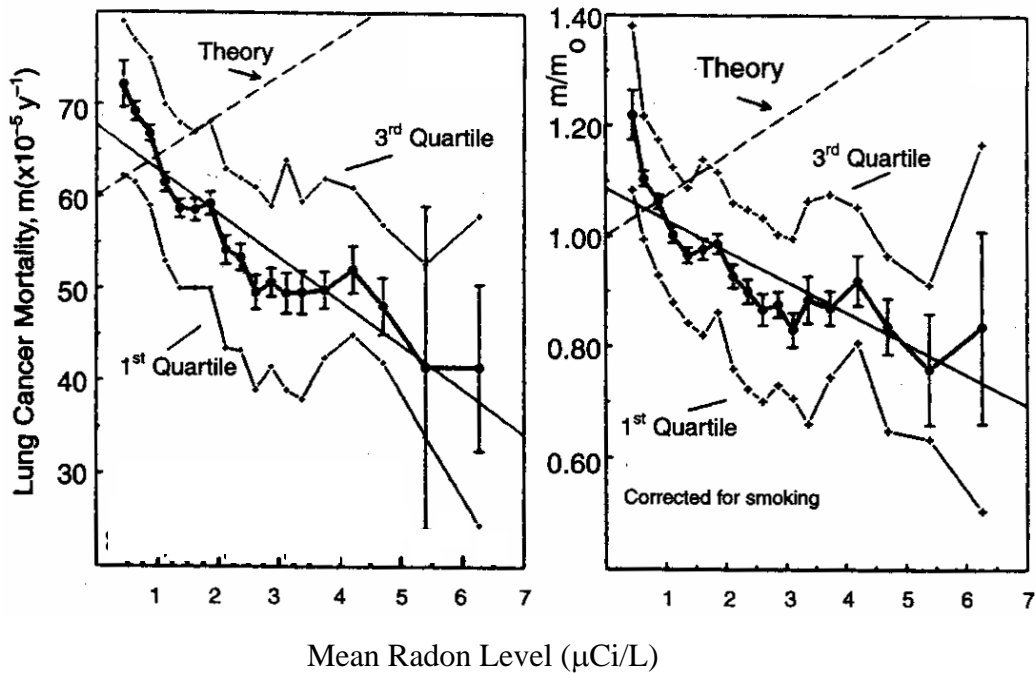


**Figure 38. Lung cancer relative risk for males vs. radon concentration for indoor radon from Cohen study**

### 6.6.2 Theory and Research-Based Issues

A number of research findings and theoretical arguments have been used to question radiological health-effect estimates. Two of the more important issues include *energy averaging* and the *bystander effect* [43]. The bystander effect relates to the finding that cancers may be induced in cells that have not been damaged by radiation, but are in close proximity to radiation-damaged cells. The significance of the bystander effect is not known at this stage. The bystander effect may increase, decrease, or have no effect on cancer risk. However, given the weight of evidence from miner and indoor radon gas studies, significant deviations from alpha-particle-induced lung cancer correlations appear unlikely.

The term *energy averaging* refers to the fact that organ dose is typically computed by averaging deposited radiation energy over the mass of the entire organ or organ compartment. For internal radiation with short penetration depths (such as alpha-particle radiation), most of the energy is deposited very close to the source rather than being distributed over the entire organ. As a consequence, some regions of the organ will

receive much higher doses than predicted by averaging. This effect was addressed earlier for embedded fragments. Another manifestation of the energy-averaging issue is the so-called *hot particle theory*; that is, a particle of an alpha-emitting material deposited in the lung will cause significant local damage to cells adjacent to the particle. Thus, a hot particle may present a greater risk than anticipated when using the standard approach for predicting lung cancer. Although the hot-particle theory was introduced more than forty years ago, testing has failed to demonstrate that the hot particle effect will result in a significant increase in the risk of lung cancer. The findings relating to hot-particle research have been summarized in a review by Bair [57].

Preferential blood-deposition of radioactive materials in some regions of an organ could also cause local hot-spots in organs. Other mechanisms, such as the direct transport of inhaled DU through the nasal cavity to the substantia nigra (as observed by Lewis) could also result in localized concentrations. In many cases, these concerns are actually accounted for by the standard methodology (e.g., localized deposition in cortical and trabecular bone regions is computed to predict leukemia and bone tumors). For the potential cancers important to this study, the effect of locally deposited DU appears to be addressed by the existing models.

## **6.7 Assessment**

An assessment of the validity and accuracy of the methodology used in this study was based primarily on the following review and evaluation. It included an assessment of uncertainties associated with the input data and mathematical models. In addition, benchmark calculations helped validate that the models and computer codes were consistent with ICRP models. Criticisms of DU dispersion models and criticisms of the basic data and methodologies for estimating radiological health effects were addressed. Furthermore, epidemiological data for U.S. and Italian veterans and for radiation workers were found to be consistent with the analysis findings and consistent with the basic methodology. Theoretical issues and criticisms of the standard methodologies for estimating radiation health effects were also addressed. Further demonstration of the validity of the methodology and predicted consequences was provided by comparing health effects estimates from this study with predictions from previous studies.

The validity of the basic methodology and predicted health risks were, in general, demonstrated by this assessment. Although uncertainties were found to be significant, the conclusions of this study were unchanged when upper bound values were used for the predicted health effects. This assessment should not be interpreted to be a general validation of the SNL National Securities Studies Department methodology for studying the consequences of terrorist use of radiological dispersal devices. Each new scenario studied possesses unique sets of conditions and environments that can differ substantially from the conditions and environments applicable to this study. Furthermore, a different approach may be required to address other scenarios. The assessment of methodologies provided by this study should be considered as a benchmark and a guide for judging the validity and accuracy of future studies. One should examine the potential effect on predictive uncertainties of the conditions and approaches used in future studies that deviate significantly from those used in the current study.

The health effects analysis for exposure to DU suggests that the standard guidelines for radiological effects from uranium exposure are consistent with basic radiological health guidelines; consequently, adherence to worker standards for uranium exposure will not present a significant radiological risk. The review also suggests that clinical health effects should not result from the chemical toxicity (heavy metal) effect of uranium. Nonetheless, the World Health Organization [1] and the Royal Society [11: p. 3] have pointed out that the implicit exposure limit of 3  $\mu\text{g}$  U/g kidney may be too high as a heavy-metal protection guideline. Although exposed individuals are unlikely to become ill at this limiting exposure level, transient indicators of renal (kidney) dysfunction are possible. Based on these observations, a reconsideration of the weapons complex guidelines for uranium exposure is recommended to determine whether the guidelines are consistent with the most recent findings and basic chemical toxicity health-protection standards.

## **7.0. Conclusions and Recommendations**

This study included a numerical analysis of the effect of DU exposure on exposed individuals, using Gulf War veterans and Iraqi civilians as a case study. The accuracy and validity of the methodology was then assessed by an uncertainty analysis, benchmark calculations, and by comparisons with veteran health statistics, epidemiological data, and comparisons with the results from previous Gulf War/DU studies. Based on this investigation, the following conclusions were reached.

### **7.1 Dispersal/Consequence Methodology**

- This study included an assessment of the methods for predicting radioisotope dispersal and health effects for the specific case of Gulf War use of DU munitions. The basic methodology was determined to be valid. The findings of this study can be used as a benchmark and a guide for evaluating the validity and uncertainties of health predictions for other radioisotope dispersal studies.

### **7.2 Weapons Complex Uranium Guidance**

- No significant radiological health risks are posed by normal handling and processing of uranium within the weapons complex, if standard safety guidelines are followed.
- Clinical health effects should not result from the chemical toxicity (heavy metal) effect of uranium, if the implicit limit of 3  $\mu\text{g}$  U/g kidney is not exceeded. Although an individual is unlikely to become ill at this maximum permitted kidney burden, transient indicators of renal dysfunction are possible.
- A reconsideration of the weapons complex guidelines for uranium exposure is recommended to determine whether the guidelines are consistent with the most recent findings and basic chemical toxicity health protection standards.

## 7.3 DU-Exposed U.S. Veterans

- DU-induced cancer risks for most Gulf War veterans are extremely small.
- Only a few U.S. veterans, in vehicles accidentally struck by DU penetrators, inhaled sufficient quantities of DU to incur an appreciable fatal cancer risk (~1%, compared to all U.S. civilian fatalities from cancer equal to 24%).
- The risk of radiation-induced cancer for DU-exposed veterans is almost entirely associated with the risk of lung cancer. All other radiation-induced cancer risks, including leukemia, are much smaller.
- The risk of radiation-induced birth defects is very small relative to the U.S. average birth defect frequency of about 8% per live birth. For the worst case, the incremental risk is about 0.03%, and for most veterans the risk is extremely small.
- For routine handling of DU munitions or occupation of tanks containing DU munitions, potential health risks are very small.
- The dominant path for DU exposure was inhalation of DU particulate. Embedded DU fragments made significant contributions to the DU concentration in the bone and other organs; however, even with fragment effects included, the risk of cancer for these organs and the risk of leukemia were very small. Ingested DU did not have a significant effect on the radiological risk.
- For veterans retaining embedded DU fragments, a review of the literature did not identify any veterans with soft-tissue sarcomas in the vicinity of fragments. Nonetheless, animal tests suggest that fragment-induced local sarcomas cannot be ruled out as a possibility.
- The risks of DU-induced cancers for veterans and DU-induced birth defects for their children are sufficiently small that any effect from DU exposure would be impossible to distinguish from background incidences of cancers and birth defects. Furthermore, veteran health statistics do not support claims of significant increases in cancers or birth defects among Gulf War veterans.
- For most DU-exposed veterans, the DU concentration in the kidney was too small to result in kidney-related health effects. However, a few Level I veterans may have

inhaled sufficient quantities of DU particulate to experience transient kidney damage. Long-term kidney health effects are not expected for any DU-exposed veterans.

- Currently, neurotoxic effects from DU exposure cannot be ruled out. Nonetheless, veteran test results to date suggest that major neurotoxic effects are unlikely. Other possible toxicity effects from DU internalization have been suggested; however, evidence for other chemically induced DU effects is not well established.
- Continued medical examination of DU-exposed veterans and tracking of veteran records is recommended to assure that no unexpected long-term health effects develop as a result of DU exposure. Some issues, such as the possibility of soft tissue sarcomas in the vicinity of DU fragments and possible neurotoxic effects, may require long-term monitoring.
- Continued basic research (e.g., animal testing) is recommended to determine the significance of possible linkages between DU exposure and chemically induced health effects such as neurotoxic effects.
- Reasonable precautions are suggested to reduce the possibility of health effects from DU exposure as a result of friendly fire, such as assuring that the ventilation system is operating following shell impact or rapidly exiting the vehicle.
- Timely post-battle screening and treatment, as required, are strongly recommended to provide accurate records for all Level I veterans.

## **7.4 DU-Exposed Iraqi Civilians**

- The radiological risk is extremely small for civilians located downwind from DU munitions use. Thus, DU is predicted to have no detectable health effects (including cancers, leukemia, and birth defects) on downwind civilians.
- Monitoring of DU in the environment suggests that DU contamination of food and water supplies has not been significant to date. Furthermore, widespread DU contamination in the distant future is unlikely.
- The most significant risk for Iraqi civilians may be for children playing in or near DU-damaged vehicles. The nominal risk of lung cancer for these children is about

0.04%, and the nominal risk of colon cancer is 0.06%. The risk of leukemia and other cancers is insignificant.

- The beta particle emission rate for DU is too low to present a risk of skin burns from direct contact with DU metal. However, a DU fragment in close contact with the skin at the same location for many years (e.g., worn as jewelry) could result in a local skin cancer risk from beta irradiation.
- Gamma radiation from nearby unburied shells, fragments, or particulate is too weak to present a significant radiological risk.
- No adverse kidney effects are predicted for Iraqi civilians exposed to DU.
- To reduce civilian risks to negligible levels, children should be discouraged from playing in or near battle-damaged vehicles.
- To assure that long-term contamination of the environment has not resulted from DU munitions use, continued monitoring of the post-battle zone environment and nearby civilians is suggested.

## References

1. World Health Organization, *Depleted Uranium Sources, Exposure and Health Effects*, WHO/SDE/PHE/01.1, Geneva, April 2001.
2. USACHPPM, “*Depleted Uranium in the Gulf*” Office of Special Assistant to the Sec. of Def. for Gulf War Illnesses, *Medical Readiness and Military Deployments (OSAGWI)*, HRA consultation no. 26-MF-7555-00D, September 15, 2000.
3. Fetter, S., and F. N. von Hippel, “The Hazard Posed by Depleted Uranium Munitions,” *Science and Global Security*, **8**, 125-161, 1999.
4. The Royal Society, *The Health Hazards of Depleted Uranium Munitions Part I*, London, UK, March 2002.
5. Parkhurst, M. A., F. Szrom, R. A. Guilmette, T. D. Holmes, Y. S. Cheng, J. L. Kenoyer, J. W. Collins, T. E. Sanderson, R. W. Fliszar, K. Gold, J. C. Beckman, and J. A. Long, *Capstone Depleted Uranium Aerosols: Generation and Characterization, Volumes 1 and 2*. PNNL-14168, Prepared for the U.S. Army by Pacific Northwest National Laboratory, Richland, Washington, October 2004.
6. Rostker, B., *Environmental Exposure Report: Depleted Uranium in the Gulf (II)*, Second Interim DoD report, 2000179-0000002, [www.gulflink.osd.mil/du](http://www.gulflink.osd.mil/du), July 28, 2003.
7. Andrews, W. S., E. A. Ough, B. J. Lewis, and L. G.1. Bennett, “Ballistic Properties of Depleted Uranium and Biological Consequences,” *Journal of Battlefield Technology*, **6**, No. 1, March 2003.
8. Lederer, C. M., and V. S. Shirley, *Table of Isotopes, 7<sup>th</sup> Edition*, John Wiley & Sons, NY, 1978.
9. Rostker, B., Office of the Special Assistant for Gulf War Illnesses (available through [www.ngwrc.org/Dulink/DU\\_Map.htm](http://www.ngwrc.org/Dulink/DU_Map.htm)) released to the Presidential Special Oversight Board (former Senator W. Rudman) on November 19, 1998, in Washington, DC.
10. Fahey, D., “The Depleted Uranium Issue in the Wake of the 2003 Iraq War,” presentation to Nuclear Policy Research Institute, *The Health Effects of Depleted Uranium Munitions*, New York Academy of Medicine, NYC, NY, June 2003.
11. The Royal Society, *The Health Hazards of Depleted Uranium Munitions Part II*, London, UK, March 2002.
12. U.S. Department of Energy, DOE STANDARD SAFT-0072 (DRAFT): *Guide to Good Practices for Occupational Radiological Protection in Uranium Facilities*, Washington, DC, January 2000.
13. Lemercier, V., X. Millot, E. Ansoborlo, F. Ménétrier, A. Flüry-Hérard, Ch. Rousselle, and J. M. Scherrmann, “Study of Uranium Transfer Across the Blood-Brain Barrier,” *Rad. Prot. Dos.*, **105** 2003.

14. Benson, K. A., "Evaluation of Health Risks of Embedded Depleted Uranium Shrapnel on Pregnancy and Offspring Development," *Envir. & Occup. Health Project Summary DoD-121*, Medsearch, December 31, 2002.
15. International Commission on Radiological Protection, ICRP Publication 60, *1990 Recommendations of the International Commission on Radiological Protection*, Pergamon, NY, 1991.
16. CIA Atlas of the Middle East, January 1993.
17. UNEP, *Desk Study of the Environment in Iraq*, United Nations Environmental Programme, 2003.
18. Araneta, M. R. G., K. M. Scglangen, L. D. Edmonds, D. A. Destiche, R. D. Merz, C. A. Hobbs, T. J. Flood, J. A. Harris, D. Krishnamurti, "Prevalence of Birth Defects Among Infants of Gulf War Veterans in Arkansas, Arizona, California, Georgia, Hawaii, and Iowa," *Birth Defects Research (Part A)* **67**, 2003.
19. McDiarmid, M. A., K. Squibb, S. Engelhardt, M. Oliver, P. Gucer, P. D. Wilson, R. Kane, M. Kabat, B. Kaup, L. Anderson, D. Hoover, L. Brown, and D. Jacobson-Kram, "Surveillance of Depleted Uranium Exposed Gulf War Veterans: Health Effects Observed in an Enlarged Friendly Fire Cohort," *JOEM* **43**, December 12, 2001.
20. Riegle, D. W., Jr., A. M. D'Amato, *The Riegle Report, US Chemical and Biological Warfare-Related Dual Use Exports to Iraq and their Possible Impact on the Health Consequences of the Gulf War*, U.S. Senate, 103rd Congress, 2<sup>nd</sup> Session, May 25, 1994.
21. Bleise, A., P. R. Danesi, W. Burkart, "Properties, Use and Health Effects of Depleted Uranium (DU): A General Overview," *Jour. Envir. Rad.*, **64**, 2003.
22. Bem, H., and F. Bou-Rabi, "Environmental Consequences of Depleted Uranium Use in the 1991 Gulf War," *Envir. Inter.*, 2003.
23. United Nations Environmental Programme (UNEP), *Depleted Uranium in Bosnia and Herzegovina Post-Conflict Environmental Assessment*, March 10, 2003.
24. International Commission on Radiological Protection, *Limits of Intakes of Radionuclides by Workers*, ICRP publication 30, Pergamon, NY, 1979.
25. International Commission on Radiological Protection, *Human Respiratory Tract Model for Radiological Protection*, ICRP Publication 66, Pergamon, NY, 1994.
26. International Commission on Radiological Protection, *Age-Dependent Doses to Members of the Public from Intake of Radionuclides*, ICRP Publication 69, Pergamon, NY, 1995.
27. Pellmer, T. C., J. B. Hogan, K. A. Benson, and M. R. Landauer, *Toxicological Evaluation of Depleted Uranium in Rats: Six Month Evaluation Point*, Armed Forces Radiobiology Research Institute, VA, February 1998.
28. Lewis, J., personal communication, University of New Mexico College of Pharmacy, May 2004.

29. Mettler, F. A., Jr., M.D., and A. C. Upton, M.D., *Medical Effects of Ionizing Radiation*, 2<sup>nd</sup> Ed., W.B. Saunders Co., Philadelphia, 1995.
30. National Cancer Institute, [http://seer.cancer.gov/csr/1975\\_2002/sections.html](http://seer.cancer.gov/csr/1975_2002/sections.html), 2002.
31. Hahn, F. F., R. A. Guilmette, and M. D. Hoover, "Implanted Depleted Uranium Fragments Cause Soft Tissue Sarcomas in the Muscles of Rats," *Envir. Health Persp.*, **10**, No. 1, January 2002.
32. Leggett, R. W., and T. C. Pellmar, "The Biokinetics of Uranium from Embedded DU Fragments," *Journal of Environmental Radioactivity*, **64**, 2003.
33. Physicians Committee for Responsible Medicine, *Birth Defect Statistics*, February 26, 2004.
34. Agency for Toxic Substance and Disease Registry, *Summary of the ATSDR Soil-Pica Workshop*, Atlanta, GA, June 7–8, 2000.
35. Science Applications International Corporation, *Hazard Prediction Assessment Capability (HPAC), User Guide Version 4.0.1*, Prepared for the Defense Threat Reduction Agency, HPAC-UG-01-U-ROC0, April 19, 2002.
36. Dietz, L. A., *Some Consequences of Using Depleted Uranium Metal*, Presented at a Public Forum, Jonesborough, TN, November 12, 1994.
37. Federal Facilities Assessment Branch, Division of Health Assessment and Consultation, Agency for Toxic Substances and Disease Registry, *Health Consultation Colonie Site*, Colonie, NY, August 15, 2003.
38. Turner, D. B., *Workbook of Atmospheric Dispersion Estimates, An Introduction to Dispersion Modeling*, Lewis Publishers, Chapel Hill, NC, 1994.
39. Dietz, L. A., CHEM-434-LAD, *Investigation of Excess Alpha Activity Observed in Recent Air Filter Collections and Other Environmental Samples*, technical report, Knolls Atomic Power Laboratory, Schenectady, NY, January 24, 1980.
40. MathSoft Engineering and Education, *Mathcad 2001 Professional User's Guide With Reference Manual*, 2001.
41. University of Washington School of Medicine, *Urine Sediment Findings*, <http://eduserv.hscer.washington.edu/hubio562/urinary/proteinuria.html>, Seattle, WA, February 2000.
42. Environmental Protection Agency, *Estimating Radiogenic Cancer Risks Addendum: Uncertainty Analysis*, EPA 402-R-99-003, May 1999.
43. National Council on Radiation Protection and Measurements, *Evaluation of the Linear-Nonthreshold Dose-Response Model for Ionizing Radiation*, NCRP Report No. 136, Bethesda, MD, June 4, 2001.
44. National Council on Radiation Protection and Measurements, *Uncertainties in Fatal Risk Estimates Used in Radiation Protection*, NCRP Report No. 126, Bethesda MD, October 17, 1997.

45. BEIR V, *Health Effects Exposure to Low Levels of Ionizing Radiation*, National Academy Press, Washington, DC, 1990.
46. Guilmette, R. A., M. A. Parkhurst, G. Miller, F. F. Hahn, L. E. Roszell, E. G. Daxon, T. T. Little, J. J. Whicker, Y. S. Cheng, R. J. Traub, G. M. Lodde, F. Szrom, D. E. Bihl, K. L. Creek, and C. B. McKee, *Human Health Risk Assessment of Capstone Depleted Uranium Aerosols*. Prepared for the U.S. Army by Battelle under Chemical and Biological Defense Information Analysis Center Task 241, DO 0189, Aberdeen, Maryland, (PNWD-3442), October 2004.
47. Szrom F., E. G. Daxon, M. A. Parkhurst, G. A. Falco, and J. W. Collins, *Level II and Level III Inhalation and Ingestion Dose Calculations*. Prepared for the U.S. Army by Battelle under the Chemical and Biological Defense Information Analysis Center Task 241, DO 0189, Aberdeen, Maryland, (PNWD-3480), October 2004.
48. Flanders, L., "Mal de Guerre," *The Nation*, March 7, 1994.
49. Committee to Review the Health Consequences of Services During the Persian War, Medical Follow-up Agency, Institute of Medicine, National Academy Press, Washington, DC, 1996.
50. Cowan, D. N., R. F. DeFraitcs, G.C. Gray, M.B. Goldenbaum, and S.M. Wishik, "The Risk of Birth Defects Among Children of Persian Gulf War Veterans," *New England Journal of Medicine* 336 **23**, 1997.
51. Parsons, R. J., "The Balkan DU Cover-up," *The Nation*, April 9, 2001.
52. Investigative Commission, Italian Ministry of Defense, *Preliminary Report of the Investigative Committee Established by the Italian Ministry of Defense on the Incidence of Malignant Neoplasia Among Military Personnel Involved in Operations in Bosnia and Kosovo*, March 19, 1994.
53. Presidential Advisory Committee, *Presidential Advisory Committee Presidential Advisory Committee on Gulf War Illnesses*, Final Report, Chapter 3, May 5, 2005.
54. Busby, C., "Health Risks Following Exposure to Aerosols Produced by the Use of Depleted Uranium Weapons," Green Audit, Presented at *Res Publica conference on DU*, Prague, Czech Republic, November 24–25, 2001.
55. National Cancer Institute, [http://seer.cancer.gov/csr/1975\\_2002/sections.html](http://seer.cancer.gov/csr/1975_2002/sections.html), 2002.
56. Sweet, W., "Chernobyl's Stressful After Effects," *IEEE Spectrum*, November 1996.
57. Bair, W. J., Current Status of the Hot Particle Theory (A Review of Current Experimental and Theoretical Approaches), IRPA Proceedings, Paris, June 6, 2002.

## Appendix A: Nuclear Basics

This appendix (1) introduces basic nuclear concepts; (2) provides a brief discussion of radiation exposure and dose quantification; and (3) discusses the relationship between radiation dose and the consequent risk of health effects. The methodology used to estimate radiation dose and health effects for Gulf War exposure to DU is discussed in Appendix E.

### A1. Atomic and Nuclear Structure

The nucleus of an atom is made up of positively charged protons and uncharged neutrons. The atomic number  $Z$  equals the number of protons in the nucleus, and the mass number  $A$  equals the total number of nucleons (protons plus neutrons). All atoms possessing the same atomic number are identified as the same chemical element and generally have essentially identical chemical characteristics, regardless of their mass number. However, the nuclear characteristics of an atom depend on the number of protons and neutrons in the nucleus. Species of atoms having the same atomic number, but different mass numbers, are referred to as isotopes. The nucleus of the element uranium contains 92 protons ( $Z = 92$ ), and the nuclei of naturally occurring uranium isotopes are found to contain either 142, 143, or 146 neutrons. Thus, the naturally occurring isotopes of uranium have mass numbers of 234, 235, and 238, respectively.

### A.2. Activity and Half-life

The process of radiation emission by unstable nuclides is called radioactive decay, and radioactive isotopes are called radioisotopes. Nuclear decay typically results in the emission of alpha or beta particles and gamma rays ( $\alpha$ ,  $\beta$ , and  $\gamma$ , respectively). An alpha particle is actually a highly stable cluster of two neutrons and two protons, identical to a helium nucleus. A beta particle is a negatively or positively charged particle (electron or positron, respectively) emitted from the nucleus, and gamma radiation is electromagnetic radiation emitted from a nucleus.

The total number of atoms of a radioisotope  $\mathcal{N}$  at time  $t$  is

$$\mathcal{N}(t) = \mathcal{N}_0 e^{-\lambda t},$$

where  $\lambda$  is the *decay constant* ( $s^{-1}$ ) and  $\mathcal{N}_0$  is the initial number of atoms. The decay constant is a fundamental property for each species of radionuclide. The number of nuclear transformations (disintegrations) per second is called its *activity*  $\mathcal{A}$  of the isotope. If only one isotope in a substance is radioactive and its daughter product is stable, then its activity is given by

$$\mathcal{A}(t) = \lambda \mathcal{N}(t).$$

Activity is often given in units of *curies* (Ci), equal to  $3.7 \times 10^{10}$  disintegrations per second or *becquerel* (Bq), equal to 1 disintegration per second. The specific activity  $\tilde{\mathcal{A}}$ , in Bq/g, is defined in terms of the atom density  $N$  (atoms/cm<sup>3</sup>) and mass density  $\rho$  (g/cm<sup>3</sup>) as,

$$\tilde{\mathcal{A}} \equiv \lambda \frac{N}{\rho}.$$

Radionuclides are commonly characterized by a half-life  $t_{1/2}$ . The half-life is the time in which half the number of atoms of a particular radionuclide decays to another nuclide or a lower energy state than the original radionuclide. The half-life is inversely proportional to the decay constant,

$$t_{1/2} = 0.693 / \lambda.$$

The majority of natural and depleted uranium consists of the U-238 radioisotope, which decays with a half-life of  $4.51 \times 10^9$  years.

Radioisotopes often decay to form other radionuclides that are also unstable. When radioactive decay produces a number of radionuclides in a sequence, the radioisotope sequence is referred to as a *decay chain* or *decay series*. When the parent radionuclide has a much longer half-life than the subsequent daughter nuclides, the shorter half-life daughter products will eventually exhibit the same decay rate as the parent radionuclide. For these conditions the daughter products are said to be in secular equilibrium with the parent nuclide.

### **A.3. Ionizing Radiation**

Ionizing radiation includes all types of radiation capable of displacing electrons from atoms to form ions (an ion is an atom possessing a net electrical charge). Important types of ionizing radiation relevant to this study include alpha particles, beta particles, and gamma radiation.

Because alpha and beta particles are charged, they will interact with the charged atomic electrons of any substance that they penetrate. The incident charged particle can transfer a sufficient fraction of its kinetic energy to the atomic electrons to remove orbital electrons from the atoms of the target material. This process will produce an ion-pair (the ionized atom and liberated electron) and result in a loss in energy for the incident radiation. The number of ionized atoms per unit path length increases with increasing mass and electrical charge of the incident radiation. For example, the mass of an alpha particle is more than 7,000 times greater than the mass of a beta particle; and the charge of an alpha particle is twice the charge of a beta particle. An alpha particle produces about 500 times more ion-pairs per cm than are produced by beta particles of the same energy. Because charged particles directly interact with orbital electrons, they do not penetrate deeply into matter. A massive alpha particle moves relatively slowly compared to other less massive particles of the same energy. As a consequence, the probability of interaction with atomic electrons is high for alpha particle, and they lose energy by ionization far more rapidly than other types of radiation, resulting in a very small range of penetration.

Unlike alpha particles, beta particles are not emitted at some characteristic energy for each decay of a particular type of radioisotope. Instead, beta particles exhibit a spectrum of energies characterized by a maximum and average energy. The decay energy is divided between the beta particle and an anti-neutrino or neutrino. Anti-neutrinos have an extremely small probability of interaction with matter; consequently, anti-neutrinos do not contribute to radiological risk. Low-mass beta particles can penetrate to greater depths than the heavier alpha particles. Because the alpha and beta particles directly ionize atoms, they are characterized as directly ionizing radiations.

Gamma radiation can be viewed as a high-energy electromagnetic wave or particle. Because gamma radiation is uncharged, it does not interact on a continuous basis with atomic electrons and is far more penetrating than alpha or beta radiation. Nonetheless, gamma radiation can produce a number of high-energy electrons by several different processes as it penetrates matter. These high-energy electrons subsequently ionize many atoms as they, in-turn, penetrate matter. Because of this two-step process, gamma radiation and other uncharged particle radiations are referred to as indirectly-ionizing radiations.

#### **A.4. Source Strength and Particle Flux**

Source strength  $s_R$  describes the emission rate of nuclear particles, in particles/sec, resulting from nuclear disintegration. Source strength depends on the composition and quantity of radioisotopes in the source and the number of each type of particle emitted per disintegration from each radioisotope. If one radioisotope species emits only one particle per disintegration, and essentially all radiation escapes the source, then  $s_R = \mathcal{A} \times (3.7 \times 10^{10} \text{ particles/s})$ , where  $\mathcal{A}$  is given in curies. This simple relationship of source strength to activity does not apply if more than one type of particle is emitted, and the relationship does not distinguish between source strengths of particles of the same type that are emitted at different energies. Also, absorption, scattering, and other types of particle interactions within the source can alter the relationship of source strength to activity.

Source strength does not characterize the radiation incident upon living tissue. *Particle flux*  $\phi_R$ , in units of particles/cm<sup>2</sup> s, is used to express the incident radiation at a particular location. The particle flux incident on a particular organ will depend on whether one is exposed externally to direct radiation from the source or internally to radioactive material that has been inhaled, ingested, or embedded in the body. In general, the flux level will depend on the distance from the source. For a point source of radiation type  $R$  in a vacuum, the particle flux decreases because of geometric attenuation as the inverse square of the distance  $r$  from the source; that is,

$$\phi_R(r) = \frac{S_R}{4\pi r^2}.$$

If air or other materials occupy the space between the source and an exposed individual, these materials may scatter or absorb some of the incident particles resulting in a reduction in the magnitude of the incident particle flux.

## A.5. Dose Concepts

Although particle flux can be used to express the magnitude of the incident radiation, the particle flux does not directly provide the dose absorbed by an individual or organ. Dose is a quantitative measure of radiation exposure. A number of dose concepts are used in radiation safety analysis, regulation, and monitoring. The most important concepts and units are discussed in the following.

### Absorbed Dose and Linear Energy Transfer

When radiation interacts with matter, it can cause damage to the material that absorbs the incident radiation energy. The extent of damage induced in a given mass of material is roughly proportional to the energy absorbed, which is called the *absorbed dose*  $D$ . The SI unit for absorbed dose is the *gray* (Gy). One gray is equal to an absorbed radiation dose of 1 joule per kilogram. An older unit of radiation dose is the *rad*. One Gy = 100 rad.

An important consideration for determining the biological effects of radiation is the rate of energy loss per unit distance traversed by the radiation. The higher the rate of linear energy transfer (LET), the more effective the radiation is in causing biological damage. Heavy charged particles, such as alpha particles, have much higher LET than gamma photons or beta particles. Although alpha particles have a high LET, internal organs are protected from external alpha radiation because alpha particles produced by nuclear decay do not penetrate human skin. On the other hand, if alpha-emitting material is ingested or inhaled, alpha radiation can produce cell damage in the living tissue of internal organs with potentially serious consequences.

## Equivalent Dose

The biological effect from radiation depends on the type and energy of the radiation as well as the magnitude of the absorbed dose. To account for the effect of different forms of radiation, a quantity called the *relative biological effectiveness* (RBE) is used. The RBE is defined as the ratio of the absorbed energy from 200-keV x-rays required to produce a given biological effect to the absorbed energy from another radiation to produce the same effect. The RBE is used to obtain radiation weighting factors  $W_R$ . The International Committee on Radiation Protection (ICRP) has identified the values for  $W_R$  given in Table A-1.

The radiation weighting factor for alpha particles requires some discussion. The weighting factor can be dependent on the particular health effect under consideration and on whether the relative risk is applied to high or low dose rates. According to Reference [1], the weighting factor of 20 for alpha particles applies to risks from low dose rate exposures. For high dose rate exposures, the radiation weighting factor should be 10.

**Table A-1. ICRP 60 radiation weighting factors for various radiations [2]**

Type of Radiation	$W_R$
X-rays, gamma rays, beta particles	1
Neutrons	
thermal energy	5
0.01 – 0.1 MeV	10
0.1 – 2 MeV	20
2 to 20 MeV	5
Alpha particles, fission fragments	20

Radiation-weighted doses  $H$  incorporate the relative biological effectiveness of different forms of radiation. The ICRP calls the radiation-weighted dose the *equivalent dose* and uses the *sievert* (Sv) as the unit of measure. The equivalent dose  $H_T$  in tissue or organ  $T$  is defined by the ICRP as

$$H_T = \sum_R W_R D_{T,R} ,$$

where  $D_{T,R}$  is the absorbed dose in Gy from radiation  $R$  averaged over the tissue or organ  $T$ . In U.S. Nuclear Regulatory Commission (NRC) regulations, the radiation-weighted dose unit is the *rem* (one rem = 0.01 Sv).

### Effective Dose and Committed Dose

The probability of a detrimental effect in any organ is generally taken to be proportional to the dose equivalent in that tissue or organ. Because of differences in sensitivity, however, the proportionality factors differ from organ to organ. The relative sensitivity to detrimental effects is expressed as a tissue-weighting factor  $W_T$ . Table A-2 provides the tissue weighting factors recommended in ICRP 60. If different organs receive different doses, the weighting factors in Table A-2 are used to calculate an effective dose  $H_E$ . These weighting factors are currently under review for revision.

**Table A-2. ICRP 60 tissue weighting factors  $W_T$  based on sensitivity to tumor induction [2]**

Tissue or Organ	$W_T$
Gonads	0.20
Bone marrow (red)	0.12
Colon	0.12
Lung	0.12
Stomach	0.12
Bladder	0.05
Breast	0.05
Liver	0.05
Esophagus	0.05
Thyroid	0.05
Skin	0.01
Bone surface	0.01
Remainder	0.05

From the preceding paragraph, we observe that the effective dose is given by,

$$H_E = \sum_T W_T H_T;$$

hence,

$$H_E = \sum_T W_R \sum_R W_T D_{T,R}.$$

Following ingestion or inhalation of radioactive materials, the dose rate will generally be time dependent. The concepts of dose rates and committed dose were established primarily to predict radiological effects associated with inhaled or ingested radioactive materials. Absorbed dose rate  $\dot{D}$  and equivalent dose rate  $\dot{H}_T$  are the absorbed dose and equivalent dose received per unit time, with units Gy/s and Sv/s, respectively. The time integral of the equivalent dose rate  $\dot{H}_T$  over a specified period  $\tau$  is called the *committed equivalent dose*:

$$H_T = \int_{\tau} \dot{H}_T(t) dt .$$

Similarly a committed effective dose is defined as

$$H_E = \int_{\tau} \dot{H}_E(t) dt .$$

## A.6. Radiation Health Effects

Radiation sources are often categorized as either *external* sources, originating outside the body, or *internal* sources, resulting from inhalation or ingestion of radioactive substances (Figure A-1). Exposure to either external or internal radiation can cause both *somatic* effects (in which injury is incurred by the irradiated individual) and hereditary effects, which are genetic effects passed on to the children of an individual receiving germ cell radiation damage. Radiation injuries can be further classified as either *deterministic* or *stochastic* health effects. A deterministic effect is one for which there is a direct causal relationship between the exposure and the observed effect. A stochastic effect is one in which the probability (rather than the severity) of an induced health effect is proportional to dose. Stochastic effects occur among unexposed as well as exposed individuals. Radiation-induced cancers and genetic effects are stochastic.

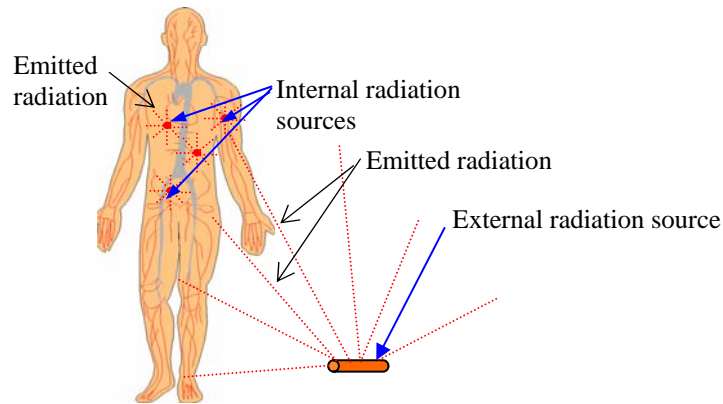


**Figure A-1. Illustration of internal and external radiation sources**

## **Large Acute Doses – Early Health Effects**

Large doses received over short time periods threaten both the short- and long-term health of exposed individuals. If exposures are sufficiently intense, exposed organs are damaged, causing radiation sickness or death within days or months. Radiation-induced sickness is a deterministic effect. A deterministic effect is one for which (1) a certain minimum dose must be exceeded before the effect is observed; (2) the magnitude of the effect increases with the size of the dose; and (3) there is a clear, unambiguous causal relationship between the exposure and the observed effect. Once the threshold dose has been exceeded, the fraction of the exposed population in which the health effect occurs (the health effect's incidence) rises rapidly with increasing dose until the effect appears in all the exposed individuals. Estimates of the threshold for radiation sickness caused by whole body gamma-ray exposure range from 0.5 to 1 Gy. The threshold for early deaths because of whole body gamma-ray exposures is about 2.5 Gy.

## **Late Health Effects**

Populations receiving large acute doses that are insufficient to cause early fatalities are subject to increased risk of stochastic health effects, including cancer and genetic effects. Cancers and genetic effects may also result from chronic exposures to low levels of radiation. The radiological risks posed by small acute doses or moderately large doses received at low dose rates are more controversial than risks from high dose rates. Statistically significant associations of radiation doses with cancer have not been

demonstrated below about 0.05 to 0.1 Sv. Although the induction of cancers in humans from low radiation doses has not been clearly demonstrated, based on theoretical considerations, there does not appear to be a threshold radiation dose below which the risk of any induced cancers would be zero. Nonetheless, some types of cancers may not be induced by radiation exposure; and other types of cancers have been found to exhibit a high-dose threshold.

Radiation-induced genetic effects have not been observed in humans at any dose; however, animal testing suggests that radiation-induced genetic effects are probable for humans as well. The inability to clearly observe radiation-induced genetic effects in humans is believed to result from the relatively low risk of radiation-induced genetic effects compared to the much higher risk of spontaneous birth defects and birth effects because of other causes (alcohol, smoking, malnutrition, etc.). Conservative extrapolations of data from animal experiments are used to estimate the risk of radiation-induced genetic effects for humans.

The traditional practice for estimating cancer risks has been to extrapolate the dose-response curve linearly to zero dose as indicated in Figure A-2, curve (a). This procedure is referred to as the *linear non-threshold hypothesis* (LNT). The linear nonthreshold model has been challenged by some as being too conservative and by others as being too optimistic. Alternatives to the LNT model are also presented in Figure A-2. Curve (b) illustrates a linear response for low-to-intermediate dose range with a nonlinear trend in the high-dose range (linear-quadratic response); curve (c) is an example of a threshold dose response model; curve (d) is for a supralinear response, giving a greater effect per unit dose at low doses than at high doses; and curve (e) shows a hormetic response (radiation dose health benefit) at low doses.

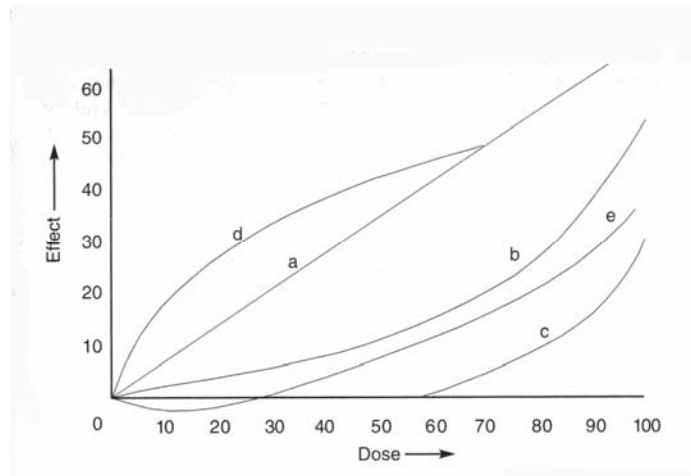


**Figure A-2. Dose-response curves for acute radiation doses [3]**

The National Council on Radiation Protection and Measurements (NCRP) has recently carried out an exhaustive review of research to determine the appropriateness of the linear nonthreshold model [3]. The report also observes “that the rates of cancer in most populations exposed to low level radiation have not been found to be detectably increased, and that in most cases the rates appeared to be decreased.” However, the report concludes that “because of the limitations of statistical power and the potential for confounding, low-dose epidemiological studies are of limited value in assessing dose-response relationships and have produced results with sufficiently wide confidence limits to be consistent with an increased effect, a decreased effect, or no effect.” Nonetheless, experiments and theoretical models have led the NCRP authors to conclude that the expected dose response “is linear without threshold at low-to-intermediate doses.” The authors also state, “Although other dose-response relationships for mutagenic and carcinogenic effects of low-level radiation cannot be excluded, no alternative dose-response relationship appears to be more plausible than the linear-nonthreshold model on the basis of present scientific knowledge.”

It is commonly accepted that linear extrapolation from high doses is proper for high-LET radiation. For low-LET radiation, on the other hand, there is evidence to suggest that linear extrapolation from high acute doses overestimates the cancers attributable to chronic or small acute doses because it ignores the capability of biological systems to repair themselves.

## **Radiation-Induced Cancer Mechanisms**

Cancer is defined as a localized growth from uncontrolled cell reproduction that can spread to other parts of the body [4]. Cancer can be induced by damage to the DNA in the nucleus of a cell. Each cell in the human body experiences thousands of spontaneous DNA damage events a day from thermodynamic instabilities and chemical attack by reactive chemicals produced during normal biological processes. Single-strand breaks of the DNA molecule are very common occurrences from spontaneous processes and are rapidly repaired from the mirror half of the DNA molecule. Nonetheless, about one out of  $10^6$  damage events results in a spontaneous cell mutation.

In addition to spontaneous processes, radiation and many chemicals can damage DNA molecules and induce cancers. Radiation-induced DNA damage can result from the direct effect of radiation ionization of the DNA molecule or from indirect effects resulting from the production of reactive chemicals that can interact with organic molecules within the cell. About one-third of the damage results from direct radiation interaction, and two-thirds from indirect chemical effects. Although single-strand breaks are a common form of spontaneous DNA damage, double-strand breaks are caused only by ionizing radiation. Double-strand breaks are extremely difficult to repair; consequently, radiation induced DNA damage is not in general identical to spontaneous mutations [5].

DNA damage that is not properly repaired and does not lead to cell death can result in cancer induction. However, a subsequent sequence of events is required for a mutation to develop into cancer. The three main phases required for cancer development are initiation, promotion, and progression. Initiation begins with genetic mutation in a cell. If the gene affected by DNA damage plays a role in cell growth, reproduction, or differentiation, the mutated cell may exhibit a predisposition for aberrant cellular growth and behavior. For the next stage, promotional agents, such as bile acids, are required to stimulate the growth of mutated cells. For full malignancy to develop in the progression phase, however, an accumulation of further gene mutations in pre-cancerous cells is required [6].

The preceding discussion illustrates some of the complexities and factors associated with cancer induction. These types of considerations and other research have

led researchers to conclude (1) a variety of influences, including spontaneous mutations, can lead to cancer induction; (2) cancer induction is a stochastic health effect (wherein the dose correlates with the probability of cancer induction, but not the severity of the cancer); (3) cancer is typified by a latency period between the time of exposure to the time of cancer induction; and (4) for low-LET radiation exposures at low doses or low dose rates, repair processes can reduce the probability of cancer induction.

## A.7. Risk Coefficients

The ICRP estimates that a collective dose of 100 person-Sv (0.1 Sv to 1000 people,  $10^{-3}$  Sv to 100,000 people, etc.) will result in five radiation-induced cancer fatalities in an affected general population (including children). This relationship is expressed by a risk coefficient  $p_c = 0.05$  cancer fatalities/Sv. For adult radiation workers,  $p_c = 0.04$  cancer fatalities/Sv. The risk to adult workers is lower because children (included in the general population) are generally more sensitive to radiation than are adults. Similar risk coefficients can be used for genetic effects. The equilibrium risk coefficient for genetic defects  $p_g$  is about 0.008/Sv for adult workers and about 0.013/Sv for the general population. The equilibrium risk refers to the genetic risk per generation that is established after several generations. The first-generation risk coefficient is at least a factor of five smaller than the equilibrium value [7]. A summary of the ICRP probability coefficients is presented in Table A-3.

**Table A-3. ICRP risk coefficients for cancers and hereditary effects for low dose rate exposures [2]**

Exposed Population	$p$ (Effect/Sv)		
	Fatal Cancer	Nonfatal Cancer	Hereditary Effect
<i>Adult Workers</i>	0.04	0.008	0.008
<i>Whole Population</i>	0.05	0.010	0.013

## References:

1. Environmental Protection Agency, *Estimating Radiogenic Cancer Risks*, EPA 402-R-93-076, June 1994.
2. International Commission on Radiological Protection, ICRP Publication 60, *1990 Recommendations of the International Commission on Radiological Protection*, Pergamon, NY, 1991.
3. National Council on Radiation Protection and Measurements, *Evaluation of the Linear-Nonthreshold Dose-Response Model for Ionizing Radiation*, NCRP Report No. 136, Bethesda MD, June 4, 2001.
4. Baggaley, A., ed., *Human Body*, DK, NY, 2001.
5. Cooper, J. R., K. Randle, and R. S. Sokhi, *Radioactive Releases in the Environment*, Wiley, West Sussex, England, 2003.
6. Mettler, F. A., Jr., M.D., and A. C. Upton, M.D., *Medical Effects of Ionizing Radiation*, 2<sup>nd</sup> Ed., W.B. Saunders Co., Philadelphia, PA, 1995.
7. National Council on Radiation Protection and Measurements, *Risk Estimates for Radiation Protection*, NCRP Report No. 115, Bethesda, MD, December 31, 1993.

## **Appendix B: DU Mass Internalized**

The quantity of DU internalized must be determined to assess both chemical and radiological health effects. The methods selected were based upon the most reliable source of data or methodology for each scenario. The general approach used to compute internalized DU mass is described in Section 3 of the text. Computational details are discussed in this appendix.

### **B.1. Aerosolized DU Mass**

For most inhalation exposure cases studied, the calculation of internalized DU mass required estimates of the quantity of DU aerosolized during penetrator impact and the quantity of DU particulate resuspended during post-impact activities. Data for DU aerosolization and resuspension were obtained from the Capstone test program. The exception to this approach was for the analysis of DU inhalation for Level I veterans. The analysis for Level I veterans in Section B.3 was based on measured DU concentrations in the urine of friendly fire veterans.

#### **Capstone Program**

The U.S. Army recently sponsored a program referred to as the Capstone DU Aerosol Characterization and Risk Assessment Program, which included a careful test program conducted by Pacific Northwest National Laboratories [1]. The test program consisted of a series of tests carried out within an enclosed structure referred to as the Superbox. In all tests, 120 mm DU rounds were fired at either Abrams tanks or BFVs. Tests were conducted with the vehicle ventilation system turned on and with the ventilation system turned off. A variety of impact locations and angles were explored, and some tests included two successive hits by DU penetrators. All tests were highly instrumented and a very large volume of detailed data was accumulated on the particulate generated by impact. Aerosol data include time-dependent DU particulate size distributions, aerosolized mass, and solubility [1].

## In-Vehicle Resuspended DU Mass

The inhaled DU mass can be estimated for a child at play or a veteran working in a destroyed military vehicle by using the resuspended DU aerosol densities from the Capstone report [1: p. 5.42]. Shortly after firing DU penetrators at armored vehicles, Capstone recovery crews entered the vehicles wearing respirators and personal air samplers. Data from the personal air samplers provided in-vehicle resuspended DU aerosol densities ranging between 0.06 and 0.97 mg/m<sup>3</sup>. Thus, the average DU air concentration was about 0.5 g/m<sup>3</sup> and the maximum was about 1 g/m<sup>3</sup>. For one of the two test shots, where two penetrators were fired (PI-3/4), the measured resuspended DU air concentration was lower than for all tests where only a single penetrator was fired. The other two-shot test (PII-1/2) was for a BFV rather than an Abrams tank. For this test, the resuspended DU air concentration was two to three times greater than the resuspended DU air concentration measured for the PI-3 test in which a BFV was struck by a single penetrator. In the absence of a clearly demonstrated correlation between number of rounds and resuspended DU air concentration, the resuspended DU air concentration will be assumed to correlate directly with the number of shots fired.

DU internalization for a child playing in a DU-contaminated vehicle is for chronic exposure rather than for acute exposure, and the mass internalized must be expressed as a mass inhalation rate  $\dot{m}$  rather than a mass  $m$ . The DU mass inhalation rate is

$$\dot{m} = R_b C_{iv} O_c .$$

Here,  $R_b$  is the breathing rate (m<sup>3</sup>/d),  $C_{iv}$  is the in-vehicle DU air concentration (g/m<sup>3</sup>), and  $O_c$  is the fraction of the elapsed time that is spent in the DU-contaminated vehicle. The nominal in-vehicle duration for a child is difficult to bound; consequently, an arbitrary high post-battlefield exposure time of 1000 hours was assumed. One-third of the exposure time (~300 hrs) was assumed to occur within a destroyed military vehicle over a 10 year period; thus,  $O_c = 300/(24 \times 365 \times 10) = 0.0034$  is the in-vehicle occupation fraction for a child over a 10-year period. For a veteran working in or exploring a DU-contaminated vehicle, inhalation of resuspended DU is over a relatively brief period of time; consequently, the biokinetic analysis for veterans inhaling resuspended DU is treated as an acute exposure rather than a chronic exposure.

## **DU Mass Released to Environment**

The quantity of DU released into the environment must be known in order to estimate the DU exposure for nearby veterans and civilian populations. Although the Capstone test program provided excellent information on the quantity of impact-generated DU aerosols released inside target vehicles, very little information is available for the mass of DU released external to the target vehicle. For these tests, the Superbox building completely enclosed the target vehicle and nearby environment. This artificial environment did not provide realistic external aerosol densities because of building confinement and the absence of wind dispersion. Furthermore, some of the DU mass released into the environment may have resulted from the impact of the DU round with the backstop after exiting the target vehicle. In the Iraq battle situation, a DU penetrator that both entered and exited a vehicle would most likely be deposited in the sand. Sand burial would be unlikely to make a significant contribution to aerosol generation.

### **120 mm Penetrators**

To provide an estimate of the DU released into the environment, the Capstone test data were used to first obtain the DU mass released inside the test vehicle. For crossing shots (penetrator both enters and exits vehicle), DU will be released inside the vehicle upon entering and exiting the vehicle, as shown in Figure B-1. Here we assume that the quantity of aerosolized DU released externally during impact is roughly the same as the quantity of aerosolized DU released internally during impact with the opposite vehicle wall (i.e.,  $m_0 \approx m_2$ ). Furthermore, we assume that the quantity of aerosolized DU released into the vehicle during penetrator entry is roughly the same as the quantity of aerosolized DU released into the environment during penetrator exit through opposite vehicle wall (i.e.,  $m_1 \approx m_3$ ). Hence,  $m_0 + m_3 \approx m_1 + m_2$ , or the mass released internal to the vehicle, is approximately equal to the mass released external to the vehicle. For the two tests in which the DU penetrator did not exit the vehicle, the quantity of DU measured by aerosol monitors external to the vehicle was very small; consequently, as illustrated in Figure B-1, most of the DU particulate released into the environment probably occurred as the penetrator exited the vehicle. The preferential deposition within the vehicle can be inferred from the Capstone deposition tray data [1: Attach. 1, p. 5.37]

and was observed by Hanson et al. from their penetrator test data for 30 mm DU penetrators [2].

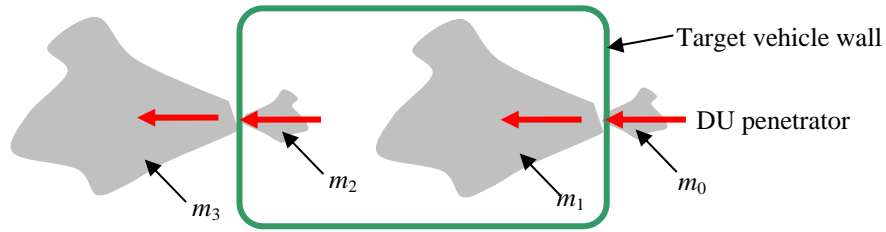


**Figure B-1. Schematic illustration of DU aerosol release during DU penetrator crossing shot through an armored vehicle**

The air concentration for DU released inside the vehicle is provided as a function of time in Table S.1 in the Capstone report for six tests representing six different scenarios. The internal volumes of a tank and BFV are about  $7.2 \text{ m}^3$  [3: p 86] and  $10 \text{ m}^3$  [1: Attach. 1, p. 4.51], respectively. Using these volumes and the data from Table S.1 in the Capstone report, the time-dependent masses of DU suspended in the vehicle air were calculated and plotted in Figure B-2. The total aerosolized DU mass in the vehicle is the inferred DU aerosol mass within the first few seconds following penetration. From Figure B-2, we find that for a tank, the total in-vehicle DU aerosol mass is about 60 g for a crossing shot and 100 g for a shot fired into the breach (no exit). Figure B-2 also shows a total in-vehicle aerosol DU mass of about 30 g for a BFV.

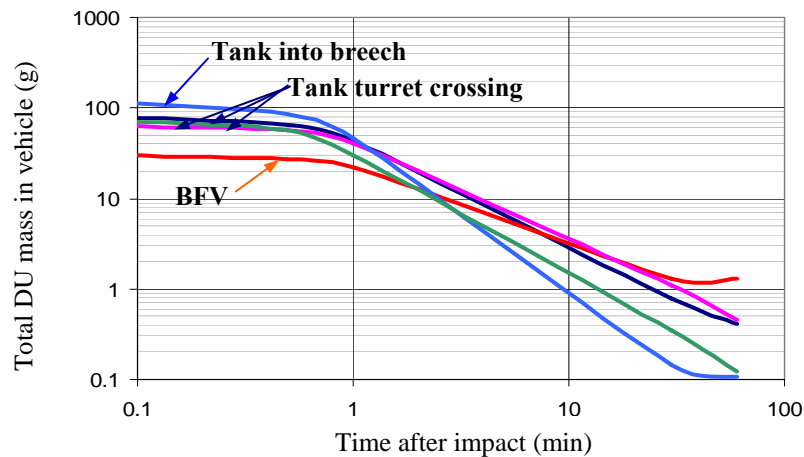


**Figure B-2. Time-dependent DU masses suspended in test vehicle air (no ventilation) based on capstone test data**

Taking the largest inferred value for the in-tank DU mass and the inferred value for the BFV DU mass, the in-vehicle DU aerosolized masses are 100 g and 30 g for the tank and BFV targets, respectively. Using the assumption that the DU mass released as an aerosol within the vehicle is equal to the aerosolized mass released into the environment, the ex-vehicle DU aerosolized masses are also 100 g for a tank and 30 g for a BFV. (This approach may overestimate the ex-vehicle DU mass for a tank because the 100 g value is for a no-exit shot rather than a crossing shot.) The DU masses released for an Iraqi tank and light vehicle are assumed to equal the mass released for a U.S. tank and U.S. BFV, respectively.

### **30 mm Penetrators**

The Capstone test program did not use 30 mm DU penetrators during the penetrator tests; however, Hanson et al. performed 30 mm penetrators tests using armor plate as a target [2]. For these tests, typically 1 to 2% of the penetrator mass (~5 g) was aerosolized on the entrance side of the armor plate and an average of about 20% on the exit side (corresponding to the inside of a vehicle). One of the five test shots did not penetrate the armor. For this shot, less than 1% of the penetrator mass was released on the entrance side of the armor. Stolfi, et al. conducted tests using A-10 aircraft to fire 30 mm rounds against two Soviet T-62 tanks [4]. A total of 93 DU rounds struck the two tanks during seven passes. Only 18% of the penetrator impacts resulted in perforation, and only 10% of the rounds fired struck the tanks. Many of the penetrators that struck the tanks without perforation caused extensive damage.

For the SNL high-density-of-targets analysis, an infinitely long column of vehicles was assumed to be struck by both 30 mm shells and shrapnel from cluster bombs. The relative amount of damage caused by each type of weapon was not determined, and the amount of DU released per penetrator impact is uncertain. Because the length of the penetrator is directly proportional to penetration depth, the short length of the 30 mm penetrator will reduce the probability of penetration relative to the long 120 mm DU rounds. Most of the 30 mm DU penetrators did not penetrate the tanks during the impact tests conducted by Stolfi et al; consequently, entrance and exit of a tank by a 30 mm penetrator appears unlikely. The possibility of entrance and exit by a 30 mm

penetrator hitting a light vehicle is uncertain. A review of the Hanson study was unable to determine whether the armor plate used in the test applies to tanks, light vehicles, or neither. Furthermore, 30 mm DU penetrators are fired from aircraft flying above their targets. If a penetrator both enters and exits the vehicle, the exit may be beneath the vehicle, reducing the amount of DU lofted into the surrounding air. Given all of these possibilities, the simple assumption will be used that about 5 g of DU particulate will be released into the atmosphere per impact with a light vehicle (i.e., the quantity of DU released into the atmosphere corresponds to the typical release on the entrance side of the armor plate from the Hanson et al. test data).

The number of impacts per m of column is also uncertain. From the tests by Stolfi et al., two tanks hit by 93 penetrators in seven passes correspond to about 6.6 hits per vehicle per pass. Estimating an average of about 10 targets per 10 m of column (many targets side by side per length of column) and assuming that roughly half of these targets are destroyed by cluster bombs gives an average number of about 3 hits per m of column. Thus, the estimated line source strength is 15 g DU/m (3 hits/m x 5 g DU/hit). In order to allow for the many uncertainties implicit in this estimate, a very large uncertainty (a factor of 10) was used in the uncertainty analysis.

## **B.2. DU Dispersal into the Environment**

The aerosols entrained in the air during battle are carried by the wind and dispersed in the atmosphere. Also, DU particulate deposited on the ground can be resuspended by wind or human and animal activities, over an extended period of time. Both the initial “puff” of DU aerosols entrained in the wind and the resuspended DU can be inhaled by nearby troops and civilians.

## Dispersal Methodology

The effect of DU on downwind civilian populations depends on how DU released during impact is dispersed into the environment, deposited on the ground, and subsequently resuspended. The dispersion of DU particulate following impact can be estimated using the Gaussian puff model, given by

$$C(x, y, z, t) = C_q(t) C_{xy}(x, y, t) C_z(z, t),$$

where  $C$  is the concentration ( $\text{g}/\text{m}^3$ ) of DU at position  $x$ ,  $y$ ,  $z$  and time  $t$ . The parameter  $C_q(t)$  is the time-dependent depleted source term that accounts for the removal of DU from the puff from deposition. The parameters  $C_{xy}$  and  $C_z$  are defined by

$$C_{xy}(x, y, t) = \exp\left[\frac{-(x-ut)^2}{4K_x(t)t}\right] \exp\left[\frac{-y^2}{4K_y(t)t}\right], \text{ and}$$

$$C_z(z, t) = \exp\left[\frac{-(z-H)^2}{4K_z(t)t}\right] \exp\left[\frac{-(z+H)^2}{4K_z(t)t}\right].$$

Here,  $u$  is the wind speed (m/s), and  $H$  is the effective release height (m) of the puff. The parameters  $K_x$ ,  $K_y$ , and  $K_z$  are the eddy diffusivities ( $\text{m}^2/\text{s}$ ) in the  $x$  (downwind),  $y$  (cross-wind), and  $z$  (vertical) directions. The eddy diffusivities are given by

$$K = \frac{\sigma^2}{2t},$$

where  $\sigma$  is the standard deviation (m). The standard deviations are approximated by

$$\sigma = c_1 x(1 + c_2 x)^{-c_3},$$

where the parameters  $c_1$ ,  $c_2$ , and  $c_3$  are specified by stability class in Table B-1. Stability classes are defined in Table B-2. For this study, it is assumed that  $\sigma_x = \sigma_y$ . The parameter  $H$  is the puff release height (m).

**Table B-1. Parameters for  $\sigma$  formulas for various atmospheric stability classes in a rural environment [5]**

Class	Conditions	$\sigma_y$ parameters			$\sigma_z$ parameters		
		$c_1$	$c_2$	$c_3$	$c_1$	$c_2$	$c_3$
<b>A</b>	Extremely Unstable	0.22	0.0001	½	0.200	0	–
<b>B</b>	Moderately Unstable	0.16	0.0001	½	0.120	0	–
<b>C</b>	Slightly Unstable	0.11	0.0001	½	0.080	0.0002	½
<b>D</b>	Neutral	0.08	0.0001	½	0.060	0.0015	½
<b>E</b>	Slightly Stable	0.06	0.0001	½	0.030	0.0003	1
<b>F</b>	Moderately Stable	0.04	0.0001	½	0.0160	0.0003	1
<b>G</b>	Strongly Stable	Not used in this study					

**Table B-2. Meteorological conditions used to define atmospheric stability class [5]**

Wind Speed (m/s)	Sun High	Cloudy	Nighttime
< 2	A	B	G
2 – 3	A-B	C	E-F
3 – 4	B-C	C	D-E
> 4	C-D	D	D

For dry deposition (no rain), the depleted source term is given by

$$C_q(t) = \frac{q \exp[-v_d I(t)]}{8(\pi t)^{\frac{3}{2}} \sqrt{K_x(t)K_y(t)K_z(t)}} .$$

The parameter  $Q_0$  is the initial quantity of DU (g) released in the puff,  $v_d$  is the deposition velocity for dry deposition, and  $I(t)$  is defined by

$$I(t) \equiv \left\{ \left( \frac{4t}{\pi K_z(t)} \right)^{\frac{1}{2}} \exp \left[ \frac{\mathcal{H}^2}{4K_z(t)t} \right] \right\} - \frac{\mathcal{H}}{K_z(t)} \operatorname{erf} \left[ \frac{\mathcal{H}}{\sqrt{4K_z(t)t}} \right] .$$

For wet deposition (washout by rain), the depleted source term is

$$C_q(t) = \frac{q \exp \left[ -\Lambda \frac{x}{u} \right]}{8(\pi t)^{\frac{3}{2}} \sqrt{K_x(t)K_y(t)K_z(t)}} ,$$

where the parameter  $\Lambda$  is the washout constant ( $s^{-1}$ ).

The deposition areal density ( $g/m^2$ ) of DU at the ground surface can be predicted for dry deposition using the standard formulation,

$$\zeta(x, y) = v_d \int_0^{\infty} C(x, y, z, t) dt .$$

Wet deposition is modeled using the washout constant  $\Lambda$  ( $s^{-1}$ ) in the equation

$$\zeta(x, y) = \int_0^{t_{\max}} \int_0^{z_{\max}} \Lambda \cdot C(x, y, z, t) dz dt ,$$

where  $t_{\max}$  is chosen as upper bound for the duration of deposition and  $z_{\max}$  is the maximum axial extent of the puff at  $t_{\max}$ .

## DU Dispersal and Deposition

The dispersal and deposition of DU at the battle location will depend on the atmospheric conditions at the time of the battle. Wind speeds between 2 and 15 m/s and frequent thunderstorms occurred during many of the battles involving DU munitions [6].

To estimate the ground deposition from DU impact with hard targets, calculations were performed assuming wet and dry deposition for a wind speed of 15 m/s using class C and class D weather conditions. These calculations were then repeated for wind speeds of 2 m/s using classes A, C, and E weather conditions.

The assumed washout constant for wet deposition was  $\Lambda = 0.00004 \text{ s}^{-1}$ . For the particle range of interest with heavy rainfall conditions, this value for  $\Lambda$  was determined to be reasonable choice [7: p. 20]. The relatively standard dry deposition velocity for particles ( $v_d = 0.0003 \text{ m/s}$ ) was also found to fairly well represent the recommended deposition velocity range for dry weather conditions and particle sizes of interest. The predicted DU areal density for wet deposition is plotted in Figure B-3 as a function of distance for class A, C, and E conditions assuming low wind speed and a release of 100 g DU into the environment. The Mathcad technical calculational tool [8] was used to carry out calculations and provide most of the plots used in this report.

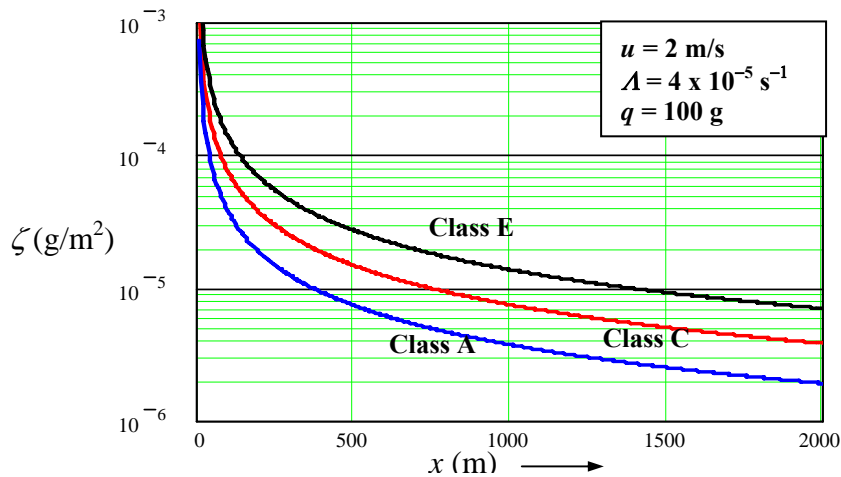


**Figure B-3. DU wet deposition density vs. x-distance for classes A, C, and E low wind speed**

Figure B-4 provides the predicted DU areal density for wet deposition for class C and class D conditions assuming high wind speed. Similar predictions were made for dry deposition (not shown). The quantity of deposited DU was found to be significantly greater for wet deposition than for dry deposition; consequently, only wet deposition is assumed in this study. The highest depositions for distances up to 1 km are observed from

these figures to result from wet deposition, class E conditions, and low wind speed. The inhaled mass as a function of distance, shown in Figure B-5, is obtained by time-integrating the product of the DU air concentration multiplied by the breathing rate. Here, a breathing rate of  $1 \text{ m}^3/\text{hr}$  was used.

For the best-estimate conditions, class C weather conditions, wet deposition, and an average wind speed of  $8 \text{ m/s}$  were used. The height of release was selected to be equal to the impact height. The explosive effect of impact and rapid oxidation of the uranium metal will loft much of the DU particulate above the height of impact. However, particulate release into the environment during penetrator entrance and exit may not be well characterized by standard approximations relating release height to explosive energy. To examine the sensitivity to release height, calculations were performed for  $2 \text{ m}$ ,  $10 \text{ m}$ , and  $30 \text{ m}$  release heights. The analysis showed that close to the vehicle, the assumed  $2 \text{ m}$  release height resulted in the highest inhaled and deposited DU masses. At longer downwind distances, release height had no significant effect on the inhaled and deposited DU masses. Based on these findings, the release height was set equal to the impact height.

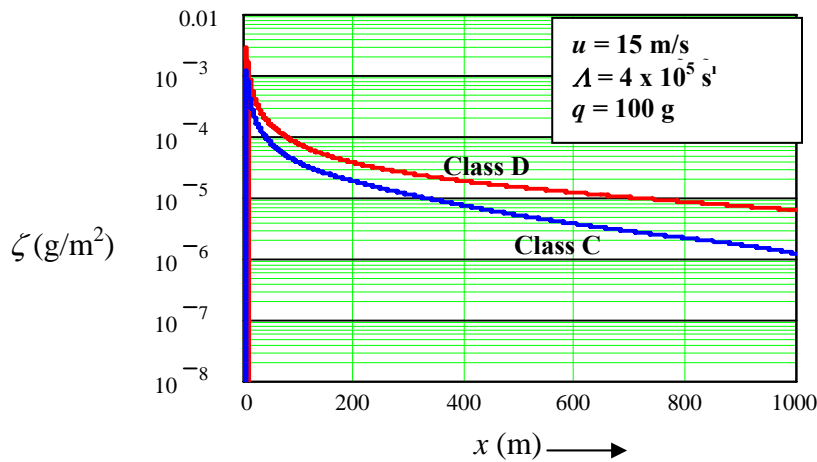


**Figure B-4. DU wet deposition density vs. x-distance for classes C and D, high wind speed**

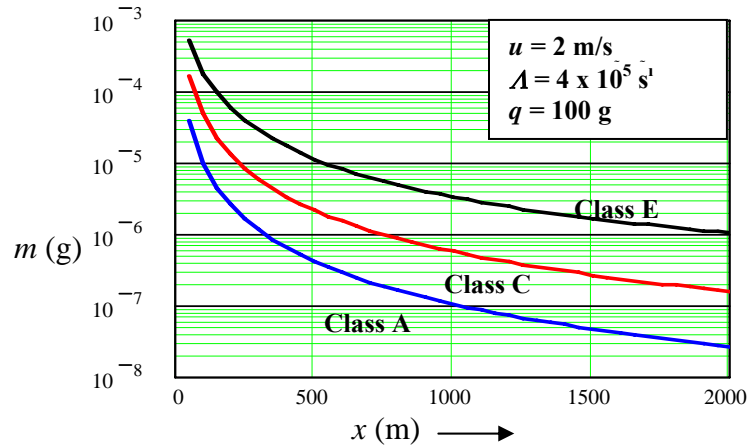


**Figure B-5. DU inhaled mass vs. x-distance for classes A, C, and E, low wind speed**

### Multiple Targets

The predicted DU release and dispersal from a single target vehicle will be less than the DU air concentrations and depositions that would result from multiple near-by targets. Multiple targets and very high target-density battles require formulations that account for the distributed nature and additive effect of a number of DU release sites. Two types of multiple targets were assumed. The first class of multiple targets was a battlefield array of tank targets in a tank battle. The second class was a densely packed, long line of light vehicle targets strafed by aircraft using a mixture of conventional and DU munitions.

#### Tank Array

The deposition for a column of target vehicles, represented by the geometry illustrated in Figure 16 in the main text, is obtained by defining a new position variable  $Y$  as

$$Y_{n_T} = |n_T \mathcal{D} - y|,$$

where  $\mathcal{D}$  is the tank separation distance and  $n_T$  is the index number for each target vehicle. The contribution to the DU air concentration at time  $t$ , position  $x, y, z$  is

$$C_{n_T}(x, y, z, t) = C(x, Y_{n_T}, z, t),$$

and the total (composite) concentration at time  $t$ , position  $x, y, z$  from all target vehicles  $N_T$  is

$$C_T(x, y, z, t) = \sum_{n_r=0}^{N_r} C_{n_r}(x, y, z, t).$$

The predicted depositions and inhaled masses, using this methodology, are presented in Figures 17 and 18 in the main text of this report.

### High Density of Targets

To account for DU release from a very long, high density of targets (e.g., the Highway of Death), a simple model was used in which the DU released during the battle is treated as an infinite line source. The basic dispersion equation for a line source is obtained by integrating over  $y$  from minus infinity to plus infinity, yielding

$$C(x, z, t) = C_{qL}(x)C_x(x, t)C(z, t),$$

where  $C$  is the concentration of DU at position  $x, y, z$  and time  $t$ . Here,

$$C_x(x, t) = \exp\left[\frac{-(x-ut)^2}{4K_x(t)t}\right],$$

and the definition for  $C(z, t)$  remains unchanged. The depleted source term for wet deposition for a line source is

$$C_{qL}(x) = \frac{q' \exp\left[-A \frac{x}{u}\right]}{4\pi t \sqrt{K_x K_z}}.$$

Here,  $q'$  is the initial source strength per unit length. At long distances, the effect of temperature inversion layer reflection may become important. Standard methods were used to include the effect of trapping (reflection) by a temperature inversion layer.

### Resuspension

For a child playing in soil external to a destroyed vehicle and for downwind civilians and veterans, the DU inhalation rate is given by

$$\dot{m} = R_b R_{scale} \zeta_0 O_c k(t).$$

Here,  $R_{scale}$  is a scaling factor for differing conditions,  $\zeta_0$  is the initial areal density for deposited DU, and  $k(t)$  is a time-dependent resuspension coefficient. The *Garland*

*resuspension factor* is used to express the time dependence of resuspended particulate when exposed to typical weather conditions. The Garland resuspension factor can be expressed as

$$k(t) = \frac{a}{t} + b.$$

For the standard Garland model  $a = 1.2 \times 10^{-6}$  d/m and  $b = 0$ . The Royal Society has suggested a modification to the standard Garland resuspension factor where  $b$  is set to  $10^{-9} \text{ m}^{-1}$  to account for long-term resuspension [9: Annex B, pp. 2-3]. To obtain closed form solutions for the biokinetic model, a roughly equivalent exponential form of the resuspension factor equation was developed; that is,

$$k(t) = a \exp(-\lambda_a t) + (b \cdot c) \exp(-\lambda_b t).$$

Here,  $c = 15$ ,  $\lambda_a = 0.1 \text{ d}^{-1}$ , and  $\lambda_b = 0.0025 \text{ d}^{-1}$ . A high scale factor ( $R_{scale} = 100$ , typical for a desert environment) was assumed [9: Annex B, p. 4].

### **B.3. Level I Veterans**

For Level I veterans, DU was internalized by inhalation, by ingestion, and by DU fragments embedded in the body. Because exposure times, the number of shells hitting the target vehicle, and other data are not well known for Level I veterans, some of these uncertainties were avoided by using a method employed by Fetter and von Hippel [10]. Fetter and von Hippel inferred inhaled DU mass from measured DU concentrations in veteran urine. Veteran urine data were also used to estimate the dissolution rate of embedded DU fragments. Standard methods, discussed previously in this appendix, were used to estimate the ingested DU mass.

#### **Inhaled DU for Veterans**

McDiarmid's team monitored the uranium mass in urine for a number of Level I veterans at seven and eight years after exposure [11]. Measurements were made for both veterans with embedded fragments and veterans that did not retain embedded fragments. For the inhalation analysis, the DU-urine data used was for veterans that did not retain shrapnel in their bodies. To infer the quantity of DU intake, a biokinetic analysis was

required to predict the time-dependent movement of DU through the body. The methodology used for the biokinetic analysis is discussed in Appendix C.

An examination of McDiarmid's data for Level I veterans with no embedded fragments found an average value of about  $0.02 \mu\text{g}$  DU/g creatinine at eight years after exposure [11]. This concentration of DU in creatinine can be reproduced by using the biokinetic model and an average inhaled DU mass of 250 mg. Figure B-6 presents a plot of the predicted time-dependence of the DU mass/g of creatinine for the nominal case. The plot includes both the inhalation-only and inhalation-plus-fragment cases. A similar approach was used to obtain the maximum inhaled mass. Using an inhalation mass of 4 g and solving the biokinetic equations gives a calculated value at eight years equal to the measured value of  $0.3 \mu\text{g}$  DU/g creatinine. Based on this analysis, the nominal and maximum inhaled DU masses for Level I veterans were estimated to be about 250 mg and 4 g, respectively.

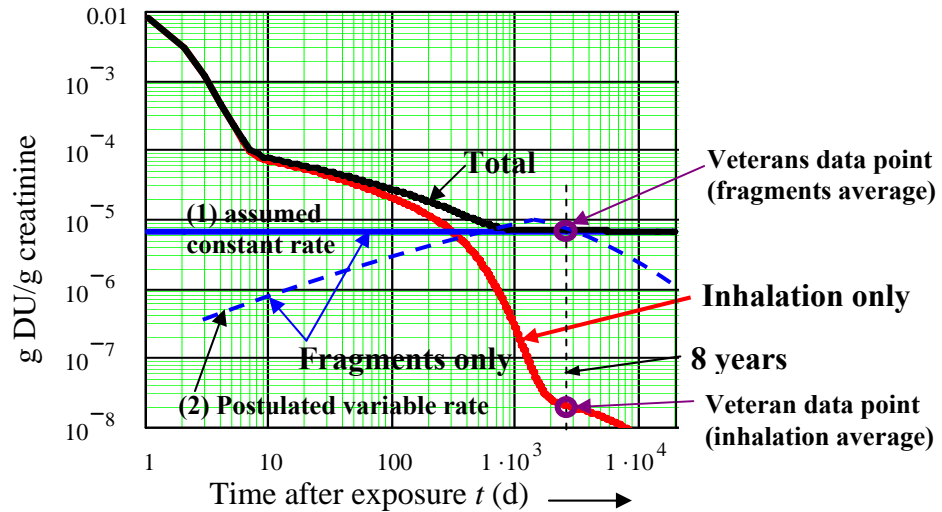


**Figure B-6. Predicted DU in creatinine vs. time for inhalation of 250 mg of DU and a fragment dissolution rate of  $6.7 \mu\text{g}$  DU/g creatinine**

## Embedded Fragments and Ingested DU

For veterans with embedded DU fragments, dissolution of the fragments by the blood results in a continuing supply of uranium to the blood and subsequent distribution to the body's organs. The measured DU in the urine, from veterans' test data at eight years, was used to obtain the dissolution rate for DU fragments. Subsequent calculations for the distribution of DU to the principal organs were based on the assumption that the inferred dissolution rate is approximately constant with time, as shown by curve (1) in Figure B-6. Studies with rats implanted with DU pellets show an increase in the DU excretion rate in urine over a period of 500 days after implanting the pellets [12]. However, the data show some tendency toward reaching a maximum. For Level I veterans, test data typically show an initial increase in the DU excretion rate that reaches a peak at about six years, followed by a declining excretion rate [11], as illustrated in curve (2) of Figure B-6. Based on the limited data, the assumption of an approximately constant dissolution rate appears to generally overestimate the fragment contribution to DU organ concentrations.

McDiarmid et al. measured the DU level in the urine for veterans retaining DU shrapnel. The concentration of uranium in the urine ranged between 0.18 and 39.1  $\mu\text{g}$  per g of creatinine, with an average concentration of about 6.7  $\mu\text{g}$  per g of creatinine [11] (shown in Figure B-6). The average adult male excretes about 1.7 g of creatinine per day, and 63% of DU dissolved in the blood is excreted in the urine. Thus, the nominal blood-dissolution rate for DU fragments is about  $[(6.7)(1.7)]/(0.63) = 18$   $\mu\text{g}$  per day. For the maximum DU case, we use the maximum measured dissolution rate of 39  $\mu\text{g}$  per g of creatinine. Applying the approach used for the nominal case and rounding up gave a maximum dissolution rate of about 160  $\mu\text{g}$  per day. In summary, the fragment nominal and maximum DU dissolution rates are 18 and 160  $\mu\text{g}$  per day, respectively.

## References:

1. Parkhurst, M. A., F. Szrom, R. A. Guilmette, T. D. Holmes, Y. S. Cheng, J. L. Kenoyer, J. W. Collins, T. E. Sanderson, R. W. Fliszar, K. Gold, J. C. Beckman, and J. A. Long, *Capstone Depleted Uranium Aerosols: Generation and Characterization, Volumes 1 and 2* (PNNL-14168), Prepared for the U.S. Army by Pacific Northwest National Laboratory, Richland, Washington, October 2004.
2. Hanson, W. C., J. C. Elder, H. J. Ettinger, L. W. Owens, *Particle Size Distribution of Fragments Fired Against Armor Plate Targets*, Los Alamos Laboratory, LA-5645, Los Alamos, NM, October 1974.
3. USACHPPM, *Depleted Uranium -Human Exposure and Health Risk Characterization in Support of the Environmental Exposure Report "Depleted Uranium in the Gulf" of the Office of Special Assistant to the Secretary of Defense for Gulf War Illnesses, Medical Readiness and Military Deployments (OSAGWI)*, HRA consultation no. 26-MF-7555-00D, September 15, 2000.
4. Stolfi, R., J. Clemens, and R. McEachin, *Combat Damage Assessment Team A-10/GAU-8 Low Angle firings Versus Individual Soviet Tanks*, February-March 1978, Volume 1, Air Force/56780, February 2, 1979.
5. Cooper, J. R., K. Randle, R. S. Sokhi, *Radioactive Releases in the Environment*, Wiley, West Sussex, England, 2003.
6. Riegler, D. W., Jr., and A. M. D'Amato, *The Riegler Report, US Chemical and Biological Warfare-Related Dual Use Exports to Iraq and their Possible Impact on the Health Consequences of the Gulf War*, U.S. Senate, 103d Congress, 2<sup>nd</sup> Session, May 25, 1994.
7. Simmons, J. R., G. Lawson, and A. Mayall, *Radiation Protection Methodology for assessing the radiological consequences of routine releases of radionuclides to the environment*, European Commission, EUR 15760 EN, 1995.
8. MathSoft Engineering and Education, *Mathcad 2001 Professional User's Guide with Reference Manual*, 2001.
9. The Royal Society, *The Health Hazards of Depleted Uranium Munitions Part II*, London, UK, March 2002.
10. Fetter, S., and F. N. von Hippel, "The Hazard Posed by Depleted Uranium Munitions," *Science and Global Security*, **8**, 125-161, 1999.
11. McDiarmid, M. A., K. Squibb, S. Engelhardt, M. Oliver, P. Gucer, P. D. Wilson, R. Kane, M. Kabat, B. Kaup, L. Anderson, D. Hoover, L. Brown, and D. Jacobson-Kram, "Surveillance of Depleted Uranium Exposed Gulf War Veterans: Health Effects Observed in an Enlarged Friendly Fire Cohort," *JOEM* **43**, December 12, 2001.
12. Leggett, R. W., and T. C. Pellmar, "The biokinetics of uranium from embedded DU fragments," *Journal of Environmental Radioactivity*, **64**, 2003.



## Appendix C: DU Biokinetics

Established biokinetic models are provided by the International Commission on Radiological Protection (ICRP) [1, 2, 3]. Although standard computer codes are currently available that utilize the ICRP models, the basic formulations given by these models were adapted for this study and used with the Mathcad calculational tool [4]. This approach was used to provide the flexibility required to address some of the unique characteristics associated with DU munitions exposure. The overall biokinetic model is schematically illustrated in Figure 21 of the main text.

### C.1. Inhalation Model

Inhaled DU particulate is deposited within the respiratory system and is subsequently transported by ciliary action and by blood absorption. Hence, DU will be transported from one region of the respiratory system to another, to lymph nodes, and to the GI tract. DU dissolved in the blood will either be eliminated in the urine or deposited among various organs. The DU deposited in organs will be eventually reabsorbed by the blood and eliminated in the urine. Basic models were developed for this study for both acute and chronic inhalation.

#### Particle Deposition

For DU internalization by inhalation, the particle size distribution must be known in order to obtain the proper deposition fractions in the various regions of the respiratory system. The Activity Median Aerodynamic Diameter (AMAD) and the geometric standard deviation  $\sigma_g$  are used to characterize the particle size distribution. The AMAD is the diameter in an aerodynamic particle size distribution for which the activity of particles having greater diameters make up 50% of the total activity. It is usually assumed that the particle distribution is lognormal, as given by

$$P(d) = \frac{1}{d [\ln(\sigma_g)] \sqrt{2\pi}} \exp \left\{ -\frac{[\ln(d) - \ln(d_A)]^2}{2[\ln(\sigma_g)]^2} \right\},$$

where  $P$  is the relative number of particles of diameter  $d$  and  $d_A = \text{AMAD}$ . When using the biokinetic model given by ICRP 66 [2], the default geometric standard deviation is used; that is,

$$\sigma_g = 1 + 1.5 \left\{ 1 - \frac{1}{\left[ 1 + 100(d_A)^{1.5} \right]} \right\}.$$

To estimate  $d_A$ , measured values were reviewed from the Capstone study [5: Attach. 1, p. 6.42]. The data from this study are immense and vary over time and from case to case. Nonetheless, impact generated aerosols were found to be reasonably characterized by assuming a bimodal distribution with peaks at about 0.5  $\mu\text{m}$  and 5  $\mu\text{m}$ . Regional respiratory system depositions were obtained from Reference [2] for nose and mouth breathers for 0.5 and 5- $\mu\text{m}$  AMAD particle distributions. (Nose breathing is 100% inhalation through the nose, but mouth breathing is actually 60% mouth and 40% nose.) The regional depositions are presented in Table C-1. These data are for a particle density of 3  $\text{g}/\text{cm}^3$  and a breathing rate of 1.2  $\text{m}^3/\text{hr}$ . Although nose breathing results in a higher deposited fraction, mouth breathing is more likely for the most challenging scenarios; and mouth breathing deposits more particulate in the slowly cleared alveolar region (AI in Figure C-1). To account for the bimodal distribution and a mix of nose breathers and mouth breathers, a simple average of the deposition fractions was used, as shown in Table C-1. The regions of the respiratory system referred to in Table C-1 are identified in Figure C-1 and are defined in Figure 21.

**Table C-1 Fractional deposition in respiratory regions for 0.5 and 5- $\mu\text{m}$  AMAD nose and mouth breathers**

Region	0.5 $\mu\text{m}$ AMAD		5 $\mu\text{m}$ AMAD		Average
	Nose Breather	Mouth Breather	Nose Breather	Mouth Breather	
<b>ET<sub>1</sub></b>	0.09	0.022	0.33	0.12	0.14
<b>ET<sub>2</sub></b>	0.10	0.04	0.40	0.36	0.23
<b>BB</b>	0.008	0.013	0.02	0.10	0.035
<b>bb</b>	0.022	0.022	0.011	0.04	0.02
<b>AI</b>	0.12	0.13	0.05	0.12	0.10
<b>Totals</b>	0.34	0.227	0.811	0.74	0.525

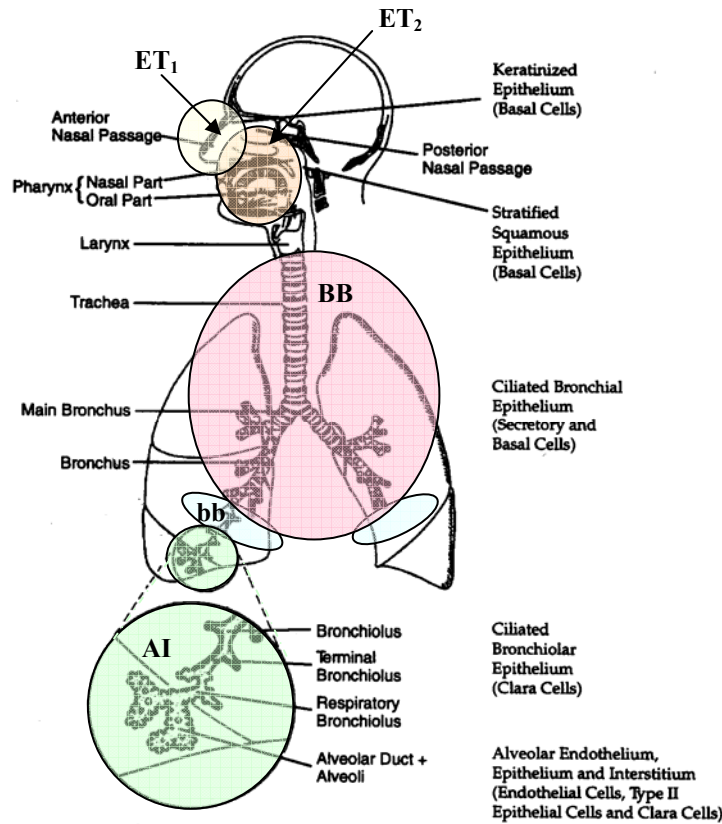


**Figure C-1. Anatomical regions of the respiratory tract [2]**

## Particle Transport

Particle transport processes, such as ciliary action and macrophage uptake, move particulate to the GI tract and lymph nodes, respectively. The cilia are hair-shaped cells on the walls of regions of the respiratory tract that move particles entrained in the mucous layer toward the extrathoracic region (ET<sub>2</sub>). Macrophages are specialized white blood cells in the lymph system that engulf foreign bodies. To determine the rate of clearance from the respiratory system, the fractional depositions are further broken down into compartments within each respiratory region. The fractions of particulate for each compartment of a region  $f_{Dc}$  are given in tables provided by the ICRP. The use of separate compartments is required to account for differing clearance rates within each region. Using the ICRP 66 model [2] for deposition and particle transport, the deposition fractions and clearance rates from particle transport  $\lambda_{ic}$  shown in Table C-2 were obtained. The symbol LN stands for lymph node, and the subscript SEQ indicates

sequestered particulate. Note that the symbol  $f$  is used throughout this report to represent the fraction relative to the amount inhaled or ingested.

**Table C-2. Respiratory region deposition fractions and transport rates**

Region	Compartment	Fraction*	$f_{Dc}$	To	$\lambda_{ic}$ (d <sup>-1</sup> )	
ET <sub>1</sub>	ET <sub>1</sub>	1.0	0.14	Environment	1	
ET <sub>2</sub>	ET <sub>2</sub>	0.9995	0.23	GI tract	100	
	ET <sub>seq</sub>	0.0005	1.2 x 10 <sup>-3</sup>	LN <sub>ET</sub>	0.001	
BB	BB <sub>1</sub>	0.5	0.017	ET <sub>2</sub>	10	
	BB <sub>2</sub>	0.5	0.017	ET <sub>2</sub>	0.03	
	BB <sub>seq</sub>	0.007	2.4 x 10 <sup>-4</sup>	LN <sub>TH</sub>	0.01	
Bb	bb <sub>1</sub>	0.5	0.01	BB <sub>1</sub>	2	
	bb <sub>2</sub>	0.5	0.01	BB <sub>1</sub>	0.03	
	bb <sub>seq</sub>	0.007	1.4 x 10 <sup>-4</sup>	LN <sub>TH</sub>	0.01	
AI	AI <sub>1</sub>	0.3	0.03	bb <sub>1</sub>	0.02	
	AI <sub>2</sub>	0.6	0.06	bb <sub>1</sub>	0.001	
	AI <sub>3</sub>		0.1	0.01	bb <sub>1</sub>	0.0001
					LN <sub>TH</sub>	0.00002

\* Compartment fraction within region

The rate of clearance from a compartment  $c$  for particle transport only is given by

$$\frac{df_{ic}(t)}{dt} = -\lambda_{ic} f_{ic}(t),$$

where  $t$  is the time in days following inhalation; and the parameter  $\lambda_{ic}$  is the clearance rate for particle transport. Solving the above equation gives

$$f_{ic}(t) = f_{Dc} \exp(-\lambda_{ic} t).$$

The model used in this study did not account for the radiological effect of DU particulate in transit through the various respiratory tract compartments. This omission, however, will be insignificant because movement through these compartments is rapid and the specific activity for DU is very low. More importantly, the preceding discussion did not account for absorption by the blood. The blood absorption rate will depend on the chemical composition and other characteristics of the inhaled particulate. Particulate generated by impact is primarily the insoluble oxide U<sub>3</sub>O<sub>8</sub>. A small fraction of the particulate consists of the more soluble oxide UO<sub>3</sub> [5]. A review of the data suggests that

the particle solubility can be represented by two solubility components  $\mathcal{F}_r$  and  $\mathcal{F}_s$  (rapid and slow, respectively) with component fractions and dissolution rates shown in Table C-3 [5: p. E.7].

**Table C-3. Rapid and slow DU particle component fractions and dissolution rates**

Component	$\mathcal{F}$	$\lambda$ (d <sup>-1</sup> )
<b>Rapid</b>	0.20	8
<b>Slow</b>	0.80	0.004

With the exception of region ET1, the absorption rate is assumed to be identical for all respiratory regions. No blood absorption is assumed for region ET1. The general time dependence of the DU mass for each compartment is given for the rapid and slow fractions by

$$f_{cr}(t) = f_{Dc} \mathcal{F}_r \exp[-(\lambda_{tc} + \lambda_r)t]$$

and  $f_{cs}(t) = f_{Dc} \mathcal{F}_s \exp[-(\lambda_{tc} + \lambda_s)t]$ .

No blood absorption occurs in region ET1; thus, for region ET1,  $f_s = f_r = 0$ . The total time-dependent fraction for compartment  $c$  is

$$f_c(t) = f_{cr}(t) + f_{cs}(t).$$

For the lymph nodes, the basic form of the equation is

$$f_{LN_r}(t) = f_{seq} \mathcal{F}_r \exp(-\lambda_r t) [1 - \exp(-\lambda_{tc} t)].$$

The equation used to determine the contribution to the thoracic lymph nodes from the AI<sub>3</sub> compartment includes the effect of transport to bb<sub>1</sub> as well as transport to LN<sub>TH</sub>.

### **Blood Redistribution**

A fraction of the DU remaining in the respiratory system will be absorbed by the blood. DU absorbed by the blood will either be eliminated in the urine or deposited in other organs of the body. The rate of transfer of DU from the respiratory system compartment  $c$  to the blood for the rapid fraction is

$$\frac{df_{Brc}(t)}{dt} = \lambda_r F_r f_c(t) = \lambda_r F_r f_{Dc} e^{-(\lambda_{ic} + \lambda_r)t}$$

The analysis predicts that 52.5% of the inhaled DU is deposited in the lungs, and the remainder is exhaled. About 30% of the inhaled DU will be passed to the gastrointestinal (GI) tract, 14% is expelled through the nose, and the remaining 8.5% in the respiratory system will be absorbed by the blood. The fraction inhaled DU entering the blood stream via the GI tract is only 0.4%. Because the relative contribution of inhaled DU entering the blood stream through the GI pathway is small compared to the contribution directly absorbed from the respiratory system, the GI tract contribution to the blood was not included in the inhalation analysis.

For inhaled DU, the distribution of DU to the major organs was estimated using the data, summarized in Table C-4, provided by ICRP 69 [3] and ICRP 30 [1]. Some simplifications were used; for example, the transfer of DU from the blood to major organs was assumed to be instantaneous. Furthermore, this analysis does not include the fraction of the DU absorbed by the blood from these organs and then distributed back to the organs. These approximations, however, have a small effect relative to the uncertainty in the data and other approximations used in this analysis.

**Table C-4. Inhaled DU distribution and decay parameters for organ compartments [1, 3]**

<b>Organ - Compartment</b>		$\gamma_o$	$\lambda_o$ (d <sup>-1</sup> )	<b>To</b>
Kidney	1	0.12	0.099	Urine
	2	0.0005	3.80 x 10 <sup>-4</sup>	Blood
Bone	1	0.127	3.46 x 10 <sup>-2</sup>	Blood
	2	0.023	1.39 x 10 <sup>-4</sup>	Blood
Soft tissue	1	0.065	0.035	Blood
	2	0.003	1.90 x 10 <sup>-5</sup>	Blood
Liver	1	0.015	0.099	Blood
			0.0069	Liver 2
	2	0.001	1.90 x 10 <sup>-4</sup>	Blood

The typical equation for the rate of change of the concentration of DU in organ  $o$  compartment 1 from the rapid dissolution fraction in respiratory system compartment  $c$  is

$$\frac{df_{o1rc}(t)}{dt} = \gamma_{o1}\lambda_r f_{rc}(t) - \lambda_{o1}f_{o1rc}(t),$$

where  $\gamma_{o1}$  is the fraction of DU in the blood apportioned to organ  $o$  compartment 1, and  $\lambda_{o1}$  is the corresponding removal rate. The parameter  $f_{o1rc}(t)$  is the fraction of inhaled DU in organ  $o$  compartment 1 at time  $t$  for rapid dissolution from respiratory compartment  $c$ . Thus, we can write

$$\frac{df_{o1rc}(t)}{dt} = \left[ \gamma_{o1}\lambda_r f_{Dc} F_r e^{-(\lambda_{ic} + \lambda_r)t} \right] - \lambda_{o1}f_{o1rc}(t).$$

Multiplying by the integrating factor  $e^{\lambda_{o1}t}$  and solving, we obtain the time-dependent fraction for each organ compartment

$$f_{o1rc}(t) = \frac{\gamma_{o1}\lambda_r F_r f_{Dc}}{\lambda_{ic} + \lambda_r - \lambda_{o1}} \left[ e^{-\lambda_{o1}t} - e^{-(\lambda_{ic} + \lambda_r)t} \right].$$

For the bone, the simple model provided by ICRP 30 was used; however,  $\gamma_{o1}$  was reduced to 0.127 to be consistent with more recent data from ICRP 69 (total to bone = 15%). The rapid-exchange soft tissue compartment used in ICRP 69 does not significantly affect long-term biokinetic behavior and was not included. The fraction of the inhaled DU distributed to each organ was obtained by summing all compartment contributions. For the kidney, bone, and soft tissue, compartments 1 and 2 are assumed to behave independently of each other. For the liver, however, about 7% of the DU removed from compartment 1 is deposited in compartment 2. The equation for liver compartment 2 is

$$f_{o2rc}(t) = \frac{\gamma_{o1}\lambda_{12}\lambda_r F_r f_{Dc}}{\lambda_{ic} + \lambda_r - \lambda_{o1}} \left[ \frac{e^{-\lambda_{o1}t} - e^{-\lambda_{o2}t}}{\lambda_{o2} - \lambda_{o1}} - \frac{e^{-(\lambda_{ic} + \lambda_r)t} - e^{-\lambda_{o2}t}}{\lambda_{o2} - \lambda_{ic} - \lambda_r} \right],$$

where  $\lambda_{12}$  is the rate constant for DU from Liver-1 to Liver-2.

## Chronic Inhalation

Chronic inhalation refers to prolonged inhalation exposure to DU, such as that of a child playing in a contaminated area or civilians living downwind from a battle zone and exposed to resuspended DU. The mass  $m$  deposited in the body organs can be estimated using the basic approach for acute inhalation; however, the equations must now be developed for a quasi-continuous source (multiple discrete events) rather than effectively a one-time inhalation of a fixed quantity of DU. For a child playing inside a DU-contaminated vehicle, the DU aerosol is generated each time the child plays in the vehicle. Although the quantity of DU present will decline slowly over time because of weather intrusion and carry-out on shoes and clothing, the quantity of DU in the tank was (for conservatism) assumed to remain unchanged during the entire 10-year span. External to the vehicle, the amount of DU available for resuspension declines quickly over time (see Appendix B). For this case, equations must be developed that account for the time-dependent nature of the resuspended air concentration.

### In-Vehicle Resuspension

For a child playing inside a vehicle, it was shown in Appendix B that the time-independent DU mass inhalation rate is given by  $\dot{m} = R_b C_{iv} O_c$ . Appendix B defined the parameters  $R_b$ ,  $C_{iv}$ , and  $O_c$  as the breathing rate, the DU air concentration, and the fraction of the elapsed time spent in the DU-contaminated vehicle. Writing the differential equations for DU deposition and transport in respiratory compartment  $c$  for the fast DU fraction and solving gives

$$m_{cr}(t) = \frac{f_{Dc} F_r \dot{m}}{\lambda_{tc} + \lambda_r} \left( 1 - e^{-(\lambda_{tc} + \lambda_r)t} \right).$$

Corresponding equations are developed for the slow-dissolution components. Differential equations were then written for the time-dependent DU mass  $m_{olrc}$  deposited in the major organs. The typical equation for the mass of DU in organ  $o$  compartment 1 from the rapid dissolution fraction in respiratory system compartment  $c$  is

$$m_{olrc}(t) = S_{Ar}(t) + S_{Br}(t),$$

where

$$S_{Ar}(t) \equiv \left( \frac{f_{Dc} F_r \dot{m}}{\lambda_{tc} + \lambda_r} \right) \left( \frac{\lambda_r \gamma_{o1}}{\lambda_{tc} + \lambda_r - \lambda_{o1}} \right) (e^{-(\lambda_{tc} + \lambda_r)t} - e^{-\lambda_{o1}t}),$$

and

$$S_{Br}(t) \equiv \left( \frac{f_{Dc} F_r \dot{m}}{\lambda_{tc} + \lambda_r} \right) \left( \frac{\lambda_r \gamma_{o1}}{\lambda_{o1}} \right) (1 - e^{-\lambda_{o1}t}).$$

The equations for the liver follow the pattern discussed previously for acute DU inhalation. Using this approach, the DU time-dependent masses were computed for major organs. For the exposure of a child, an organ mass equal to 30% of the standard adult organ mass was assumed. Following the 10-year period of occasional in-vehicle play, DU will be slowly removed from the respiratory system and other organs. DU in the various respiratory system compartments reach equilibrium concentrations by 10 years. As a consequence, the post-exposure (subscript  $p$ ) DU mass in each respiratory system compartment  $m_{pcr}(t)$  is simply

$$m_{pcr}(t) = \frac{f_{Dc} F_r \dot{m}}{\lambda_{tc} + \lambda_r} (e^{-(\lambda_{tc} + \lambda_r)(t-t_e)}),$$

where  $t_e$  is the 10-year exposure time in days. For other organs, the general equation for the post-exposure period  $m_{polrc}(t)$  is given by

$$m_{polrc}(t) = [m_{olrc}(t_e)] e^{-\lambda_{o1}(t-t_e)} + \left( \frac{f_{Dc} F_r \dot{m}}{\lambda_{tc} + \lambda_r} \right) \left( \frac{\lambda_r \gamma_{o1}}{\lambda_{tc} + \lambda_r - \lambda_{o1}} \right) (e^{-\lambda_{o1}(t-t_e)} - e^{-(\lambda_{tc} + \lambda_r)(t-t_e)}).$$

As usual, the equations for the liver differ from other organs.

### Ex-vehicle Inhalation

External to the vehicle, the resuspended DU is time-dependent. Using the exponential equivalent of the Garland resuspension factor (see Appendix B), a differential equation was written and solved to obtain the mass in respiratory compartment  $c$  for fast blood absorption; that is,

$$m_{cr}(t) = V_{Ar}(t) + V_{Br}(t), \quad \text{where}$$

$$V_{Ar}(t) \equiv f_{Dc} F_r \frac{a R_{scale} O_c \zeta R_b}{\lambda_a - (\lambda_{tc} + \lambda_r)} \{ \exp[-(\lambda_{tc} + \lambda_r)t] - \exp(-\lambda_a t) \},$$

and 
$$V_{Br}(t) \equiv f_{Dc} \mathcal{F}_r \frac{(b \cdot c) R_{scale} O_c \zeta R_b}{\lambda_b - (\lambda_{ic} + \lambda_r)} \{ \exp[-(\lambda_{ic} + \lambda_r)t] - \exp(-\lambda_b t) \}.$$

Corresponding equations are developed for the slow-dissolution components. The parameters  $\lambda_a$ ,  $\lambda_b$ ,  $a$ ,  $b$ , and  $c$  are the parameters used in the exponential form of the Garland model discussed in Appendix B. The parameter  $\zeta$  is the areal density from DU deposition.

Differential equations were then written for the time-dependent DU mass  $m_{o1rc}$  deposited in the major organs incorporating the above respiratory system equations. The typical equation for the concentration of DU in organ compartment  $o$  from the rapid dissolution fraction in respiratory system compartment  $c$  is

$$m_{o1rc}(t) = M_r(t) - M_{Ar}(t) - M_{Br}(t), \quad \text{where}$$

$$M_r(t) \equiv \lambda_r \gamma_{o1} f_{Dc} \mathcal{F}_r R_{scale} \left( \frac{a O_c \zeta R_b}{\lambda_a - (\lambda_{ic} + \lambda_r)} + \frac{(b \cdot c) O_c \zeta R_b}{\lambda_b - (\lambda_{ic} + \lambda_r)} \right) \frac{\{ \exp(-\lambda_{o1}t) - \exp[-(\lambda_{ic} + \lambda_r)t] \}}{\lambda_{ic} + \lambda_r - \lambda_{o1}},$$

$$M_{Ar}(t) \equiv \lambda_r \gamma_{o1} f_{Dc} \mathcal{F}_r R_{scale} \left[ \frac{a O_c \zeta R_b}{[\lambda_a - (\lambda_{ic} + \lambda_r)](\lambda_a - \lambda_{o1})} \right] [\exp(-\lambda_{o1}t) - \exp(-\lambda_a t)],$$

and 
$$M_{Br}(t) \equiv \lambda_r \gamma_{o1} f_{Dc} \mathcal{F}_r R_{scale} \left[ \frac{(b \cdot c) O_c \zeta R_b}{[\lambda_b - (\lambda_{ic} + \lambda_r)](\lambda_b - \lambda_{o1})} \right] [\exp(-\lambda_{o1}t) - \exp(-\lambda_b t)].$$

The equations for the liver follow the pattern discussed previously for acute DU inhalation. Using this approach, the DU time-dependent masses were computed for major organs.

## C.2. Ingestion and Embedded Fragments

The analysis for ingested DU and for DU embedded in the body is simpler than for inhaled DU in that the analysis does not require modeling of the deposition in the various respiratory compartments or the subsequent removal competition between ciliary and dissolution mechanisms.

## Ingested DU

It is generally assumed that for the GI tract, DU absorption by the blood takes place in the small intestines. The rate parameters for the stomach  $\lambda_{ST}$ , small intestines  $\lambda_{SI}$ , upper large intestines  $\lambda_{ULI}$ , and lower large intestines  $\lambda_{LLI}$  are given in Table C-5. The fraction of the ingested DU absorbed by the blood  $f_1$  is obtained from

$$f_1 = \frac{\lambda_B}{\lambda_B + \lambda_{SI}},$$

where  $\lambda_B$  is the rate constant for absorption by the blood. From ICRP 30,  $f_1 = 0.05$  for rapid dissolution, and  $f_1 = 0.002$  for slow dissolution. This equation gives values of 0.3 and  $0.012 \text{ d}^{-1}$  for  $\lambda_B$  for the rapid and slow constituents, respectively. Using the values of  $F_r$  and  $F_s$ , we obtain the effective values  $\lambda_B = 0.088 \text{ d}^{-1}$  and  $f_1 = 0.014$ . Thus, 1.4% of the ingested impact-generated DU is absorbed by the blood.

**Table C.5. GI system transport rates**

Organ	Symbol	To	$\lambda_t \text{ (d}^{-1}\text{)}$
Stomach	<i>ST</i>	Small Intestines	24
Small Intestines	<i>SI</i>	Upper large intestines	6
		Blood ( <i>B</i> )	0.088
Upper large intestines	<i>ULI</i>	Lower large intestines	1.8
Lower large intestines	<i>LLI</i>	Feces Excretion	1

## Acute Ingestion

For acute ingestion, the time-dependent DU fraction for the stomach is simply

$$f_{ST}(t) = e^{-\lambda_{ST}t}.$$

The time-dependent DU fraction in the small intestines is obtained by solving

$$\frac{df_{SI}(t)}{dt} = -\omega_{SI}f_{SI}(t) + \lambda_{ST}e^{-\lambda_{ST}t},$$

where  $\omega_{SI} \equiv [\lambda_{SI} + \lambda_B]$ . Multiplying through by the integrating factor  $e^{\omega_{SI}t}$  and integrating, we obtain

$$f_{SI}(t) = \frac{\lambda_{ST}}{\omega_{SI} - \lambda_{ST}} \left( e^{-\lambda_{ST}t} - e^{-\omega_{SI}t} \right).$$

Using the same basic approach for the upper large intestines as for the small intestines gives

$$f_{ULI}(t) = \lambda_{SI} \frac{\lambda_{ST}}{\omega_{SI} - \lambda_{ST}} \left[ \left( \frac{e^{-\lambda_{ST}t} - e^{-\lambda_{ULI}t}}{\lambda_{ULI} - \lambda_{ST}} \right) - \left( \frac{e^{-\omega_{SI}t} - e^{-\lambda_{ULI}t}}{\lambda_{ULI} - \omega_{SI}} \right) \right].$$

For the lower large intestines,

$$f_{LLI}(t) = \lambda_{ULI} \theta_1 \left[ (\theta_2)(e^{-\lambda_{ULI}t} - e^{-\lambda_{LLI}t}) + \theta_3(e^{-\lambda_{ST}t} - e^{-\lambda_{LLI}t}) - \theta_4(e^{-\omega_{SI}t} - e^{-\lambda_{LLI}t}) \right],$$

$$\text{where } \theta_1 \equiv \frac{\lambda_{SI} \lambda_{ST}}{\omega_{SI} - \lambda_{ST}}, \quad \theta_2 \equiv \frac{1}{(\lambda_{LLI} - \lambda_{ULI})} \left[ \frac{1}{(\lambda_{ULI} - \omega_{SI})} - \frac{1}{(\lambda_{ULI} - \lambda_{ST})} \right],$$

$$\theta_3 \equiv \frac{1}{(\lambda_{LLI} - \lambda_{ST})(\lambda_{ULI} - \lambda_{ST})}, \quad \text{and} \quad \theta_4 \equiv \frac{1}{(\lambda_{ULI} - \omega_{SI})(\lambda_{LLI} - \omega_{SI})}.$$

The blood-redistribution of ingested DU to the major target organs (kidneys, bones, etc.) can be estimated using the basic methods discussed in preceding sections. For acute ingestion of DU, it is easily shown that the time-dependent fraction of DU in organ  $o$  compartment 1 is given by

$$f_{o1}(t) = \frac{\gamma_{o1} \lambda_{ST} \lambda_B}{\omega_{si} - \lambda_{ST}} \left[ \left( \frac{e^{-\lambda_{ST}t} - e^{-\lambda_{o1}t}}{\lambda_{o1} - \lambda_{ST}} \right) - \left( \frac{e^{-\omega_{SI}t} - e^{-\lambda_{o1}t}}{\lambda_{o1} - \omega_{SI}} \right) \right].$$

## Chronic Ingestion

Assuming a chronic ingestion at a rate  $R_i$  (g/d), the time-dependent mass of DU in the organs of the GI tract (subscript  $go$ ) quickly reaches an equilibrium level given by an equation of the form

$$m_{go}(t) = \frac{R_i O_c}{\lambda_{go}} (1 - e^{-\lambda_{go}t}).$$

For chronically ingested DU, the time-dependent mass of DU absorbed by the blood and deposited in target organ  $o$  is approximately

$$m_{o1}(t) = \frac{\gamma_{o1} R_i O_c f_1}{\lambda_{o1}} (1 - e^{-\lambda_{o1}t}).$$

## Embedded Fragments

For embedded fragments, distribution by the blood of dissolved DU to various organs was found from experiments with rats to be roughly equivalent to the distribution given by standard ICRP models [6]. For a constant dissolution rate of  $R_d$  ( $\mu\text{g/d}$ ), the distribution to the body's organs can be estimated using

$$\frac{dm_{o1}(t)}{dt} = \gamma_{o1}R_d - \lambda_{o1}m_{o1}(t),$$

where  $m_{o1}(t)$  is the mass in organ  $o$  compartment 1. By simple substitution, we obtain

$$m_{o1}(t) = \frac{\gamma_{o1}R_d}{\lambda_{o1}}(1 - e^{-\lambda_{o1}t}).$$

For a constant rate of fragment dissolution, the mass in major organs increases in a manner similar to the case of chronic ingestion.

## References:

1. International Commission on Radiological Protection, *Limits of Intakes of Radionuclides by Workers*, ICRP Publication 30, Pergamon, NY, 1979.
2. International Commission on Radiological Protection, *Human Respiratory Tract Model for Radiological Protection*, ICRP Publication 66, Pergamon, NY, 1994.
3. International Commission on Radiological Protection, *Age-dependent Doses to Members of the Public from Intake of Radionuclides*, ICRP Publication 69, Pergamon, NY, 1995.
4. MathSoft Engineering and Education, *Mathcad 2001 Professional User's Guide With Reference Manual*, 2001.
5. Parkhurst, M. A., F. Szrom, R. A. Guilmette, T. D. Holmes, Y. S. Cheng, J. L. Kenoyer, J. W. Collins, T. E. Sanderson, R. W. Fliszar, K. Gold, J. C. Beckman, and J. A. Long, *Capstone Depleted Uranium Aerosols: Generation and Characterization, Volumes 1 and 2*, PNNL-14168, Prepared for the U.S. Army by Pacific Northwest National Laboratory, Richland, Washington, October 2004.
6. Leggett, R. W., and T. C. Pellmar, "The Biokinetics of Uranium from Embedded DU Fragments," *Journal of Environmental Radioactivity*, **64**, 2003.



## Appendix D: DU Chemical Health Effects

The principal concern associated with internalized uranium is chemical damage to the kidney. Other chemically induced health concerns, such as neurotoxic effects, have been postulated to result from internalization of uranium. Although potential effects identified in this appendix are associated with heavy metal toxicity, research suggests that some of these potential effects may be enhanced by low-level radiological exposure resulting from alpha particle emission from uranium.

### D.1. Uranium Physical and Chemical Properties

Uranium is a naturally occurring heavy metal found in a variety of chemical forms in soil, rock, and water. It has an atomic number of 92 and a relative atomic mass of 238.0289 u. The melt temperature is 1132 °C, and the boiling point is 3818 °C. The density of uranium metal is 18.9 g/cm<sup>3</sup>, nearly twice the density of lead. Uranium is a strong reducing agent, particularly in aqueous solutions. It exhibits valance states +3, +4, +5, and +6 in the crystalline form; and U<sup>4+</sup> and U<sup>6+</sup> are stable forms in aqueous media. The element is commonly associated with oxygen as the uranyl ion UO<sub>2</sub><sup>++</sup>. Uranium is considered to be a reactive metal and reacts with nonmetallic elements to form a variety of inter-metallic compounds as well as cationic and anionic salts.

Uranium metal is pyrophoric; that is, when in the form of a fine particulate, it ignites readily in air, producing uranium oxides. The pyrophoric burning of DU particulate in air, following impact of DU munitions on hard targets, produces several uranium oxides; the primary oxides produced are U<sub>3</sub>O<sub>8</sub> and UO<sub>3</sub>. The initial reaction of uranium metal with water forms uranium dioxide UO<sub>2</sub>. In moist environments, UO<sub>2</sub> will gradually form hydrated oxides. The reaction is strongly influenced by the presence of impurities. The addition of 0.75% of titanium, used as an alloy with DU in U.S. penetrators, appears to slow the oxidation rate appreciably. Microbial action, the presence of oxygen, salinity, and other factors affect the rate of corrosion of DU munitions in the environment [1].

## D.2. Uranium Chemistry in the Body

The solubility and the chemical and physiological properties of uranium compounds will depend on the type of compound and the physical form of the compound. In general,  $U_3O_8$  and  $UO_3$  are slowly soluble, and  $UO_3$  dissolves more rapidly. The uranyl ion  $UO_2^{++}$  is the most common and bioavailable chemical form of uranium that has been dissolved in body fluids. Uranyl ions form stable complexes with carbonates and phosphate ligands in biological fluids and tissues. Some important characteristics relating to the chemistry of internalized uranium include the following [2]:

- Uranium shares chemical properties with calcium, and the bicarbonate complex dissociates in the relatively low pH of the bone. As a consequence, dissolved uranium will deposit on bone surfaces.
- Uranium is also deposited in the kidney, liver, lymph nodes, and other organs in small quantities.
- Serum and egg albumin readily complex with uranyl ions.
- About 40% of uranium found in the blood is protein-bound uranium; the remainder is mostly uranyl bicarbonate complex.
- The uranyl ion can bind with the phosphoryl group of DNA.

Information on the chemical toxicity effects of uranium on humans has been obtained to a large extent by extrapolations from animal testing. These results are buttressed by data available from medical records for accidental human exposures, for uranium workers, and for DU-exposed Gulf War veterans. Guidance is also provided by in vitro experiments.

## D.3. DU Effect on Kidney

The kidney, shown in Figure D-1, is the principal target organ for uranium toxicity. Kidneys contain many urine-making units called nephrons. Blood enters the glomerulus where it is filtered. The filtrate flows into the proximal tubules that are in intimate contact with a capillary system. Water and other substances carried in the proximal tubules are

reabsorbed by the blood in the capillaries. The remaining filtrate in the tubules passes through a collecting duct and then into the bladder where the filtrate is subsequently eliminated from the body as urine. The acid environment of urine in the kidney tubules frees uranium, enabling it to attack the cells on the tubule surface. Complexes of uranium with proteins and phospholipids in the proximal tubules are considered to be the principal source of kidney damage. Nephrotoxic effects range from microscopic lesions in the tubular epithelium for low concentrations, to tubular necrosis for high concentrations.

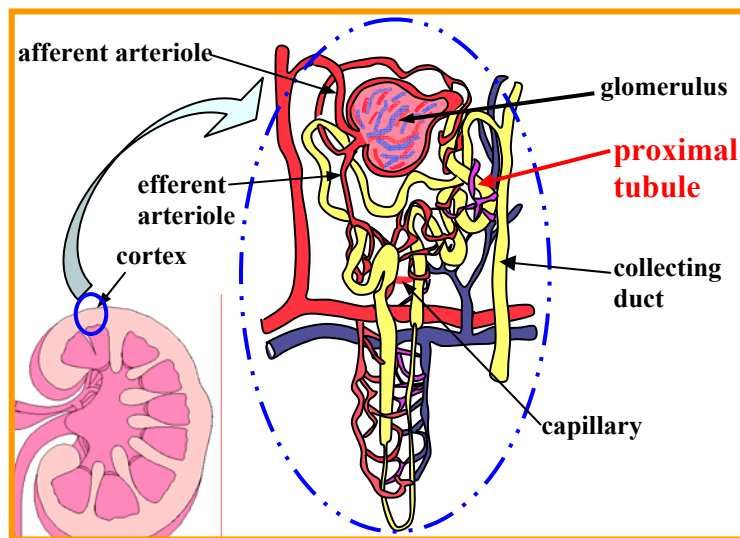


**Figure D-1. Kidney and nephron structure with proximal tubules**

For chronic exposures, uranium concentrations as low as  $0.1 \mu\text{g U/g}$  of kidney have been reported to show symptoms of slight effects on the kidney. Symptoms of slight effects are reported for acute exposures to uranium for uranium concentrations as low as  $1.0 \mu\text{g U/g}$  of kidney. Although effects on the kidney are measurable at these low exposures, illnesses have not been observed. Between 3 and  $10 \mu\text{g U/g}$  of kidney, protracted kidney damage has been observed [3: Appendix 1, p. 63]. The LD/50 concentration is the uranium kidney burden that would result in deaths to 50% of the exposed population without medical intervention. The LD/50 level for internalized uranium is estimated at about  $50 \mu\text{g}$  of DU per gram of kidney [4]. Kidney failure fatalities are predicted to occur within a few days after exposure at LD/50. However, the Royal Society points out that “kidney function can be reduced by about two-thirds without any obvious symptoms, and the ability of the kidney to recover apparently

normal function even after large intake of uranium, has implications for the evaluation of the health of veterans” [3: p. ix]. One must also keep in mind that the dose of 50 µg of U per gram of kidney for LD/50 is based on very limited human data and extrapolations from animal testing. Accurate health-effects predictions and unambiguous interpretation of veteran data are difficult because of the limited data base and the variability in human sensitivity for kidney-damage from uranium exposure. Our current understanding suggests that individuals surviving kidney damage from acute DU exposure are unlikely to experience long-term kidney health effects. Nonetheless, the DU kidney concentrations predicted for some Level I veterans were substantial, and continued monitoring of these veterans is recommended.

The traditional (implicit) guideline for limiting uranium intake is a maximum kidney burden of 3 µg of uranium per gram of kidney. The World Health Organization (WHO) [1] and the Royal Society [3: p. 3] have pointed out that the chemical toxicity effects on the kidney result at lower doses than previously assumed; consequently, they have concluded that current permissible exposure levels are too high. The uranium kidney concentrations for no effect and the LD/50 level are compared to the traditional exposure guideline in Table 8 of the main text of this document. Established guidelines for permissible exposure levels for uranium chemical toxicity are compared to guidelines for lead and beryllium in Table D-1.

**Table D-1. Chemical toxicity guidelines [5, 6]**

<b><u>Tolerable Intake - Public</u></b>		<b><u>(µg/kg body/day)</u></b>
Soluble uranium compounds		0.5
Insoluble uranium compounds		5.0
<b>Air Concentration Permissible Exposure Levels (PEL)</b>		
<b><u>OSHA*</u></b>	<b><u>PEL (mg/m<sup>3</sup>)</u></b>	
Soluble uranium		0.05
Insoluble uranium		0.25
Lead		0.05
Beryllium		0.002

\* OSHA = U.S. Occupational Safety and Health Administration

## D.4. Neurotoxic Effects

Extensive studies of exposure to lead have shown neurotoxic effects associated with alterations in membrane-bound enzymes. Because uranium is a heavy metal analogous to lead, it may be associated with neurotoxic effects as well. Some animal testing has been performed that addresses this issue. Lemercier et al. performed experiments with rats that showed that internalized uranium can cross the blood-brain barrier [7]. Pellmar et al. studied rats implanted with DU pellets. For these tests, a comparison of DU excretion rates per body mass suggests that the average and maximum DU organ-concentrations for the rats was about five times greater than the corresponding DU concentrations for Gulf War veterans. Although Pellmar found that excitability of neurons in the hippocampus was reduced for rats with significant quantities of implanted DU, no behavioral differences were observed from a battery of behavioral tests [8]. The hippocampus area (shown in Figure D-2) is associated with learning and memory. Lewis conducted uranium inhalation testing on rats to determine if DU can enter the brain directly through the nasal cavity without crossing the blood-brain barrier. Although not currently quantified, preliminary results show that uranium passed directly to the brain and appears to be preferentially deposited in the substantia nigra area of the brain (associated with motor control) [9].

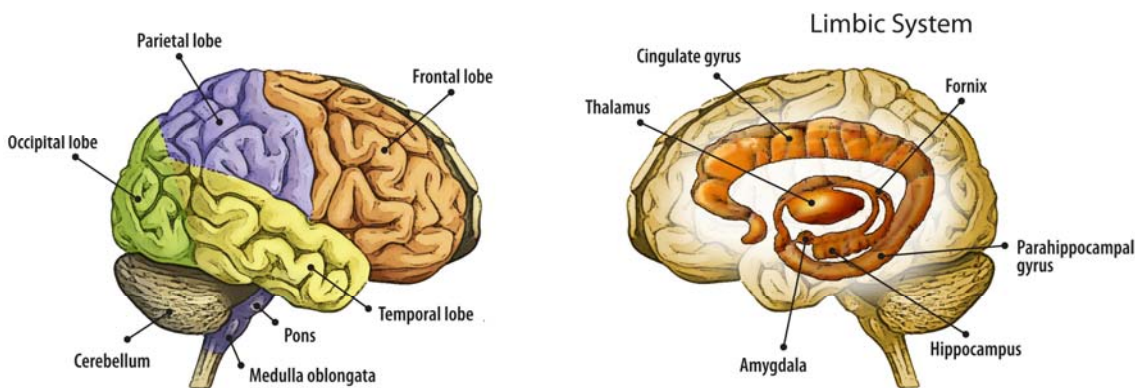


**Figure D-2. Anatomy of brain showing location of hippocampus**

McDiarmid and her staff have carried out a medical evaluation of a number of friendly fire veterans from the 1991 Gulf War. McDiarmid's team observed a statistically lower score for one type of neurocognitive test (computer-based problem solving) for veterans with high uranium concentrations in their urine [10]. Among the tested veterans, however, the slight neurocognitive effects did not appear to significantly affect normal functioning. Furthermore, as pointed out by the Royal Society [3], stress and anxiety resulting from their wounds and exposure cannot be ruled out as a contributing effect. A reassessment reported by McDiarmid in 2000 did not show evidence of an association between DU exposure and neurocognitive performance [10]. Although the results of veteran testing do not suggest significant neurotoxic effects from DU internalization, the potential for heavy metal neurotoxic effects found in animal testing warrants further study on this topic.

## **D.5. Other Chemical Effects**

Some evidence has been reported for other chemical effects associated with uranium internalization. *In vitro* studies suggest that DU can induce malignant transformations with frequencies similar to those observed with the nonradioactive heavy metal carcinogens, nickel and lead [3]. Studies by Benson et al. on female rats with DU implants [11] have shown that uranium can cross the placental barrier; however, physical maturation features and reflex behavior of newborn pups did not differ from the control group. Initial veteran test results for DU-exposed veterans suggested a possible linkage between high levels of the hormone prolactin with DU internalization. This finding, however, was disputed by the National Academy of Science, and the possible association of DU with prolactin levels was not found during McDiarmid's 2000 reassessment. Furthermore, no excess health effects of any type have been observed from epidemiological studies for uranium workers [12].

## References:

1. World Health Organization, *Depleted Uranium Sources, Exposure and Health Effects*, WHO/SDE/PHE/01.1, Geneva, April 2001.
2. Venugopal, B., and T. D. Luckey, *Metal Toxicity in Mammals*, Plenum Press, NY, 1978.
3. The Royal Society, *The Health Hazards of Depleted Uranium Munitions Part II*, London, UK, March 2002.
4. U.S. Department of Energy, DOE STANDARD SAFT-0072 (DRAFT): *Guide to Good Practices for Occupational Radiological Protection in Uranium Facilities*, Washington DC, January 2000.
5. Harley, N. H., E. C. Foulkes, L. H. Hilborne, A. Hudson, and C. R. Anthony, *A Review of Scientific literature as it Pertains to Gulf War Illness*, Rand report, 1999.
6. U.S. Occupational Safety and Health Administration, *U.S. Code of Federal Regulations 29 CFR 1910.96: Ionizing Radiation*, Office of the Federal Register, National Archives and Records, January 1, 1991.
7. Lemercier, V., X. Millot, E. Ansoborlo, F. Ménétrier, A. Flüry-Hérard, Ch. Rousselle, and J. M. Scherrmann, "Study of Uranium Transfer Across the Blood-Brain Barrier," *Rad. Prot. Dos.*, **105** 2003.
8. Pellmar, T. C., J. B. Hogan, K. A. Benson, and M. R. Landauer, *Toxicological Evaluation of Depleted Uranium in Rats: Six Month Evaluation Point*, Armed Forces Radiobiology Research Institute, VA, February 1998.
9. Lewis, J., personal communication, University of New Mexico College of Pharmacy, May 2004.
10. McDiarmid, M. A., K. Squibb, S. Engelhardt, M. Oliver, P. Gucer, P. D. Wilson, R. Kane, M. Kabat, B. Kaup, L. Anderson, D. Hoover, L. Brown, and D. Jacobson-Kram, "Surveillance of Depleted Uranium Exposed Gulf War Veterans: Health Effects Observed in an Enlarged Friendly Fire Cohort," *JOEM* **43**, December 12, 2001.
11. Benson, K. A., "Evaluation of Health Risks of Embedded Depleted Uranium Shrapnel on Pregnancy and Offspring Development," *Environmental & Occupational Health Project Summary DoD-121*, Medsearch, December 31, 2002.
12. Bordujenko, A. "Military Medical Aspects of Depleted Uranium Munitions," *ADF Health* **3**, September 2002.



# Appendix E: Radiological Health Effects

## E.1. Internal Radiation Analysis

Using the time-dependent DU organ concentrations presented in Section 4 of the main text, internal radiation doses were computed by applying the standard dose analysis methods described in the following sections.

### Dose Calculation Methodology

Radiation from organs that contain radioactive materials (source organs,  $i$ ) may cause damage in other nearby organs (target organs,  $T$ ) as shown in Figure E-1. Radiation from radioactive materials within the target organ can also cause damage to the target organ. In the latter case, the target organ is also the source organ. For DU, the most significant radiation is from alpha particle emission. Because the range of alpha particles is very short, the radiation for the target organ is often from radioactive materials within the target organ, rather than from other organs.

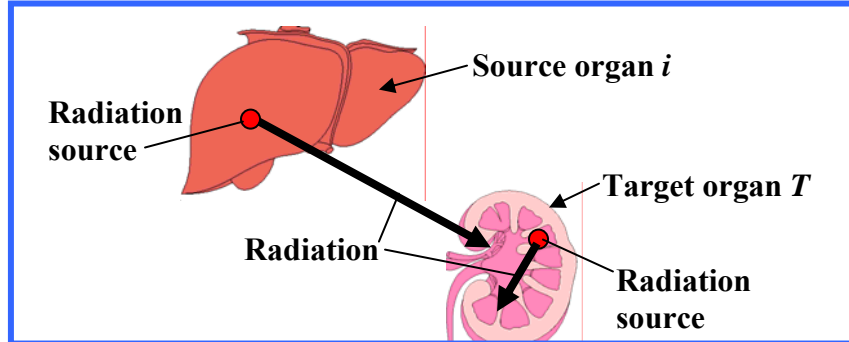


**Figure E-1. Illustration of internal radiation source and target organ definition**

For simplicity, the internal dose estimate was made for alpha particle emission, assuming that the DU penetrator consists of 100% U-238. Radiation from other uranium isotopes, daughter products, beta and gamma emission, and trace actinides increases the effective dose by less than 20%. These effects were accounted for in the simplified model by increasing all calculated doses by the factor  $F_{OI} = 1.20$ .

The 20% correction discussed in the previous paragraph should be a good approximation for alpha particle emissions by U-234, U-235, and trace actinides. Although the effects of beta and gamma radiation are very small, a brief discussion of their contribution to dose may be useful to aid understanding. The biological effects of various radiations are directly proportional to the radiation weighting factor  $W_R$ , the number of emissions of the radiation per U-238 decay  $F_R$ , and the energy of the radiation  $E_R$ . For alpha particles, the product of these factors is about 85 MeV. For beta particles emitted by DU, the product is about 0.9 MeV. Thus, the contribution of beta particles to the dose from internalized DU is about  $[(0.9/85) \times 100] = 1\%$ . For gamma radiation, the product of the three factors is about 0.05 MeV; hence, the gamma contribution to dose from internalized DU is only  $[(0.05/85) \times 100] = 0.06\%$ . Although gamma radiation is more penetrating than alpha or beta radiation, the effect on internal dose is very small relative to alpha particle emission.

The lifetime effective dose to compartment  $c$  of target organ  $T$  from each source organ  $i$  is given by

$$H_{c,i} = \int_0^{t_i} \left\{ \lambda_{238} F_{oi} \frac{m_i(t) N_A}{m_c A_R} [\text{AF}(T_c \leftarrow S_i)] E_R c \right\} W_R dt,$$

or

$$H_{c,i} = \lambda_{238} F_{oi} \frac{N_A W_R}{m_c A_R} [\text{AF}(T_c \leftarrow S_i)] E_R c \int_0^{t_i} m_i(t) dt.$$

Here,  $\lambda_{238}$  is the decay constant in days for U-238,  $m_i(t)$  is the time-dependent uranium mass (kg) in source organ  $i$ ,  $N_A$  is Avogadro's number,  $A_R$  is the relative atomic mass,  $E_R$  is the energy released per disintegration,  $c$  is a conversion factor ( $1.6 \times 10^{-13}$  J/MeV),  $W_R$  is the radiation weighting factor (equal to 20),  $m_c$  is the mass (kg) of compartment  $c$  of the target organ, and  $t_i$  is the duration in days. The parameter  $\text{AF}(T_c \leftarrow S_i)$  is the fraction of the radiation energy from source organ  $i$  absorbed by target organ compartment  $c$ . A summary of the organ masses used in this study is given in Table E-1.

The equivalent dose from all source organs for each compartment  $c$  of a specific target organ  $T$  is given by

$$H_c = \sum_i H_{c,i},$$

and the equivalent dose to a compound organ  $T$  is

$$H_T = \sum_c H_c A_c,$$

where  $A_c$  is the weighting factor assigned to compartment  $c$  of target organ  $T$ . Finally, the effective dose from all exposed organs is

$$H_E = \sum_{\text{all } T} W_T H_T,$$

where  $W_T$  is the target organ weighting factor.

**Table E-1. Assumed adult organ masses [1, 2]**

Organ		Mass (kg)	
		Component	Total
<b>Lungs</b>		1.00	1.00
<b>Kidney</b>		0.31	0.31
<b>Liver</b>		1.80	1.80
<b>Soft Tissue Organs</b>	Brain	1.40	33.71
	Gonad	0.35	
	Spleen	0.18	
	Muscle	28.00	
	Adrenals	0.14	
	Pancreas	0.10	
	Thymus	0.02	
	Stomach	0.15	
	SI wall	0.64	
	ULI wall	0.21	
	LLI wall	0.16	
	Thyroid	0.02	
	Skin	2.60	
	Bladder wall	0.045	
<b>Bone</b>	Cortical	4.00	6.50
	Trabecular	1.00	
	Red Marrow	1.50	
	Surface	0.12	
<b>Each Lymph Node</b>		0.015	0.015

## E.2. Internal Dose Calculation

The principal organs examined for inhaled DU and embedded DU fragments include the lungs, bone surface, bone marrow, kidney, liver, lymph nodes, gonads, and the brain. For ingested DU, the principal organs are the stomach, small intestines, upper large intestines, and lower large intestines. Weighting parameters, values for  $AF(T \leftarrow S)$ , and compartment masses for adults are listed in Table E-2 for the principal organs. These parameters and the preceding equations were used to obtain the effective dose for exposed individuals. For the lung, a number of source organ and target compartment organs must be included in the calculations. Calculations for the bone addressed both bone cancers (sarcomas) from radiation exposure of the bone surface and leukemia from radiation exposure of bone marrow. Uranium is generally considered to be a bone-volume seeker. For bone volume seekers, the radioisotope is assumed to be uniformly distributed throughout the cortical bone and the trabecular bone. The cortical bone is the hard bone mass making up the bone surface, illustrated in Figure E-2 (a). The trabecular bone consists of the many struts within the marrow region, illustrated in Figure E-2 (b). The ratio of the amount of uranium deposited on trabecular surfaces to that deposited on cortical surfaces is 1.25 [2].

DU particulate sequestered in the extrathoracic and thoracic regions is carried by the lymph to the extrathoracic and thoracic lymph nodes. DU is slowly removed from the lymph nodes by dissolution and absorption by the blood. The brain and gonads are two of the many soft tissue organs. The brain and gonads were singled out for examination because the issues have been raised relating neurotoxic effects and birth defects.

A summary of the dose calculations is provided in Tables E-3, E-4, and E-5 for Level I veterans, Levels II and III veterans, and civilians, respectively. The organ doses presented in these tables are equivalent doses; thus, they have been adjusted by a radiation weighting factor, but have not been corrected by organ weighting factors. The effective dose in the last row, however, is the sum of the organ-weighted dose for all organs.

**Table E-2. Parameters for computing effective dose from internal radiation [1–4]**

Organ	Compartment	$W_T$	$A_c$	$m_c$ (kg)*	Source	$AF(T_c \leftarrow S_i)$
Lung	BB basal	0.12	0.1665	$4.3 \times 10^{-4}$	BB <sub>1</sub>	0
					BB <sub>2</sub>	$5.4 \times 10^{-4}$
					BB <sub>seq</sub>	0.135
	BB secretory		BB <sub>1</sub>	0.144		
			BB <sub>2</sub>	0.192		
			BB <sub>seq</sub>	0.0515		
	bb		bb <sub>1</sub>	0.233		
			bb <sub>2</sub>	0.237		
			bb <sub>seq</sub>	0.111		
			AI	$7.06 \times 10^{-5}$		
AI		0.333	1.10	AI	1.0	
Bone	Surface	0.01	1.0	0.12	Trabecular	0.025
					Cortical	0.01
	Red Marrow				Trabecular	0.05
					Cortical	0.0
Lymph Nodes	Extrathoracic	0.05	0.001	0.015	Extrathoracic	1.0
	Thoracic	0.12	0.001	0.015	Thoracic	1.0
Kidney		0.025	1.0	0.31	Kidney	1.0
Liver		0.05	1.0	1.80	Liver	1.0
Soft Tissues	Gonads	0.20	1.0	33.71	Soft Tissues	1.0
	Brain	0.05				
Stomach		0.05	1.0	0.15	Stomach	1.0
Small Intestines		0.05	1.0	0.64	SI	1.0
Upper Large Intestines		0.12	1.0	0.21	ULI	1.0
Lower Large Intestines		0.12	1.0	0.16	LLI	1.0

\* Organ masses are for adults

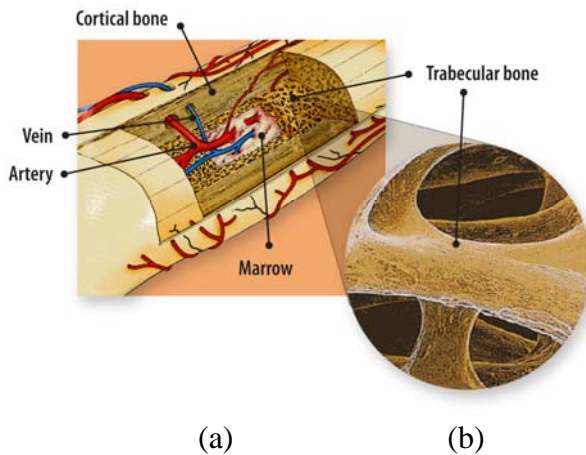


**Figure E-2. Bone structure: (a) overall and (b) trabecular bone**

**Table E-3. Level I veteran lifetime equivalent doses from DU exposure**

Organ	Inhalation-Only (Sv)		Inhalation + Fragment (Sv)	
	Nominal	Maximum	Nominal	Maximum
Lung	0.125	2.0	0.125	2.0
Bone surface	$8.7 \times 10^{-3}$	0.14	0.104	0.69
Bone marrow	$1.1 \times 10^{-3}$	0.017	0.012	0.083
Lymph nodes	0.02	0.31	0.02	0.31
Kidney	$3.0 \times 10^{-3}$	0.048	0.046	0.30
Liver	$1.1 \times 10^{-3}$	0.018	$1.6 \times 10^{-3}$	0.021
Soft tissue	0.0005	0.008	0.005	0.035
Effective Dose	0.015	0.25	0.019	0.265

**Table E-4. Veteran Levels II and III lifetime internal equivalent doses from DU exposure**

Organ	Level II (Sv)		Level III (Sv)	
	Nominal	Maximum	Nominal	Maximum
Lung	0.02	0.300	$6.0 \times 10^{-6}$	0.0040
Bone surface	$1.5 \times 10^{-3}$	0.021	$1.5 \times 10^{-7}$	$2.8 \times 10^{-4}$
Bone marrow	$1.8 \times 10^{-4}$	0.003	$1.8 \times 10^{-8}$	$3.4 \times 10^{-5}$
Lymph nodes	0.003	0.047	$3.3 \times 10^{-7}$	$6.2 \times 10^{-4}$
Kidney	$5.0 \times 10^{-4}$	0.007	$5.0 \times 10^{-8}$	$9.6 \times 10^{-5}$
Liver	$1.8 \times 10^{-4}$	0.003	$1.8 \times 10^{-8}$	$3.6 \times 10^{-5}$
Soft tissue	$8.3 \times 10^{-4}$	0.001	$8.3 \times 10^{-9}$	$1.6 \times 10^{-5}$
Effective Dose	0.0025	0.038	$2.5 \times 10^{-7}$	$5.0 \times 10^{-4}$

**Table E-5. Lifetime equivalent internal radiation doses for civilians from DU exposure**

Organ	Battle Zone –Child (Sv)		Downwind Civilian (Sv)	
	Nominal	Maximum	Nominal	Maximum
Lung	0.041	0.164	$3.3 \times 10^{-6}$	$5.3 \times 10^{-5}$
Bone surface	$6.1 \times 10^{-3}$	0.024	$2.2 \times 10^{-7}$	$3.6 \times 10^{-6}$
Bone marrow	$7.3 \times 10^{-4}$	$3.0 \times 10^{-3}$	$2.7 \times 10^{-8}$	$4.4 \times 10^{-7}$
Stomach	0.002	0.006	–	–
Small intestines	0.0015	0.004	–	–
Large Intestines	0.064	0.19	–	–
Soft tissue	$3.4 \times 10^{-4}$	$1.3 \times 10^{-3}$	–	–
Effective Dose	0.013	0.044	$4.1 \times 10^{-6}$	$6.5 \times 10^{-6}$

## **Radiological-Health Effects**

The possible radiation health effects that might be associated with internal DU exposure include cancers and hereditary effects. A brief discussion of risk, as used in this study, is also provided.

### **Risk Definition**

Risk is the unrealized potential for harm. Harm can include death, injury, financial loss, or any other undesirable outcome. Risk can be understood in terms of incidences in a large population group and is usually expressed as a fraction; that is, risk = (number of incidences in a population)/(size of population). Risk can also be expressed as a percentage. For example, if 10,000 individuals in a sample of 100,000 unexposed people are found to spontaneously incur a specific health effect, then the risk from spontaneous causes is 10%. If another group of 100,000 people is exposed to a specific dose of a toxin that has a 1% chance (incremental risk) of inducing the same health effect, then the total risk for the health effect is 11%. For this case, the predicted number of incidences will be 10,000 from spontaneous causes and 1,000 from toxic exposure for a total of 11,000 incidences of the health effect. All risk projections used in this study were absolute risk projections. The *absolute risk* is the projected excess risk, rather than the *relative risk* (the ratio of the number of excess cases to the number of cases in the unexposed population).

### **Risk Estimation Method**

The net risk of radiation-induced fatal cancers is typically predicted by multiplying effective dose estimates by the dose-risk probability coefficients for fatal cancers in Table A-3. The risks of specific cancers can be estimated by multiplying the equivalent dose for each organ by the dose-risk probability coefficients for fatal cancers for specific organs given in Table E-6 [4]. The risk coefficients provided in Table E-6, however, are not entirely consistent with the risk coefficients in Tables A-3 combined with the weighting factors in Table A-2. When the net cancer risk predicted using the effective dose and Table A-3 differed significantly from the value obtained from the sum of the organ risks using Table E-6, the largest predicted value was used. The risks of

genetic effects were obtained by multiplying the equivalent dose to the gonads by the probability coefficients for hereditary effects in Table A-3.

**Table E-6. Fatal organ cancer probability coefficients used in this study [4]**

Organ	Cancer/Sv	
	Population	Workers
Lungs	0.0085	0.0068
Bone Marrow	0.0050	0.0040
Bone Surface	0.0005	0.0004
Colon	0.0085	0.0068
Liver	0.0015	0.0012
Stomach	0.0110	0.0088
Skin	0.0002	0.0002
Remainder	0.0050	0.0040

### Leukemia Risk

Leukemia is a malignant neoplasm in the blood-forming tissues characterized by abnormal proliferation of white blood cells. Leukemia is usually observed following whole body doses of several Gy, with peak incidences at 7 to 8 years after exposure and latency periods as short as two years. Our interest, however, relates to low-dose, low-dose-rate exposures resulting from internalized uranium deposited in the bone. No epidemiological evidence has been found to indicate the induction of leukemia as a result of uranium internalization by humans or animals. Nonetheless, DU-induced leukemia has been raised as an issue by a number of critics. For maximally exposed veterans who retain DU fragments, the projected risk for leukemia induction is about 0.03%, which is about 1/3 of the lifetime risk from spontaneous causes. One must keep in mind that the number of maximally exposed individuals is very small and the absolute risk of radiation-induced leukemia is very low. Furthermore, the EPA and others suggest that leukemia may be significantly overestimated by standard methods.

### Birth Defects

Birth defects are congenital defects of body structure or function likely to result in physical or mental handicap or death. Birth defects result from mutations in germ cells

that are passed on to progeny; hence, radiation damage to germ cell DNA may result in hereditary birth effects. Although some in utero effects on the fetus (such as mental impairment) has been found to be statistically significant for pregnant women receiving high radiation doses, no clear evidence of radiation-induced genetic birth defects has been observed in humans at any exposure level. It is believed that part of the reason radiation-induced genetic birth defects in humans have not been observed is that the percent increase in birth defects relative to the spontaneous induction of birth defects is generally too small to be detected. Thus, observation of birth defects resulting from DU exposure is highly unlikely. The risk of serious birth defects because of radiation exposure is given by the ICRP as 0.013 per person-Sv for the general population and 0.008 per person-Sv for workers [4].

### **Neurotoxic Effects**

Radiotherapy has been used extensively in the treatment of cancerous brain tumors. The neurotoxic effect resulting from high radiation doses to the brain during radiotherapy is well established. Some areas of the hypothalamus appear to be more sensitive to radiation than the white matter, and the white matter is more sensitive than gray matter or the brain stem. Behavioral effects and mental impairment resulting from high-dose treatments are clearly observed. The effect of radiation on the brain is greater for children than for adults [5]. Studies of neurotoxic effects on the brain, however, are focused on extremely high exposures resulting from radiotherapy. For radiotherapy, acute radiation doses generally ranged from 20 to 70 Gy, compared to the maximum 50-year committed dose for a DU-exposed veteran of about 0.01 Gy (at least 2000 times lower than the dose from radiotherapy). A search of the literature did not yield any research findings for neurotoxic effects in the low dose range.

### **E.3. External Dose Computation**

An approximate method was used to compute the dose and radiological risk from external radiation exposure from DU. Only gamma and beta radiation are of concern when considering external radiation exposure from DU shells or fragments.

## Gamma Dose from a DU Round

For a DU shell or large fragment, the volumetric source strength for gamma radiation  $s_{v\gamma}$  is

$$s_{v\gamma} = \frac{\lambda_{238} N_A \rho_{238} F_\gamma}{A_{238}}.$$

Here,  $\lambda_{238}$ ,  $\rho_{238}$ , and  $A_{238}$  are the decay constant, solid density, and relative atomic mass for U-238 metal. The ratio  $N_A \rho_{238} / A_{238}$  gives the atom density of U-238 (atoms/cm<sup>3</sup>), and the factor  $F_\gamma$  is the fraction of U-238 disintegrations that results in the emission of a 1 MeV gamma photon.

For external exposure, we will examine the gamma dose from an unburied 120 mm DU shell. The geometry and nomenclature used for this analysis are illustrated in Figure E-3. The gamma flux from a finite cylinder can be approximated by [6]

$$\phi_\gamma(r) = \frac{s_{v\gamma} \pi R_0^2}{4(r + \delta)} B_{air}(E, r) \int_0^{\theta(r)} \exp\{-[(\mu_{\gamma air})r + (\mu_{\gamma DU})\delta] \sec \theta\} d\theta.$$

The parameters  $R_0$ ,  $r$ , and  $\delta$  are the radius of the DU penetrator (cm), the distance from the surface of the shell, and an effective distance from the penetrator surface to an equivalent line source used to represent the volumetric cylindrical source. The symbol  $\mu_{\gamma DU}$  is the gamma attenuation coefficient in DU metal; here,  $B_{air}(E, r)$  and  $\mu_{\gamma air}$  are the buildup factor and gamma attenuation coefficient (cm<sup>-1</sup>), respectively, for air. The buildup factor accounts for the fact that a fraction of the photons that are scattered off an original trajectory toward location  $r$  will scatter back to location  $r$ . For air, this effect is small and  $B_T(E, r)$  was approximated as unity.

The angle  $\theta$ , shown in Figure E-3, is

$$\theta(r) = \text{atan} \left[ \frac{L}{2(r + \delta)} \right]$$

For a 120 mm shell,  $R_0 = 1.5$  cm and  $L = 30$  cm. The radius of the shell is sufficiently small that we can make the simplifying assumption that the equivalent line source is at

the center of the shell; that is,  $\delta \approx R_0$ . Using these relationships, the gamma flux was calculated as a function of distance from the shell and plotted in Figure E-4. To check the accuracy of the prediction using this approach, an MCNP [7] Monte Carlo gamma transport calculation was performed for DU using the same geometry assumed for the simple analysis. The data points shown in Figure E-4 are in good agreement with the approximate method. The anomaly at 500 cm is because of statistical error in the MCNP calculation at large distances from the source.

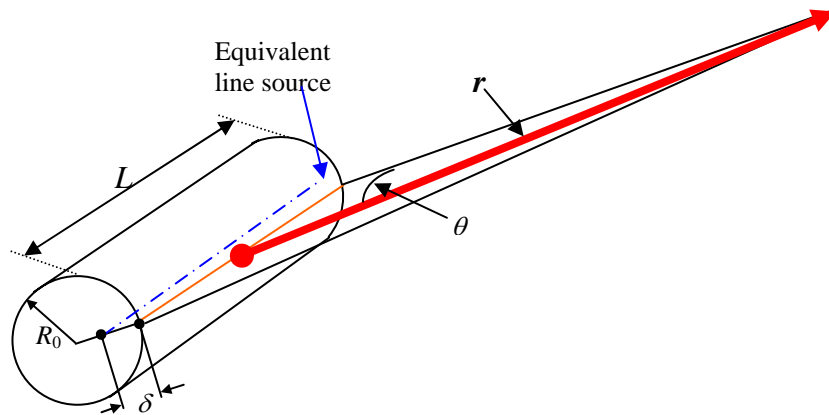


**Figure E-3. Geometry and nomenclature for estimating gamma dose from a DU shell**

The equivalent dose rate received at location  $r$ , presented in Figure 33 in the main text, was obtained using

$$\dot{H}(r) = \phi_{\gamma}(r) E \mu_{\gamma T} (1.603 \times 10^{-10}) W_R \bar{g} .$$

Here,  $E$  is the gamma energy,  $\mu_{\gamma T}$  is the gamma attenuation coefficient in tissue,  $W_R$  is the radiation weighting factor,  $\bar{g}$  is the average attenuation factor for gamma rays in the human body; and the factor  $(1.603 \times 10^{-10})$  is a conversion factor to give the dose rate in Sv/s. For gamma rays,  $W_R = 1.0$  and a value of 0.5 was assumed for  $\bar{g}$ .

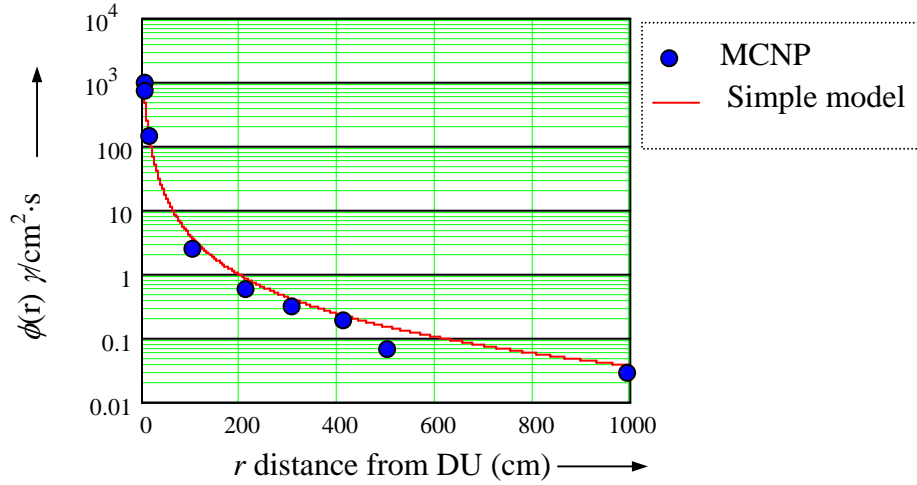


**Figure E-4. Predicted gamma flux vs. distance from a DU shell**

### Gamma Dose from a Pendant

To establish a worst-case scenario for external exposure to gamma rays, we explore the case of a 2-cm diameter DU spherical fragment worn as jewelry in the form of a pendant in close proximity to the body. In this case, the flux as a function of distance into the body  $r_b$  is (neglecting the buildup factor)

$$\phi_{\gamma}(r_b) = \phi_{\gamma s} \left( \frac{r_0}{r_b} \right)^2 e^{-\mu_{\gamma T} r_b},$$

where the spatial attenuation is now  $\sim 1/r_b^2$  and the attenuation coefficient  $\mu_{\gamma T}$  is for tissue. The effective dose as a function of distance and exposure time is

$$H_E(r_b, t_{ex}) = \phi_{\gamma}(r_b) E \mu_{\gamma T} (1.603 \times 10^{-10}) W_R t_{ex}.$$

The estimated risk of cancer to internal organs from a DU pendant is provided in Figure E-5 as a function of time. The internal organ was assumed to be located about 5 cm from the pendant surface with a typical organ weighting factor of about 0.1. After two years, the cancer risk is  $\sim 0.02\%$ .

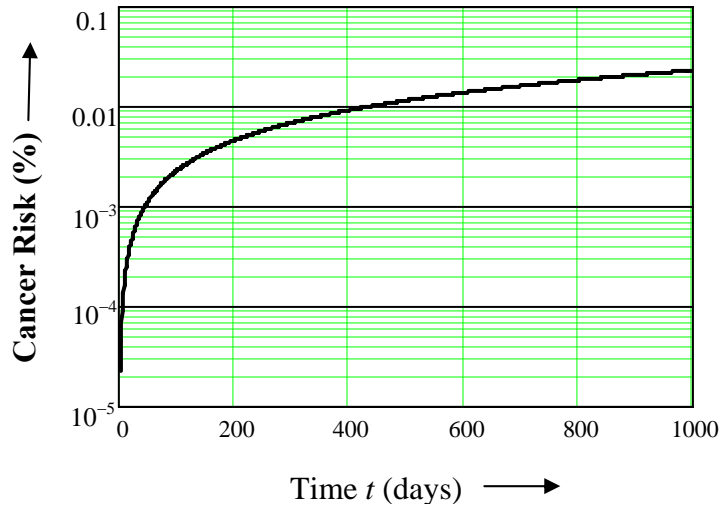


**Figure E-5. Estimated cancer risk to an internal organ vs. time assuming a 2 cm DU pendant worn close to the body**

### Beta Burns and Skin Cancer

The beta particle flux at the surface of a DU shell can be estimated using

$$\phi_{\beta s} = \frac{\lambda_{238} N_A \rho_{238} F_{\beta}}{2 A_{238} \mu_{\beta DU}}$$

The factor  $1/\mu_{\beta DU}$  is used to approximate the penetration depth of beta particles emitted by DU. The dose rate at the surface is

$$H_{\beta s} = \phi_{\beta s} \bar{E}_{\beta} \bar{\mu}_{\beta T} (1.603 \times 10^{-10}) W_R \bar{g}_{\beta} = 2.33 \text{ mSv/hr.}$$

The values for  $W_R$  and  $\bar{g}$  for beta particles are the same as those used for gammas. This estimated beta radiation dose rate at the surface is in exact agreement with the measured value [8]. The dose to the skin is obtained by simply multiplying the dose rate by the exposure time. For a pendant in direct contact with the skin, the skin dose from beta particles as a function of time in days is given in Figure E-6 along with the threshold range for beta burns (reddening) [5]. The average skin regeneration time is about one month. Thus, Figure E-7 indicates that beta burns should not result from prolonged skin contact. However, as stated in the text and shown in Figure 34 of the main text, prolonged skin contact (e.g., prolonged wearing of earrings made from DU) increases the risk of developing skin cancer at the location of contact.

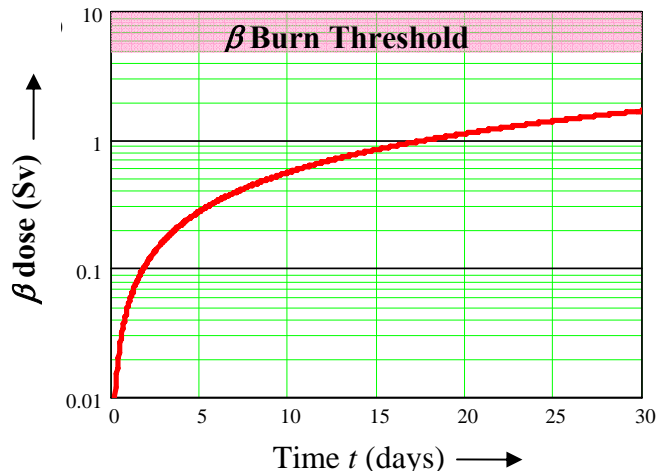


**Figure E-6. Estimated  $\beta$  dose to the skin from a DU pendant as a function of exposure time**

## References:

1. International Commission on Radiological Protection, *Limits of Intakes of Radionuclides by Workers*, ICRP Publication 30, Pergamon, NY, 1979.
2. International Commission on Radiological Protection, *Age-dependent Doses to Members of the Public from Intake of Radionuclides*, ICRP Publication 69, Pergamon, NY, 1995.
3. International Commission on Radiological Protection, *Human Respiratory Tract Model for Radiological Protection*, ICRP Publication 66, Pergamon, NY, 1994.
4. International Commission on Radiological Protection, ICRP Publication 60, *1990 Recommendations of the International Commission on Radiological Protection*, Pergamon, NY, 1991.
5. Mettler, F. A. Jr., M.D., and A. C. Upton, M.D., *Medical Effects of Ionizing Radiation*, 2<sup>nd</sup> Ed., W.B. Saunders Co., Philadelphia, 1995.
6. Glasstone, S., and A. Sesonske, *Nuclear Reactor Engineering*, Van Nostrand Reinhold Co., New York, 1967.
7. Briesmeister, J. F., Ed., "MCNP-A General Monte Carlo Code for Neutron and Photon Transport, Version 3A," *Los Alamos National Laboratory LA-7396-M Rev. 1*, Los Alamos, NM, 1986.
8. U.S. Department of Energy, DOE STANDARD SAFT-0072 (DRAFT): *Guide to Good Practices for Occupational Radiological Protection in Uranium Facilities*, Washington, DC, January 2000.

# Appendix F: Notation and Glossary

## F.1. Units

Bq	becquerel = 1 disintegration per second
Ci	curie = $3.7 \times 10^{10}$ disintegrations per second
cm	centimeter = 0.394 inches
dm	decimeter = 0.1 m
eV	electron volt = $1.6 \times 10^{-19}$ joules
Gy	gray = absorbed dose of 1 joule per kg = 100 rad
g	gram = 0.000455 pounds = 0.0073 ounces
hr	hour
J	joule = Watt·second
kg	kilogram = 1000 g = 0.455 pounds
km	kilometer = 1000 m = 0.622 miles
m	meter = 100 cm = 1000 mm = 39.4 inches = 3.28 feet
mg	milligram = 0.001 g
mm	millimeter = 0.001 m
mSv	millisievert = 0.001 Sv
ng	nanogram = $10^{-9}$ g
MeV	million electron volts = $10^6$ electron volts
s	second
Sv	sievert = Gy multiplied by radiation weighting factor
min	minute
u	atomic mass units = $1.6605 \times 10^{-24}$ g
yr	year
μg	microgram = $10^{-6}$ g = 0.000001 g
μm	micrometer = $10^{-6}$ m = 0.000001 m

## F.2. Explanation of Notation for Non-Scientist

Some non-scientists may be unfamiliar with standard scientific notation that uses powers-of-ten (i.e.,  $10^x$ ). The notation is easily understood to mean that the position of the decimal point of the number before the multiply sign is to be moved to the right by the number of decimal places indicated in the exponent (i.e.,  $x$ ) on the number 10. If the sign before the exponent is a minus (i.e.,  $10^{-x}$ ), however, the notation means  $1/10^x$ . Thus, when the exponent is negative, the decimal point is moved to the left by the number of decimal places indicated by the exponent. For example:  $2.73 \times 10^5$  is equivalent to 273,000 and  $6.25 \times 10^{-4}$  is equivalent to 0.000625.

This report also presents many plots using a logarithmic scale to show trends over ranges that would be difficult to observe using a linear scale. When a logarithmic scale is used, each major division represents a factor-of-ten change relative to the next major division (e.g., major divisions such as 0.01, 0.1, 1.0, 10, 100...). Note also that the subdivisions between major divisions are distorted, relative to a linear scale, by using a logarithmic scale.

### F.3. Symbols Used in Equations

$A$	Mass number (number of protons and neutrons in the nucleus)
$A_{238}$	Relative atomic mass for U-238 (u)
$A_r$	Relative atomic mass (u)
$\mathcal{A}$	Activity of radioactive material (Ci or Bq)
$\tilde{\mathcal{A}}$	Specific activity of radioactive material (Ci/g or Bq/g)
$a, b, c$	Coefficients used in the Garland Resuspension factor
$B_{air}$	Gamma ray buildup factor for air
$C$	Particulate concentration in air ( $\text{g}/\text{m}^3$ )
$C_{iv}$	In-vehicle aerosol concentration ( $\text{g}/\text{m}^3$ )
$c$	Conversion factor ( $1.6 \times 10^{-13} \text{ J}/\text{MeV}$ )
$c_1 - c_3$	Coefficients used to compute standard deviations
$D$	Absorbed dose (Gy)
$\mathcal{D}$	Distance between targets (m)
$d$	Particle diameter ( $\mu\text{m}$ )
$E_R$	Kinetic energy of incident radiation; i.e., $\alpha$ , $\beta$ , or $\gamma$ radiation (MeV)
$F_{OI}$	Factor to account for contribution to dose from isotopes other than U-238
$F_\beta$	Number of beta particle emissions per U-238 disintegration
$F_\gamma$	Number of 1-MeV gamma emissions per U-238 disintegration
$\mathcal{F}_r$	Fraction of particulate characterized as rapid dissolution
$\mathcal{F}_s$	Fraction of particulate characterized as slow dissolution
$f$	Fraction relative to mass internalized
$f_1$	Fraction of ingested uranium absorbed by the blood
$f_{Brc}$	Rapid fraction of DU absorbed by the blood from respiratory compartment $c$
$f_{Dc}$	Fraction of DU inhaled deposited in organ compartment $c$
$f_{ic}(t)$	Fraction in compartment $c$ at time $t$ considering only particle transport
$f_c(t)$	Fraction in compartment $c$ considering particle transport and blood absorption
$f_{cr}(t)$	$f_c(t)$ for only the rapid-dissolution particulate
$f_{LLI}(t)$	Fraction in lower large intestines at time $t$

$f_{ULI}(t)$	Fraction in upper large intestines at time $t$
$f_{LNr}(t)$	$f_c(t)$ for the rapid-dissolution particulate for the lymph nodes
$f_{olrc}(t)$	Rapid-dissolution fraction from respiratory compartment $c$ in organ $o$ 1 at time $t$
$f_{SI}(t)$	Fraction in small intestines at time $t$
$f_{ST}(t)$	Fraction in stomach at time $t$
$\bar{g}$	Average radiation attenuation factor in the body
$\mathcal{H}$	Effective height of source (m)
$H_{c,i}$	Equivalent dose to target organ compartment $c$ from source compartment $i$ (Sv)
$H_T$	Equivalent dose for organ or tissue $T$ (Sv)
$H_E$	Effective dose (Sv)
$K$	Eddy diffusivity ( $\text{m}^2/\text{s}$ )
$k$	Garland Resuspension factor ( $\text{m}^{-1}$ )
$L$	DU penetrator length (cm)
$\mathcal{M}_c$	Multiplier on estimated fatal cancer risk, used to obtain upper bound
$\mathcal{M}_g$	Multiplier on estimated genetic risk, used to obtain upper bound
$m$	Mass (g)
$\dot{m}$	Mass rate (g/s)
$m_c$	Mass of target organ compartment $c$ (kg)
$m_i$	Mass of DU in source organ $i$ (kg)
$m_{go}$	Mass in GI tract organ $o$ (g)
$m_{pcr}$	Post-exposure mass of rapid-dissolution DU in organ compartment $c$
$N$	Atom density (atoms/ $\text{cm}^3$ )
$N_A$	Avogadro's number (atoms/g-mole)
$\mathcal{N}$	Total number of atoms
$N_T$	Number of target vehicles
$n$	Neutron
$n_T$	Target index number
$O_c$	Fraction of time occupying contaminated area
$P(d)$	Relative number of particles of diameter $d$
$p_c$	Cancer risk coefficient (fatal cancers/Sv)
$p_g$	Genetic risk coefficient (Genetic birth defects/live birth/Sv)

$q$	Mass of DU (g) aerosolized and released into atmosphere
$q'$	Linear source strength (g DU/m)
$R_0$	DU penetrator radius (cm)
$R_B$	Breathing rate ( $\text{m}^3/\text{hr}$ ) or ( $\text{m}^3/\text{d}$ )
$R_d$	DU fragment dissolution rate ( $\mu\text{g}/\text{d}$ )
$R_i$	Ingestion rate (g/d)
$r$	Distance from DU penetrator or fragment (cm)
$s_{v\gamma}$	Volumetric gamma source strength (photons/ $\text{cm}^3\text{s}$ )
$t$	Time (s, d, or yrs)
$t_{1/2}$	Half-life (e.g., yrs)
$t_l$	Human lifetime following exposure (d)
$u$	Wind speed (m/s)
$v_d$	Deposition velocity (m/s)
$W_r$	Weighting factor for radiation type $R$
$W_T$	Weighting factor for tissue or organ type $T$
$x$	Downwind distance from source (m)
$y$	Crosswind distance from source (m)
$z$	Vertical distance from ground (m)
$Z$	Atomic number (number of protons in the nucleus)
$\text{AF}(T_c \leftarrow S_i)$	Fraction of radiation energy from source organ compartment $S_i$ absorbed in target organ compartment $T_c$
$\delta$	Distance from penetrator surface to an effective line source (cm)
$\phi_{\beta s}$	Beta-particle flux at surface of DU penetrator ( $\beta$ particles/ $\text{cm}^2\text{s}$ )
$\phi_R$	Particle flux for radiation type $R$ (particles/ $\text{cm}^2\text{s}$ )
$\gamma_c$	Distribution fraction for U absorbed in blood deposited in organ $c$
$\Lambda$	Particulate washout constant ( $\text{s}^{-1}$ )
$\lambda$	Decay or rate constant (e.g., $\text{s}^{-1}$ )
$\lambda_{238}$	Radioactive decay constant for U-238 ( $\text{d}^{-1}$ )
$\lambda_a, \lambda_b$	Rate constants for exponential form of Garland Resuspension factor ( $\text{d}^{-1}$ )
$\lambda_B$	Rate constant for absorption by blood in the GI tract ( $\text{d}^{-1}$ )
$\lambda_{ST}$	Transfer rate from stomach to small intestines ( $\text{d}^{-1}$ )

$\lambda_{SI}$	Transfer rate from small intestines to upper large intestines ( $d^{-1}$ )
$\lambda_{LLI}$	Excretion rate from lower large intestines ( $d^{-1}$ )
$\lambda_{ULI}$	Transfer rate from upper large intestines to lower large intestines ( $d^{-1}$ )
$\lambda_t$	Transfer rate from GI organ to other organ, blood, or feces ( $d^{-1}$ )
$\lambda_{tc}$	Rate constants for particle transport from compartment $c$ ( $d^{-1}$ )
$\lambda_r, \lambda_s$	Dissolution rate for rapid and slow-dissolution particulate ( $d^{-1}$ )
$\lambda_{c1}$	Transfer rate from target organ $c1$ to blood, urine, or other compartment ( $d^{-1}$ )
$\rho_{238}$	Density of U-238 (DU) metal ( $g/cm^3$ )
$\mu_{\gamma air}$	Gamma attenuation coefficient in air ( $cm^{-1}$ )
$\mu_{\gamma DU}$	Gamma attenuation coefficient in DU metal ( $cm^{-1}$ )
$\mu_{\gamma T}$	Gamma attenuation coefficient in tissue ( $cm^{-1}$ )
$\mu_{\beta DU}$	Beta attenuation coefficient in DU metal ( $cm^{-1}$ )
$\mu_{\beta T}$	Beta attenuation coefficient in tissue ( $cm^{-1}$ )
$\sigma$	Standard deviation for dispersion calculations (m)
$\sigma_g$	Geometric standard deviation for particle size distribution ( $\mu m$ )
$\zeta$	Areal density (g of deposited particulate per $m^2$ of ground surface)

## F.4. Glossary

**Absorbed dose:** The amount of radiation energy absorbed per unit mass of the exposed tissue or material (units: Gy or rad).

**Absorbed fraction:** The fraction of energy emitted by a radiation source in a source organ (S) that is absorbed by a target organ (T).

**Actinide:** Any of a series of chemically similar, radioactive elements with atomic numbers ranging from 89 (actinium) through 103 (lawrencium).

**Activity ( $\mathcal{A}$ ):** The number of nuclear transformations per unit time (units: Ci or Bq).

**Activity Median Aerodynamic Diameter (AMAD):** The diameter in an aerodynamic particle size distribution for which the activity of particles having greater diameters make up 50% of the total activity.

**Acute:** Short duration exposure.

**Aerosolization:** The production of an aerosol (a mist containing minute particles).

**Albumin:** A group of water-soluble proteins found in blood, muscle, egg, and milk.

**Alpha particle:** A particle emitted from the atomic nucleus of certain radioisotopes, consisting of a cluster of two neutrons and two protons.

**Alveolar-interstitial region:** Respiratory bronchioles, alveolar ducts and sacs and their alveoli and interstitial connective tissue.

**Anaplasia:** Loss of structural definition within a cell often with increased capacity for multiplication, as in a tumor.

**Aortic valve stenosis:** Abnormal narrowing of the aortic valve

**Areal density:** The mass of deposited particulate per unit surface area.

**Atomic mass (A):** The mass of an atom for a particular nuclide (u).

**Atomic mass unit (u):** A mass unit equal to 1/12 the mass of a neutral carbon-12 atom.

**Atomic number (Z):** The number of protons in the nucleus of an atom.

**Background radiation dose:** The typical radiation dose to individuals from natural and artificial (e.g., medical x-rays) sources.

**Beta burn:** Erythema (reddening of the skin) because of beta particle radiation.

**Beta particle:** A negatively or positively charged electron emitted from the atomic nucleus of certain radioisotopes.

**Biokinetic model:** A mathematical model describing the deposition, transport, blood absorption, and elimination of foreign material internalized in the body.

**Birth defect:** Congenital defects of body structure or function likely to result in physical or mental handicap or death.

**Blood-brain barrier:** A barrier between brain tissues and circulating blood that serves to protect the central nervous system.

**Bone seeker:** A radioisotope that tends to accumulate in the bones following internalization.

**Bronchial region:** The trachea and bronchi.

**Bronchiolar region:** The bronchioles and terminal bronchioles.

**Bystander effect:** Potential for cancer induction because of the effect on cells that are adjacent to cells that have been traversed by ionizing radiation.

**Burden (organ):** The total amount of a specific substance in an organ.

**Cancer:** A localized growth from uncontrolled cell reproduction, which can spread to other parts of the body.

**Carcinogen:** An agent or substance capable of inducing cancer.

**Child at play:** An Iraqi child playing inside or near a damaged military vehicle.

**Chromatid:** An individual strand of a chromosome that results from duplication.

**Chromosome:** Elements of a cell nucleus, consisting of DNA and proteins. DNA contains the genes that carry genetic information.

**Chronic:** Exposure over an extended period of time or having an effect over an extended period of time (months to years).

**Cilia:** Short hair-like outgrowths of certain cells capable of rhythmic beating.

**Class (weather):** Type of weather condition used in the analysis of pollutant dispersal and defined in Table B-2.

**Collective dose:** The sum of doses received by a specific population from exposure to a specified source of radiation.

**Committed effective dose:** The effective dose received by an individual during a 50-year period following intake of a radioactive material.

**Compound organ:** An organ described by several components to allow a more detailed radiological analysis.

**Congenital:** Present at birth (either genetic or non-genetic causes).

**Conservative assumption:** An assumption that tends to overestimate the severity of an effect.

**Cortical bone:** The hard compact shell forming a bone's surface.

**Creatinine:** A waste product of protein metabolism found in the urine.

**Daughter product:** The nuclide formed by the decay of the radioactive parent nuclide.

**Decay:** Radioactive disintegration of the nucleus of an atom.

**Decay constant ( $\lambda$ ):** The fraction of the number of atoms of a particular radioisotope that decay during a unit time (units:  $s^{-1}$ ).

**Depleted uranium:** Uranium depleted in the percentage of U-235 relative to the percentage present in natural uranium.

**Deoxyribonucleic acid (DNA):** An acid, mostly within the nucleus of a cell, that carries genetic information.

**Directly ionizing radiation:** Types of radiation (e.g., alpha and beta particles) that are capable of directly ionizing atoms in materials (secondary particle production is not necessary for ionization).

**Dose:** Dose is a quantitative measure of radiation exposure in terms of absorbed energy per mass of tissue. See absorbed dose, equivalent dose, and effective dose.

**Dose rate:** Radiation dose per unit time.

**Deterministic effect:** A deterministic effect is one for which there is a direct causal relationship between the exposure and the observed effect.

**Downwind civilian:** A civilian located away from the battlefield in the general direction of prevailing winds.

**Early health effect:** A health effect that occurs within a period of days to months following exposure.

**Effective dose:** The dose computed as the sum of the effective doses of radiation-exposed organs that have been weighted by tissue weighting factors to account for organ sensitivity (units: Sv or rem).

**Electromagnetic radiation:** Radiation made up of oscillating electric and magnetic fields propagating at the speed of light. Includes, for example, gamma radiation, visible, and infrared light.

**Electron volt (eV):** A very small unit of energy =  $1.6 \times 10^{-19}$  joules.

**Embedded Fragments:** Fragments of depleted uranium shrapnel embedded in the body.

**Energy:** The capacity of a physical system to do work or transfer heat (joules or MeV)

**Enrichment:** A process used to increase the relative abundance of one isotope of an element relative to the abundance found in the elements natural state.

**Epidemiology:** The study of the distributions of diseases in human populations.

**Flux (particle):** A particle flux is the number of particles crossing a surface per unit time.

**Epithelium:** Cellular tissue covering external surfaces of the body or lining internal organs.

**Equivalent dose:** An expression of dose that accounts for the relative biological effectiveness of different forms of radiation (units: Sv or rem).

**Extrathoracic:** Not located in the thoracic region (chest cavity).

**External radiation:** Radiation that originates from a source outside the body.

**Fetus:** Human unborn offspring beginning eight weeks after conception.

**Fission:** Splitting of the atomic nucleus.

**Fission products:** The nuclei formed by the splitting of a nucleus during fission.

**Friendly Fire Veteran:** Veterans accidentally hit by munitions fired by their own troops.

**Gamete:** Mature male or female reproductive cells.

**Gastro-intestinal (GI) tract:** The digestive system that starts from the oral cavity and proceeds to the esophagus, stomach, small intestine, large intestine, rectum and anus.

**Gaussian:** A random distribution of events, often graphed as a bell-shaped curve and used to represent a normal or statistically probable outcome.

**Gamma radiation:** Electromagnetic radiation emitted from the nucleus of an atom.

**Gene:** A segment of DNA forming a basic unit of heredity.

**Germ cell:** A sperm or egg cell.

**Glomerulus:** A closely knitted structure of capillaries found in the kidney that is responsible for filtering the blood.

**Gonad:** A sex organ, such as an ovary or testicle, which produces the gametes.

**Gray (Gy):** A radiation dose unit for absorbed radiation energy, equal to 1 J/kg.

**Half-life (radioactive):** The time in which half the atoms of radioactive species decays to form another isotope or decays to a lower energy state.

**Heavy metal:** Any metal that has a relatively high density and is toxic at low concentrations.

**Highway of Death:** A common expression that refers to the highway between Kuwait City and Basrah where U.S. aircraft destroyed a long column of Iraqi vehicles retreating from Kuwait. U.S. aircraft used 30 mm DU rounds as well as non-DU munitions.

**Hippocampus:** The region of the brain associated with learning and memory.

**Hodgkin Disease:** A neoplasm of lymphoid tissue defined by the presence of the malignant Reed-Sternberg cells.

**Hormesis:** The theory that small radiation doses can induce beneficial health effects.

**Implicit guideline (kidney):** A guideline of a maximum allowed kidney burden equivalent to 3  $\mu\text{g}$  uranium/g kidney used to set worker and public standards for maximum allowed uranium concentrations in air and water.

**Internal Radiation:** Radiation emitted from radioactive material that has been taken inside the body (e.g., inhaled or ingested).

**Internalized DU:** Depleted uranium taken into the body by inhalation, ingestion, embedded fragments, or wound contamination.

**In vitro:** Isolated from a living organism and artificially maintained.

**Ion:** An electrically charged atom.

**Ionization:** A process in which a charged particle (typically an electron) is removed from an atom.

**Ionizing radiation:** The types of radiation capable of ionizing atoms or molecules.

**Isotope:** Nuclides having the same number of protons but a different number of neutrons.

**Kinetic energy:** A form of energy associated with the motion of a body (joules or MeV).

**Late health effect:** Health effects that are not expressed until years after exposure to radiation or toxin.

**LD/50:** The dose that is lethal to 50% of the exposed individuals.

**Lesion:** An injury or other change in an organ or tissue of the body tending to impair function.

**Level I Veteran:** Gulf War veterans in vehicles hit by friendly fire DU penetrators. Rescuers of friendly fire veterans are also in the level I category.

**Level II Veteran:** A category of Gulf War veterans involved in post-combat evaluation of DU-damaged vehicles, removal of equipment, and preparation of vehicles for transport.

**Level III Veterans:** Gulf War Veterans who experienced short-term low-level exposures during or following battle.

**Lymph node:** Small organs located throughout the lymphatic system that contain immune system cells which can trap cancer cells and bacteria.

**Lesion:** An injury or other change in an organ or tissue of the body tending to impair function.

**Leukemia:** A malignant neoplasm of the blood forming organs resulting in an abnormal increase in white blood cells.

**Ligand:** An atom, molecule, radical, or ion that forms a complex around a central atom.

**Linear relationship:** A straight-line relationship.

**Linear energy transfer (LET):** The quantity of energy lost by a particular type of ionizing radiation per unit path length in a material.

**Linear nonthreshold model:** A method for predicting health effect risks that assumes a linear relationship between dose and health effect risk and assumes that no threshold exists below which there is no health effect risk.

**Low dose:** Less than 0.2 Gy.

**Low dose rate:** Less than 0.0001 Gy per minute (averaged over one hour).

**Lymph node:** Small organs located throughout the lymphatic system that contain immune system cells, which can trap cancer cells and bacteria.

**Macrophage:** A type of white blood cell that removes waste material from the body.

**Malignant:** A cancer that tends to become progressively worse and result in death if not treated; characterized by anaplasia, invasiveness, and metastasis.

**Maximally exposed:** An individual at a location or situation expected to receive the highest exposures.

**Metanalysis:** A statistical technique where all data from all available studies are combined.

**Metastasis:** The spread of cancer from one organ to another not directly connected with the organ.

**Mortality:** Death or death rate.

**Mutagen:** An agent (such as a chemical, ultraviolet light, or a radioactive element) that can induce or increase the frequency of mutation in an organism.

**Mutation:** A hereditary change in a gene or chromosome.

**Necrosis:** Death or decay of tissue in a particular part of the body.

**Nephrotoxic:** Toxic to the kidney.

**Neoplasm:** An abnormal growth of tissue in which the growth is uncontrollable.

**Nephron:** A unit of the kidney that serves to filter the blood, consisting of a filtration capsule and tubules.

**Neutron:** A neutral particle found in the nucleus of an atom.

**Neurotoxic:** Poisonous or destructive to nerve tissue.

**Neurocognitive:** Relating to cognitive functions linked to neural pathways or areas of the brain.

**Nominal exposure:** An typical or average exposure to individuals for a particular exposure scenario.

**Non-Hodgkin's Lymphoma:** Any of various malignant lymphomas that do not contain Reed-Sternberg cells and that produce symptoms similar to those of Hodgkin's disease.

**Nucleus (atomic):** The central region of an atom consisting of neutrons and protons.

**Nucleus (cell):** The nucleus is a membrane bound structure that contains the cell's hereditary information and controls the cell's growth and reproduction.

**Nuclide:** A particular species of nucleus characterized by the number of neutrons, the number of protons, and the energy state of the nucleus.

**Oncogene:** A gene that when activated can induce cancer.

**Penetrator:** The metal component of armor-piercing munitions used to pierce the wall of an armored vehicle.

**Photon:** A quantum of electromagnetic energy, regarded as a discrete particle having no mass or electrical charge. Depending on the photon energy and origin, photons can be categorized as gamma rays, X-rays, visible light, radio waves, etc.

**Plasma:** The fluid part of the blood (excluding blood cells).

**Proton:** A positively charged particle found in the nucleus of an atom.

**Proximal tubules:** Small tubules within the nephron structures of the kidney that allow water and other substances to be reabsorbed by the blood.

**Pyrophoric:** Ignites readily in air when in the form of a fine particulate.

**Radiation:** Emitted sub-atomic particles or electromagnetic waves that carry energy and propagate through space or matter.

**Radiation weighting factor:** A factor used to multiply the absorbed dose to account for the relative biological effectiveness of different radiation types or energies.

**Radioisotope:** A radioactive species of isotope.

**Radon:** A naturally occurring radioactive gaseous element formed by a sequence of natural radioactive decay stages.

**Relative biological effectiveness (RBE):** The ratio of the absorbed energy from 200-keV x-rays required to produce a given biological effect to the absorbed energy from another radiation to produce the same effect.

**Renal agensis:** This malformation occurs when a kidney fails to develop.

**Resuspension:** The resuspension of ground or surface-deposited particulate in the air by wind or human and animal activity.

**Risk:** The product of the consequence and probability of an event. For carcinogenic effects, risk is the incremental probability for developing cancer over a lifetime because of exposure to a carcinogen (unitless or %).

**Risk coefficient:** The increase in the incidence of a health effect per person exposed per unit equivalent dose.

**Risk multiplier:** A factor multiplied by the best estimate risk to obtain the upper bound risk.

**Sarcoma:** A malignant tumor arising in connective tissues.

**Secular equilibrium:** When the parent nucleus has a much longer half-life than the subsequent daughter nuclides, the shorter half-life daughter products will eventually exhibit the same decay rate as the parent radionuclide. The matching of decay rates to the parent radionuclide is called secular equilibrium.

**Self-sharpening:** A property of DU penetrators that results in continual shearing away of the mushrooming penetrator end formed by impact.

**Serum:** A clear fluid obtained upon separating whole blood into its solid and liquid components after it has been allowed to clot.

**Sievert (Sv):** A dose unit equal to 1 Gy multiplied by a radiation-weighting factor.

**Soft tissue:** In this report, soft tissues are the organs and tissues identified in Table E-1.

**Somatic effect:** A health effect from exposure to radiation or a chemical toxin that is limited to the body of an individual (rather than the individual's offspring).

**Source term:** The quantity, type, and characteristics of radioactive material released into the environment.

**Source tissue:** Tissue or organ containing a radioactive substance.

**Specific activity ( $\tilde{A}$ ):** Activity per gram of a radionuclide.

**Stochastic effect:** An effect that is characterized by probability of occurrence, where the probability of occurrence is proportional to the dose received.

**Substantia nigra:** A layer of large pigmented nerve cells in the midbrain that produce dopamine and whose destruction is associated with Parkinson's disease.

**Target tissue:** Tissue or organ in which radiation is absorbed.

**Temperature inversion layer:** A meteorological phenomenon where air temperature increases rather than decreases with height.

**Teratogen:** Any agent that interferes with normal embryonic development.

**Thoracic:** The region of the body between the neck and the abdomen.

**Tissue weighting factor:** A factor used to multiply the equivalent dose to account for the relative radiation sensitivity of various organs.

**Trabecular bone:** Trabecular bone consists of the many struts within the marrow region.

**Tricuspid valve insufficiency:** Tricuspid valve insufficiency occurs when a tricuspid valve does not close tightly enough to prevent leakage.

**Upper bound:** Here, the upper bound is the estimated maximum value for either a nominal or maximum exposure scenario that includes analysis uncertainties.

## **Distribution:**

Dr. M. Parkhurst PNNL (4 copies)

Staff Scientist  
Radiological Science and Engineering Group  
Battelle (PNNL), K3-55  
P. O. Box 999  
Richland, WA 99352

Dr. Nick Greene (3 copies)

Manager, Physical Sciences and International Security  
Science Policy Section  
The Royal Society  
6-9 Carlton House Terrace  
London SW1Y 5AG

Dr. M. Bailey

The Royal Society  
6-9 Carlton House Terrace  
London SW1Y 5AG

Dr. Lea Steel (6 copies)

Scientific Director  
Research Advisory Committee on Gulf War Veterans' Illnesses  
U.S. Department of Veterans Affairs  
2200 S.W. Gage Blvd. (T-GW)  
Topeka, KS 66622

Dr. S. Fetter

Dean: School of Public Policy  
Van Munching Hall  
University of Maryland  
College Park, MD 20742-1821

Dr. Frank N. von Hippel

Professor of Public and International Affairs  
Woodrow Wilson School  
209 221 Nassau St.  
Princeton, NJ 08544-1013

Dr. Bernard. Rostker (3 copies)

Office of Special Assistant  
Department of Defense  
5113 Leasburg Pike, Suite 901  
Falls Church, VA 22041

Dr. J. Lewis UNM

Director: Community Environmental Health Project  
University of New Mexico  
College of Pharmacy  
Albuquerque, NM 87131 0001

Dr. N. Roderick

Professor: Chemical and Nuclear Engineering Department  
The University of New Mexico  
209 Ferris Engineering Center  
Albuquerque, NM 87131-1341

George L. Hawley

National Veterans Service  
200 Maryland Ave. NE  
Washington D.C. 20002

Dr. Fred Mettler

Veterans Administration Hospital  
2100 Ridgecrest Dr. SE  
Albuquerque, NM 87108

Adrian Atizado

Assistant National Legislative Director  
National Service and Legislative Headquarters  
807 Maine Avenue SW  
Washington D.C. 20024

Dan Fahey

631 Howard St.  
San Francisco, CA 94105

Jerry Wheat

1 Manana Rd.  
Albuquerque, NM 87031

Dr. Janice Harper

Assistant Professor  
Department of Anthropology  
250 South Stadium Hall  
Knoxville, Tennessee 37996-0720

Shannon Middleton  
Health Policy Analyst  
The American Legion  
1608 K St.  
Washington D.C. 20006-2847

S. Aftergood  
1717 K St. NW  
Suite 209  
Washington D.C. 20038

Senator Jeff Bingaman  
625 Silver Avenue SW, Suite 130  
Albuquerque, NM 87102

Senator Pete V. Domenici  
Albuquerque Plaza  
201 3<sup>rd</sup> Street NW, Suite 710  
Albuquerque, NM 87102

Senator Hillary Rodham Clinton  
United States Senate  
476 Russell Senate Office Building  
Washington, DC 20510

Congressman Dennis Kucinich  
Washington Office  
1720 Longworth HOB  
Washington, DC 20510

Congresswoman Heather Wilson  
20 First Plaza NW, Suite 603  
Albuquerque, NM 87102

Professor Edward Dugan  
University of Florida  
202 Nuclear Science Bldg.  
P.O. Box 118300  
Gainesville, FL 32611-8300

50	MS245	A.C. Marshall, 245
250	CD's MS245	A.C. Marshall, 245
1	MS0102	J. Woodard, 2
1	MS0134	J. Rice, 200
1	MS0415	K.J. Almquist, 241
1	MS0415	C.A. Drewien, 241
1	MS0415	J.P. Franklin, 241
1	MS0415	J.B. Godfrey, 241
1	MS0415	S.G. Kaufman, 241
1	MS0415	T.E. Owen, 241
1	MS0415	R.A. Watson, 241
1	MS0415	D.H. Zeuch, 241
1	MS0417	W.H. Ling, 243
1	MS0417	B.J. Ash, 243
1	MS0417	M.L. Bunting, 243
1	MS0417	D.M. Fordham, 243
1	MS0417	S.W. Hatch, 243
1	MS0417	D.B. Lawson, 243
1	MS0417	S.M. Schafer, 243
1	MS0417	D.M. Teter, 243
1	MS0421	R. Moya, 240
1	MS0423	L.J. Branstetter, 247
1	MS0423	W.B. Chambers, 247
1	MS0423	R.M. Griswold, 247
1	MS0423	L.M. Sanders, 247
1	MS0423	A. Slavin, 247
1	MS0423	D.E. Waye, 247
5	MS0425	J.D. Rogers, 245
1	MS0425	L.W. Connell, 245
1	MS0425	K.J. O'Brien, 245
1	MS0425	A.C. Payne, 245
1	MS0425	B. Smith, 245
1	MS0425	L.C. Trost, 245
1	MS0425	C. Layne, 8000
1	MS0431	C. Ross, 233
1	MS0651	C. Potter, 6334
1	MS0742	D. Powers, 6870
1	MS0771	J. Kelly, 6870
1	MS0791	F. Harper, 4117
1	MS1017	L.Clevenger, 3300
1	MS1136	P. Pickard, 6872
1	MS1166	E. Blansett, 6743
1	MS1221	J. McDowell, 5000
1	MS1395	N. Wall, 6822